Design of Experiments Methodology in Studying Near-infrared Spectral Information of Model Intact Tablets

Simultaneous Determination of Metoprolol Tartrate and Hydrochlorothiazide in Solid Dosage Forms and Powder Compressibility Assessment Using Near-infrared Spectroscopy

Inauguraldissertation

zur

Erlangung der Würde eines Doktors der Philosophie

vorgelegt der

Philosophisch-Naturwissenschaftlichen Fakultät

der Universität Basel

von

Branko Z. Vranic

von Serbien

Basel, 2015

Approval

Genehmigt von der Philosophisch-Naturwissenschaftlichen Fakultät

auf Antrag von

Prof. Dr. Matthias Hamburger

und

Prof. Dr. Thierry F. Vandamme

und

Prof. Dr. Jörg Huwyler

Basel, 09.12.2014

Prof. Dr. Jörg Schibler

The Dean of Faculty

Овај рад посвећујем мојим вољенима, мојој супрузи Катарини, мом сину Лазару, мојој мајци Олги и мом оцу Зорану.

I dedicate this work to my loved ones, my wife Katarina, my son Lazar, my mother Olga and my father Zoran

Acknowledgements

This PhD project was carried out at the Department of Pharmaceutical Sciences, University of Basel, Switzerland.

I would like to express my deep appreciation and gratefulness to **PD Dr. Gabriele Betz** for giving me the opportunity to do my PhD project in her research group and under her supervision. I would like to thank her for continuous support, guidance and motivation throughout the project.

I owe the same if not more to my dear **Prof. Dr. Svetalana Ibric**. Without her help and support, I wouldn`t be where I am now.

My sincere gratitude goes to my Thesis Advisor, **Prof. Dr. Thierry F. Vandamme**, whose precious comments and guidance helped me to round up and bring the PhD thesis to an end.

I would like to thank **Prof. Dr. Matthias Hamburger** for accepting to be my Faculty Responsible and for the support.

My appreciation goes also to **Prof. Dr. Jörg Huwyler** for accepting to be the co-referee of this PhD thesis.

I would like to thank to all the former members of Industrial Pharmacy Research Group for the unique support and for the great and inspiring working atmosphere in the laboratory.

Special thanks goes to **Dr. Muhanned Saeed** who transferred to me his reach experience in near-infrared spectroscopy and chemometrics, and helped me to substantially understand this complex field.

The third project of the thesis has been accomplished with the great help of my friend and colleague **Dr. Nicolaos Gentis** to whom I owe special thanks.

I owe my deepest gratitude to my beloved wife Katarina, who has supported me with deep understanding and love through the tough periods.

My dear parents, mother Olga and father Zoran were always beside me when I needed support and wise advice. I thank them for that.

List of Abbreviations

AOTF	Acousto-optic tunable filter
API	Active pharmaceutical ingredient
BP	British pharmacopoeia
GMP	Good manufacturing practice
PCA	Principal Component Analysis
PCR	Principal Component Regression
Db1	First derivative 4 points
DR	Diffuse reflectance
DT	Diffuse transmittance
EMA	European Medicined Agency
FDA	Food and drug administration
EP	European Pharmacopoeia
FT	Fourier transformation
HPLC	High performance liquid chromatography
ICH	International conference on harmonization
LED	Light-emitting diode
MCC	Microcrystalline cellulose
MLR	Multiple linear regression
MSC	Multiplicative Scatter Correction
Ncl	Normalization by closure
PLS	Partial Least Squares
PLSR	Partial Least Squares Regression
NIR	Near infra-red
NIRS	Near infra-red spectroscopy
nle	Normalization to unit length
PASG	Pharmaceutical analytical science group
PAT	Process Analytical Technology
PC	Principal Component
PRESS	Predicted residual error sum-of-squares
RPM	Revolution per minute
SD	Standard Deviation
RSD	Relative Standard Deviation
SE	Standard Error
MTP	Metoprolol Tartrate

HTZ	Hydrochlorothiazide
SEC	Standard error of calibration
SECV	Standard error of cross-validation
SEE	Standard error of estimation
SEP	Standard error of prediction
RMSEP	Root Mean Squared Error of Prediction
RPD	Ration of Performance to Deviation
SNV	Standard Normal Variate
SST	System suitability test
TPH	Tablets per hour
USP	United States Pharmacopoeia
UV	Ultra Violet
SVM	Support Vector Machines
ANN	Artificial Neural Networks
UV-Vis	Ultra violet – visible
GCM	Global calibration model approach
BRM	Balance reference method

Abstract

Near-Infrared spectroscopy (NIRS) is applied in pharmaceutical industry for monitoring drug content during tablet manufacturing process. NIRS method, once developed and validated, is used over years and it is of critical importance to insure method robustness towards formulation, process, instrumental, acquisition and environmental factors. Design of Experiments (DoE) methodology was proposed in this work for systematic study of the effect of compression pressure, pre-compression pressure and tableting speed on Average Euclidean Distance (AED) which reflects NIR spectral features of the studied caffeine tablets, and Root Mean Squared Error of Prediction (RMSEP) as a key performance indicator of the developed NIRS calibration model for caffeine content prediction. Study was performed in diffuse reflectance (DR) and diffuse transmittance (DT) measurement mode. Tableting factors shown to have significant influence on the studied responses have been considered in the development of the robust calibration models in DR and DT mode, using Global Calibration Model (GCM) approach. Three studied factors have shown to be significant in DR mode whereas, compression pressure and tableting speed have shown significant effect on the studied responses in DT mode. Developed robust method in DT mode have shown superior performances compared to DR mode, exhibiting total error (RMSEP) of 1.21 % calculated on the independent test set. DoE setup, with the selection of factors and responses adopted in this study was not reported elsewhere.

Simultaneous NIRS quantification of two APIs in powders and tablets requires several challenges to be overcome. Overlapping absorption peaks of formulation components result in method specificity problem. Strategy for selecting the samples used for developing the prediction models is needed. Robustness of the method towards formulation factors needs to be assessed due to complex formulation. Fast and simple method for simultaneous quantification of Hydrochlorothiazide (HTZ) and Metoprolol Tartrate (MTP) in powders and tablets was proposed in work. Simulation of industrial scale tablet machine using tablet press replicator - *Presster*® was proposed as fast and cost-effective alternative for design and manufacture of tablet sets needed for NIRS calibration model development. Balance Reference Method (BRM) was proposed as an alternative to HPLC and UV-spectroscopy which are traditionally used as reference methods in NIRS model development. The proposed experimental setup was suggested for the feasibility study stage of the method development. The two model drugs were simultaneously quantified using NIRS exhibiting RMSEP of 1.69 and 1.31 mg in HTZ powder and tablet samples respectively, while MTP powder and tablet samples were predicted with RMSEP of 3.15 and 3.00 mg respectively. NIRS analysis of Metoprolol Tartrate and Hydrochlorothiazide in powders and tablets was not yet reported in the literature.

The compressibility and compatibility of a powder formulation is conventionally determined by compaction followed by destructive tensile strength and relative density measurement of the final compact. In this study, a non-destructive near-infrared spectroscopic (NIRS) was evaluated for the determination of powder compressibility and compactibility. Twelve different formulations were investigated with 2 batches produced per formulation. Relative density and tensile strength were measured using a traditional, destructive method on one tablet batch and subsequently by a developed non-destructive chemometric NIRS method on the second batch of the particular formulation. The outcomes of the two approaches were compared to validate the developed method. All data sets were fitted to the three established mathematical equations to calculate equation factors, which represent a formulation compressibility and compactibility. The study focus was set on the equation factor comparison between the traditional and the newly designed method. The results have shown a high degree similarity between the outcomes of the two methods. A discrepancy between the two methods was observed for the outcomes of the equation factors after fitting to Leuenberger equation. The approach using NIRS is suggested as a promising tool for monitoring tablet manufacturing process.

Contents

List of Figures

List of Tables

List of Equations

1. Introduction

Near-infrared spectroscopy (NIRS) is a technique becoming increasingly popular both in industry and academia. The reason is that it is very fast compared to the other analytical techniques. Very often it takes only several seconds to do a measurement. NIR is nondestructive analytical technique, which requires little or no sample preparation. It is very versatile. If sample contains molecular bonds such as C-H, N-H, O-H or S-H and if the concentration of the analyte exceeds about 0.1% of the total composition, then it is very likely that the analysis with NIRS would be feasible. Measurement procedure is quite simple and requires as little as few hours of training. There are, however, disadvantages that should be considered. The preliminary work, typical of any chemometric method, requires expertise and time. The system should be "taught" of what is in the sample relevant for the analyzed parameter. This task may be time-consuming. Currently available chemometric software packages offer user-friendly interfaces and big choice of data pre-treatments, wavelength selection algorithms, various regression methods such as multiple liner regression (MLR), partial least squares (PLS), principal components regression (PCR), neural networks (NN), support vector machines (SVM) among others. After several hours or days invested for calibration development, the multiple advantages of NIRS analysis would certainly outweigh the time required for method development.

With current advances in computer technology and user friendly chemometric software packages it is not necessary for the developer or the operator that is using the technique, to have a firm theoretical understanding of near-infrared spectroscopy (NIRS). It is, however, needed for the meaningful development of NIRS method and interpretation of the results, that the basics of the technology and chemometrics are understood. NIRS methodology contains some theoretical considerations that are not relevant in more common spectroscopic applications. Hydrogen bonding shifts dominate the spectrum. Spectral interactions and nonlinearities deviate from Lambert - Beer's law. The development of applications is significantly different from the UV-Vis and mid-IR applications. NIRS method development depends, to high extent, on statistics and chemometrics.

Near-infrared spectroscopy (NIRS) is the study of interaction of electro-magnetic radiation that spans the range from 700 to 2.500 nm (14.285 – 4.000 cm^{-1}), and the matter. Absorption in NIR spectral range is represented by overtones and combinations of the fundamental molecular vibrations from the mid-infrared (MIR) region. Overtones and combinations are mainly associated with C-H, N-H, O-H and S-H functional groups. NIRS requires the use of chemometrics to analyze the functional groups present in a sample matrix. As a quality and process control technique, NIRS is applied to analyses of raw materials, intermediate and finished products. It has been widely used in food and agricultural industries since several decades. Pharmaceutical industry is

quite slow in accepting NIRS as a common analytical technique, which could be due to the fact that there is absence of primary absorption bands that could be assigned to the analyte. In recent years, an increasing amount of research has been carried out on NIRS and its application in pharmaceutical industry. The advances in hardware and software tehchnologies have enabled the necessary growth in use of NIRS in pharmaceutical industry. The regulatory authorities promoting the innovative concepts of pharmaceutical manufacturing, stimulate the use of NIR spectroscopy which is considered as a useful process analytical technology tool.

1.1 Historical Development of NIR Spectroscopy

William Herschel's discovery of near-infrared radiation has the greatest importance for the development of NIR spectroscopy (Davies T., 1998). He was considered one of the greatest astronomers of the time. In the year of 1800, he published two papers on the heating effect in the spectrum of solar radiation. He has used a glass prism as a dispersive element to transfer the sunlight onto three thermometers with carbon-blackened bulbs. Beyond the red end of the visible electromagnetic spectrum, he observed the heating effect. Herschel defined this phenomenon as "radiant heat" considering it as a form of energy different from light. Thirty five years later, Ampere found that NIR was not a different form of energy but a light energy that spans beyond the visible spectral range. At the beginning of the 20th century, the nature of the electromagnetic spectrum was studied and explained by many scientists. James Clerk Maxwell have formulated four equations defining the propagation of light (Maxwell J. C., 2011). The work of Kirchoff, Stefan and Wien was rounded up in 1900 by the law of radiation discovered by Max Plank (Planck M., 1901).

In the first half of the 20th century, the spectral features of many organic compounds were explained and assigned to functional groups. Infrared spectroscopy was not so widely excepted and was reserved mostly for the scientists and spectroscopists. Suitable spectrometers did not exist at that time and the few existing ones were available only in governmental institutions. The first quantitative NIR application was the determination of atmospheric moisture at the Mount Wilson observatory by F.E. Fowle in 1912. In 1938, Ellis and Bath determined water content in gelatin. In the early 1940s, Barchewitz analyzed fossile fuels and Barr and Harp published the spectra of some vegetable oils. Until 1970, only about 50 scientific papers, related to NIR, had been published. In the 1930s, lead sulphide has been studied as a materials suitable for the detection of infrared light. The upcoming Second World War stimulated the development of heat sensors based on lead sulphide. After the Second World War, lead sulphide detectors, covering the wavelength region of 1000-2500 nm, became commercially available (Pasquini C., 2003).

Research in the field of NIRS was developing slowely after the Second World War. Many scientists considered the technique too complex as it was characterized by weak and overlapping absorption bands based on overtones and combination bands of fundamental MIR absorptions. The degree of absorption of NIR radiation by a matter was two to three orders of magnitude weaker compared to MIR. The baseline dependency on many instrumental, acquisition and sample properties was creating additional confusion among the scientists. The lack of chemometric software packages made the peak assignment and spectra interpretation difficult. On the other hand, very sensitive PbS detectors were commercially available together with powerful tungsten lamps as a good source of NIR radiation, and

that enabled diffuse reflection measurements of solid samples. The components of the first NIR spectrometers were relatively inexpensive which stimulated the manufacturing of the first NIR instruments.

Near-infrared spectrometers rely to a great extent on the computer technologies. Computers control NIR instruments, data acquisition and enable calibration process and data analysis that require thousands of calculations which would be inconsivable without the aid of computer. Work on diffuse light scattering in transmission and reflection by Kubelka and Munk in 1931, set a foundation for the NIR measurements of solid samples. The discovery of principal components analysis (PCA) and Mahalanobis`s mathematical approach for representing data clustering and separation in multidimensional score space, helped in further development and use of NIR spectroscopy. The first commercially available computer was launched on the market in 1950s. Several years later, programming language Fortran, was developed by the company IBM. In the beginning of 1980s, personal computers has been widely spread and became the driving force for the development of NIR instrumentation (Wahr J. A., 1996).

In the mid of 20th century there was a growing demand for fast, quantitative determinations of moisture, protein, fat and other common parameters in different agricultural products. Scientist named Karl Norris, who was working for US Department of Agriculture at that time, was assigned to solve the problem of the need for fast analysis of wheat grains. He has managed to solve the problem and provide a solution based on NIR technology. The equipment that he has used was fairly simple but able to provide sufficient performances to satisfy the needs of the market. In 1968, Ben-Gera and Norris published the work on applying multiple linear regression (MLR) to the problem of calibration related to agricultural products (Ben-Gera I. et al., 1968). In the early 1970s the first NIR laboratory instruments were launched on the market by the companies Dickey-John, Technicon and Neotec. The first process instruments were developed in Germany and UK.

In the 1980s, the microprocessors have started being integral part of the design of NIR instruments. Data acquisition was controlled by the microprocessor technology and the data manipulation was much faster. Data analysis and interpretation was enhanced by including MLR, PLS and PCA algorithms in the software packages. Companies developing chemometric software have emerged offering a various possibilities of data treatments. NIR technology has developed rapidly since 1970s. In many fields, NIR spectroscopy is now the measurement technique of choice (Saeed M., 2011).

1.2 Theory of Near Infrared Spectroscopy

1.2.1 Molecular Vibrations

Energy status of the molecules change after the NIR radiation energy is absorbed. Rotational and vibrational quantum numbers represent the changes in energy status of molecules. Vibrational energy has higher magnitude compared to a rotational energy. Molecules are in a ground energetic state, i.e. at the lowest energy level, unless excited. When the substance is irradiated with the light from NIR source, some of the molecules will absorb the photon energy and reach the higher energetic level. Most of the molecules reach the first energy level next to the ground state and very few second or higher energy level. Such a changes in rotational and vibrational energy represent the first or higher overtone absorption bands in NIR spectra. Probability of such transitions is very low, and for that reason the intensity of overtone bands is ten to hundred times weaker compared to the absorption bands from fundamental vibrations (Wilson E. B., 1955; Quack M., 1990).

Vibration of covalent bonds in a molecule does not obey Hooke`s law of harmonic motion. The quantum vibrational energy levels are not equidistant within a potential energy well. This phenomenon is called anharmonicity. Anharmonicity is reflected in the fact that the frequency of the overtones is slightly less than the integer multiples of the fundamental vibrational frequencies. This results in the overtones being found at slightly longer wavelengths than expected (Sokolnikoff, I. S. and Dickerson S. R., 1956; Rychlewski, J., 1984).

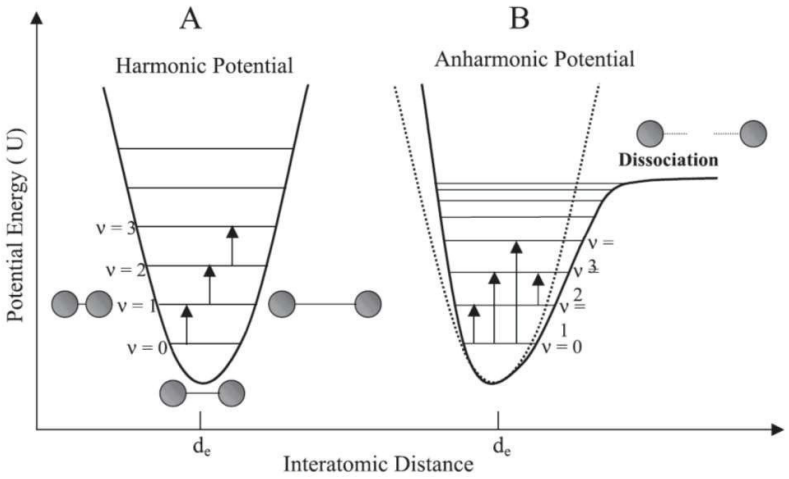

Figure 1: Schematic representation of the harmonic (A) and anharmonic (B) models for the potential energy of a diatomic molecule.

de = equilibrium distance (U = minimum) (Pasquini 2003)

1.2.2 Origin of absorption bands in NIR

When the energy of NIR light that irradiates the molecules equals the difference between two vibrational energy levels, molecules will interact with the frequencies of the light. Some frequencies of the incident radiation will be absorbed and the other partially absorbed or not absorbed at all. The dependence of the intensity of the absorbed radiation on the frequency of the incident light source constitutes the absorption spectra of a analyte. In the interaction of the matter with the light wave it is crucial that the electrical field of the electromagnetic wave can interact with the electric field of the molecules. Such an interaction results in absorption of the light by the matter. Absorption can occur only if the vibrational movement of the atoms that form the molecular bond or the atoms forming a local group of vibrating atoms, creates a change in the diplole moment.

Transitions to excited states that involve two vibrational modes at the same time are also allowed. Those are called combination bands and occur in polyatomic molecules. In NIR spectroscopy, the importance of combination bands is quite significant. Overtone absorption bands originate from the functional groups that contain C-H, N-H, O-H or S-H atomic bonds. Overtone vibrations that originate from the above mentioned covalent bonds are combined with lower-frequency fundamental bands such as C=O and C-C to generate overtone-combination bands. Combination bands are very useful in NIR spectroscopy. Unlike MIR, in NIR spectroscopy, for combination bands to occur, it is necessary that only one of the combining vibrations is active, causing a dipole change. The other may be inactive. This feature is unique and makes some vibrations visible in NIR spectral range while not observable in MIR range.

Intensity of absorption bands is dependent on the degree of the dipole change during thvibration of the covalent bonds. Covalent bonds show fundamental vibrational transitions in the region of 3000 - 4000 nm. Intensities of the combination absorption bands are around ten times weaker compared to fundamental vibrations whereas, up to thousand times weaker for the overtone vibrations. The spectral features in NIR region are dominated by overtones and combination absorption bands. (Workman J. J., 1992).

1.2.3 Sample Presentation and Measurement Modes in NIR Spectroscopy

Sample presentation to an NIR instrument is one of the critical factors affecting NIR measurements. Figure 2 illustrates sample presentation modes, i.e. diffuse reflection, diffuse transmission, specular reflection, transmission and transflection. In the case of diffuse reflection, incident light irradiates the surface of the sample, is diffusely reflected from the surface layer of the sample, and finally detected. In order to apply this measurement mode, the sample should be opaque and not transparent, e.g. powder or tablet. Diffuse transmission measurement mode is characterized by an incident light that illuminates one side of the sample, traverses the sample through pore structure, and finally the transmitted light is detected on the other side of the sample. The light takes tortuous path through the sample and is being reflected or refracted on the solid-air interfaces of the pores. Those optical phenomena are repeated multiple times and as a resul, the effective pathlength is several orders of magnitude higher compared to the nominal one. The intensity of the detected signal is usually quite weak and noisy, so it requires the use of very sensitive detectors. Specular reflection occurs at the surface of the sample where the angle of the reflected light is equal to the angle of the incident light. Transmission measurement mode is usually applied for the liquid and transparent samples. The sample shouldn`t be opaque and the scattering should be negligible. Transflection measurement mode combines transmission and reflection principles. Incident light is transmitted through the sample and reflected back from a reflective surface, which could be from teflon, ceramic or other reflective material. In this work, diffuse reflectance and diffuse transmittance measurement modes were applied for the measurement of the powder and tablet samples (Cozzolino D. and Murray I., 2002; Siesler H. W., et al., 2008).

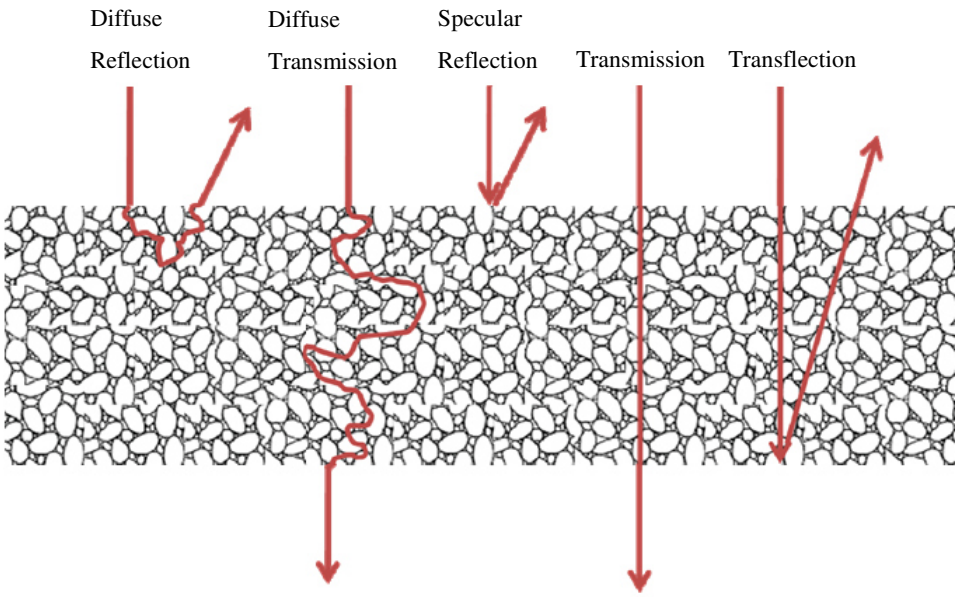

Figure 2: Diagram showing the types of light interaction in the NIR region with particulate solids. In practice, only diffuse reflection and transmission are observed

1.2.4 Diffuse Reflectance (DR) Measurement Mode

Reflectance of certain material is represented by the ratio of the light intensity reflected from a diffusely reflecting surface, I_0, and light reflected from the measured sample, I_S. Reflectance is usually reported in absorbance units, log (1/R). Apparent absorbance spectra recorded in diffuse reflectance measurement mode establish linear correlation with the concentration of the analyte, according to Lambert - Beer's law. The deviations fom the law (nonlinearities) are disregarded if insignificant or dealth with by adding additional factors to the calibration model or nonlinear terms (Wendlandt W. W. and Hecht G. H., 1966; Fuller M. P. and Griffiths P. R., 1978).

The first theory on diffuse reflection was given by Bouguer in the middle of 18th century. Bouguer assumed diffuse reflection as a sum of mirror-type reflections from the microcrystalline faces statistically distributed over all possible angles.

Lambert established a cosine law in 1760. Describing the relation between the intensity of an incident light beam, angle of incidence and the angle of an observation. The shortcoming of the theory was the fact that an ideal diffuse reflective surface, which was postulated in the theory has never been found and thus, failed to succeed in practice.

In 1888, Seeliger and the coworkers came up with an idea of diffuse reflectance radiation penetrating the surface of materials. One portion was assumed to be absorbed by the material and part returned to the surface through reflection, diffraction or refraction from the microstructure of the surface layer of the material.

In 1908., Mie set a theory described elastic scattering phenomenon and the relationship with the frequency of radiation. The main assumption of the theory was that the scattering is associated with isolated, spherical particles. According to this theory, scattering is not distributed isotropically but rather follows a complex pattern with forward scattering being more probable than the reverse scattering (Simmons E. L., 1975; Steinke J. M. and Shepherd A. P., 1988).

$$\frac{I_{\Theta scat}}{I_0} = \frac{\lambda^2}{8\pi^2 R^2} = (i_1 + i_2)$$

Equation 1: Mie Theory

λ – Single wavelength

$I_{\Theta scat}$ – Intensity of scattered radiation at distance R and angle π from the center of the scattering particle

i_1, i_2 - Complex functions of the angle of the scattered radiation, the spherical harmonics, or their derivatives with respect to the cosine of the angle of scattered radiation, the refractive index of both the sphere and surrounding medium, and the ratio of the particle circumference to wavelength

Equation 1 shows that as the wavelength increases, the intensity of the scattered radiation increases. This could explain the baseline upscaling observed in the NIR absorbance of the solid samples. Mie theory suffered from several drawbacks. Particles in real solid samples could not be considered isolated but are rather in contact with one another. The theory also didn`t consider multiple scattering phenomena.

Kubelka and Munk, in 1931., came up with a simplified solution of the radiation transfer equation. The equation 2 shows that the measured diffuse reflectance (R_∞) is dependent on the ratio of the absorption coefficient (K) and the scattering coefficient (S). Kubelka and Munk's equation is widely accepted explanation of the diffuse reflectance since it is a equation consisted of the two constants and could be experimentally tested (Kubelka P., 1948; Nobbs J. H., 1985).

$$f(R_\infty) = \frac{K}{S} = \frac{1-2R_\infty+{R_\infty}^2}{2R_\infty} = \frac{(1-R_\infty)^2}{2R_\infty}$$

Equation 2: Kubelka – Munk Equation

1.2.5 Diffuse Transmittance (DT) Measurement Mode

Interaction between NIR radiation and solid particles is characterized by the relatively weak absorbance with high scattering. This feature allows the NIR light to penetrate the solid samples with little or no requirements for sample preparation. The diffuse transmission measurements of solid samples are unique for the NIRS compared to MIR and UV spectroscopy. Transmittance of a sample is defined as the ratio of light intensity transmitted through an empty path, I_0, and light transmitted through an equal distance of a sample, I_s. Transmittance of a sample can be reported in the form of Beer-Lambert law (Zaccanti G. and Bruscaglioni P., 1988; Langhals H. G. et al., 2000):

$$\boldsymbol{A = log\left(\frac{1}{T}\right) = log\left(\frac{I_s}{I_0}\right) = abc}$$

Equation 3: Beer – Lambert Law

For a single wavelength, λ:

A – Beer-Lambert optical absorbance

T – Transmittance ratio

a – absorption coefficient, cm^{-1}

b – pathlength (or sample thickness), cm

c – concentration of absorbing material

Transmittance of NIR radiation through a solid sample composed of tightly packed particles, deviate nonlinearly from the Beer-Lambert`s law, unlike UV or VIS absorption spectroscopy. In case of spectroscopy through clear liquids where the nonlinear deviations from Beer`s law are due to changes in absorption coefficients across the concentration range, in case of diffuse transmission through solid sample, incident photons are scattered or reflected either forward or backward relative to the direction of propagation of the incident beam, I_0. The incident photons are not transmitted directly through the sample but rather take a tortuous path with multiple scattering phenomena.

Diffuse transmittance NIR spectroscopy shows the most important features is in the third overtone region, between 780-1100 nm. The absorptivity, reflectance, and scattering properties of a solid samples such as powders, granules or tablets, are dependent on various sample properties such as particle size and morphology, bulk density and index of refraction. The effective pathlength and the nonlinear deviation from the Beer's law is, however, difficult to predict in practice.

1.2.6 NIR Instrumentation

Instrumentation dedicated to NIR spectroscopy differs from the other spectroscopic instruments in the applied spectral range and specificity of the applications that it is dedicated for. Required resolution of NIR spectrometers is not as high as for the UV or MIR because NIR spectra appear as combinations and overtones of primary absorption bands of fundamental MIR vibrations. Spectral acquisition in NIR spectral region is often challenging. Measurements made in a field or on the factory production line are typical of NIRS. In laboratory, measurements are usually done in situ, with little or no sample preparation. Samples that are analysed by NIR spectroscopy are often heterogeneous, solid or opaque samples, with significant scattering properties. Large light spot area, high sample throughput and a fast spectra aquisition are prerequisits for high quality NIR measurements.

Interference-filter spectroscopy, Fourier-transform spectroscopy and acousto-optic tuneable filter spectroscopy are well known technologies suitable for NIR spectroscopy. Specific measurement cells and NIR sampling geometry are used in NIR spectroscopy for improving the acquisition efficiency of diffuselly reflected light.

NIR spectrometers could be optically set up as pre-dispersive or post-dispersive depending on the position of the wavelength selection element in the light path from the source of the radiation, sample to the detector (figure 3). In case of pre-dispersive spectrometers, sample is illuminated with monochromatic light. Light that is scattered back from the sample surface or transmitted through the sample is collected and brought to the detector. Stray light that hits the sample is also collected are delivered to the detector. Since stray light can represent a large portion of the total detected light signal, it is a major source of error in pre-dispersive NIR spectroscopy. Stray light effect can be reduced by protecting or covering the sample in order to reduce the ambiental light sample illumination.

In case of post-dispersive NIR spectrometers, sample is illuminated directly from the source of NIR radiation. Light that is scattered back from the sample or transmitted through the sample is dispersed and then delivered to the detector. As it is a case with the NIR pre-dispersive spectrometers, stray light that hits the sample is also being collected. The difference is that in case of post-dispersive instruments, only stray light of the same wavelength as that being detected is added to the signal resulting from the instrument's illumination of the sample. For that reason, the stray light represents only a small portion of the total light signal measured by the detector (Workman J. J. and Burns D. A., 2001; Osborne B. G. et al., 1993).

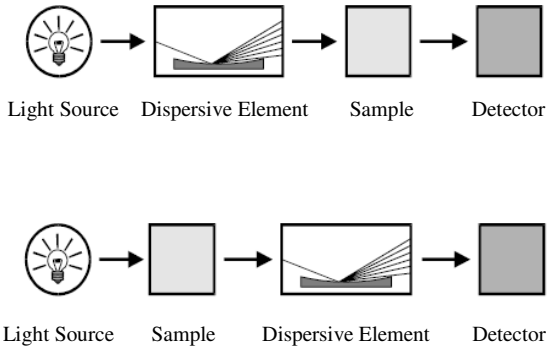

Figure 3: Pre-dispersive (above) and Post-dispersive Spectrometers

1.2.6.1 Filter instruments

Filter instruments consists of a set of 10-20 interference filters mounted on a rotating wheel positioned between the collection lenses and a detector (figure 4). It is possible to have very fast measurements, comparable to diode array spectrometers, by spinning the filter wheel at a rate of several thousands oscilations per minute. Fast Fourier transformation of the detected signal can be applied to separate the spectral data from the instrument noise. Filter instruments have simple and robust design and are suitable for not too demanding applications. Filter based instruments are often applied as an on-line moisture gauges. The main drawback of the filter instruments is the limited wavelength accuracy and low spectral resolution (Shenk J. S. and Westerhaus M. O., 1985).

Figure 4 : Rotating wheel with interference filters

1.2.6.2 Light Emitting Diodes - based instruments

Light Emitting Diodes (LED) technology is used in some applications where it is important to reduce the size of the instrument. LED-based instruments are characterized by a band width of around 30 - 50 nm. The instruments are employing multiple LEDs as sources of narrow band NIR radiation which is

then dispersed by using common dispersive elements such as gratings or interference filters. LED-based NIR instruments operating at wavelengths higher than 1100 nm are still quite expensive (Malinen J. et al., 1998).

1.2.6.3 AOTFinstruments

NIR spectrometers based on Acousto-Optical Tunable Filter (AOTF) technology have design with no moving parts, capable of reaching high scanning speed over a broad range of NIR region (figure 5). Scan speeds of up to 2000 wavelengths per second, is the advantage of AOTF technology in process analysis where fast acquisition is of critical importance. AOTF instruments are made of a birefringent TeO_2 crystal, cut in a special angle, and a piezoelectric material attached to one end of the crystal. TeO_2 crystal is excitated by an external radio frequency signal, producing an acoustic wave which propagates through the crystal and produces a variation of refractive index of the crystal. The frequency of the generated acoustic wave is determined by the radio frequency signal. The usuall radio frequency range in AOTF NIR spectroscopy is from 50 to 120 MHz. The interaction of the electromagnetic wave and the acoustic wave causes the crystal to refract narrow wavelength bands from the NIR light source. The birefringent TeO_2 crystal produces two monochromatic light beams and both or only one diffracted beam can be used by NIR instruments (figure 5). The fact that there are no moving parts makes the AOTF NIR spectrometer a good candidate for the implementation in field or production environment. The scan speed enables the on-line or in-line process-monitoring (Pasquini C., 2003).

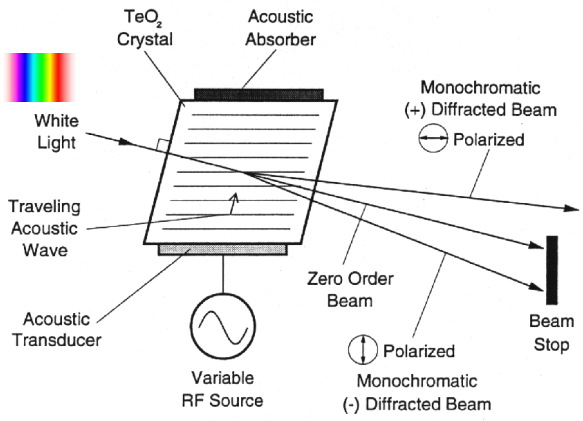

Figure 5 : Scheme of the AOTF instrument

1.2.6.4 Dispersive instruments

Diffraction grating dispersive instruments are one of the earliest NIR technologies (Figure 6). These instruments have a relatively low cost compared to the other scanning instruments employing modern technologies. The main disadvantages is the slow scan speed and low wavelength accuracy and precision. Wavelength instability deteriorates over time due to mechanically driven mechanism fatigue, which causes the unreliability of the dispersive instruments for the use in production environments (Armstrong P. R. et al., 2006).

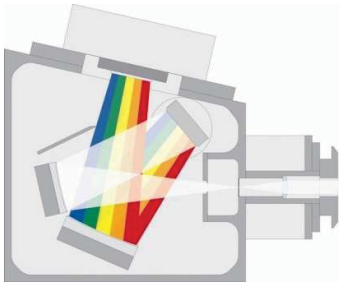

Figure 6: Diffraction Grating NIRS.

The incident light is delivered by a concave mirror on to the diffraction grating, where it is spatially split into the narrow spectral bands. A second concave mirror focuses the spectral bands of the light onto the Charge Coupled Device detector, and in that way, capturing the sample spectrum in a single acquisition.

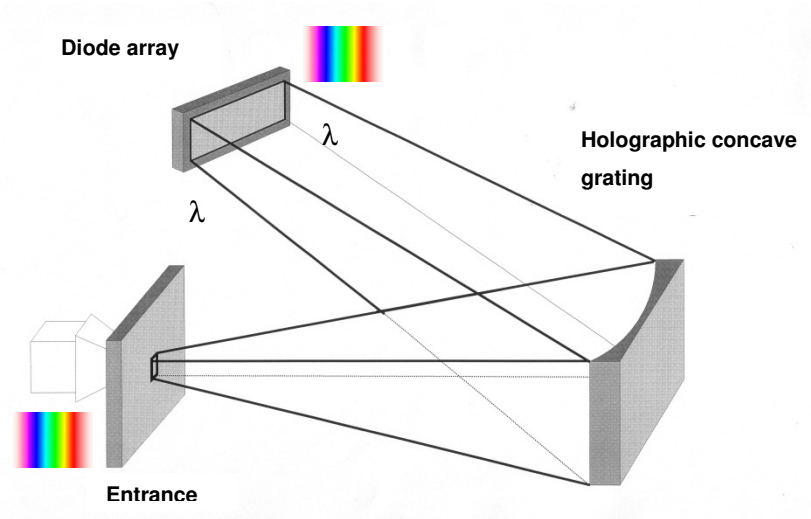

Figure 7: Diode array instrument

Recent evolution in detector technology enabled dispersive instruments to be more efficient. Construction of linear arrays of PbS and InGaAs detectors containing up to 256 independent elements allow scanning the entire spectrum in a few milliseconds (figure 7). Additionally, the innovative design eliminated the moving parts of the diode - array NIR spectrometers (Cozzolino D. et al., 2004).

1.2.6.5 Fourier-transform (FT) NIR Spectrometers

FT-NIR spectrometers offer several advantages in comparison to the other NIR technologies especialy when the high-resolution capabilities are important or if the spectrometer needs to have many options for sample presentation. The spectral resolution of FT-NIR spectrometers is constant across the spectral range and is adjusted by varying the length of the interferogram. In case of a Michelson interferometer, the length of the interferogram, i.e. the spectral resolution corresponds to the displacement of the moving mirror. Scanning speed is for that reason impared compared to e.g. diode-array spectrometers.

The FT spectrometers have a combination of three theoretical advantages, which make this technology advantages:

- All wavelengths are detected simultaneously (Fellgett's advantage)
- Wavelength accuracy is constantly maintained by a built-in laser (Connes advantage)
- High optical throughput compared to the other technologies (Jacquinot's advantage)

The resolution needed for the most NIRS applications for the analysis of pharmaceutical solid dosage forms is 8-16 cm^{-1}. This is due to the fact that the absorption bands in NIR region, originating from the combination and overtone vibrations, are broad and overlapping.

Polarization interferometer is based on a two-piece birefringent crystal wedge polarizer and birefringent compensator to modulate optical light beam in the pattern of a Fourier interferogram. Figure 8 shows that randomly polarized radiation passes through a linear polarizer and a birefringent crystal, which separates the light into two orthogonally polarized parallel light beams with a phase shift, thereby slightly rotating the plane of polarization. The phase-shifted beams are transmitted through the two-piece wedge polarizer, which then rotates the plane of polarization in the opposite direction, reducing the phase shift. The angle of polarization rotation is dependent on the effective pathlength through the wedge polarizer, and wavelength. At the initial position, the thickness of the wedge polarizer is set so that the polarization rotation angle perfectly offsets the compensator, resetting the polarization state to that of the first polarizer. In this state, the maximum light energy at all wavelengths will pass through the second polarizer. As the thickness of the wedge

polarizer varies, the polarization angle incident on the second polarizer will vary following a sinusoidal pattern between 0 and 100% transmittance; the frequency of the sinusoidal pattern will vary according to optical frequency. Therefore, the sum of the components incident on the detector will produce an optical interferogram. The optical efficiency of the device is limited by absorption in the beam path, especially as the thickness of the wedge polarizer reaches a maximum (which will limit the maximum resolution).

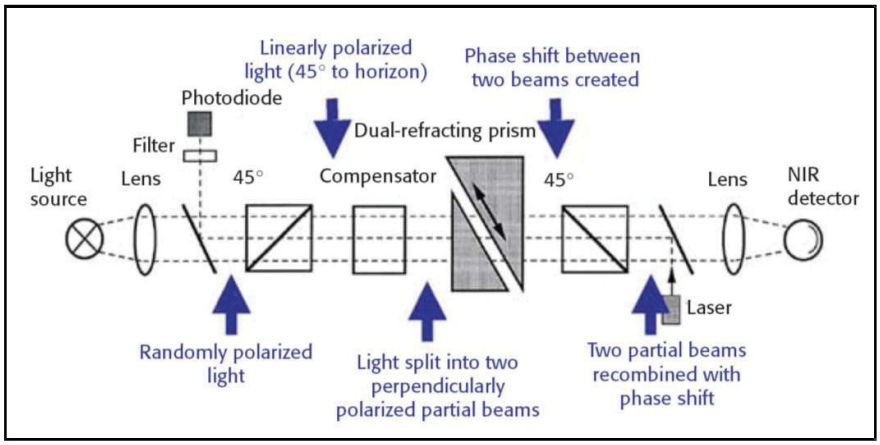

Figure 8: Scheme of the polarization interferometer. A sample is placed after the last lens and before the detector. A second lens then is needed to compensate for signal divergence through the sample. (Ciurczak 2005)

Because there is only a single optical path through the instrument (compared with the dual path of Michelson, Sagnac, or Mach-Zender interferometers), the polarization interferometer is less affected by small misalignments, which makes it more suitable form at-line applications. Additionally, simple design is more cost-effective and can be produced with a smaller footprint (Siesler H. W. et al., 2008).

1.3 Chemometrics

Chemometrics is a science that uses different mathematical and statistical methods to perform calculations on a large amount of chemical data and exctract the information relevant for the analysis of interest. The common meaning of the chemometrics refers to using linear algebra calculations, to make either quantitative or qualitative analysis of chemical data such as NIR spectra. The science of chemometrics provides to spectroscopists different ways to solve the calibration problem for analysis of spectral data. Chemometrics is the bridge between connecting the state of a chemical system to the measurements of the same system. It has become an essential part of the modern industry. Chemometric software packages have been widely used by product development scientists, process engineers, PAT specialists, and QA/QC scientists to build reliable models, ensure product quality, classify raw material and to monitor the process in real-time (Vandeginste B. G. M. et al., 1988).

1.3.1 Regression Methods

Regression methods are a useful tool for the investigation of the relationships between variables. Usually, the investigator is looking for the causal effect of one variable upon another. For example, the effect of a calorie intake on a body weight, or the effect of changes in the money value upon the inflation rate. To explore such relationships, the investigator performs regression analysis to estimate the quantitative effect of the causal variables upon the variable that they influence. The investigator also typically assesses the statistical significance of the estimated relationships, that is, the degree of confidence that the true relationship is close to the estimated relationship.

1.3.1.1 Multiple Linear Regression

Multiple Linear Regression (MLR) is a method used to model the linear relationship between a dependent variable and one or more independent variables. The dependent variable is also called predictand, and the independent variables, predictors. MLR is based on least squares theory. The model is fit in a way that the sum-of-squares of differences of observed and predicted values is minimal. The predictors in any regression problem could be inter-correlated. Inter-correlation of predictors does not prevent the use of regression, but can make difficult or impossible to assess the relative importance of individual predictors from the estimated coefficients of the regression equation. Extremely high inter-correlation of predictors, or *multicolinearity*, exacerbates any difficulty of interpreting the regression coefficients, and may call for combination of subsets of predictors into a new set of less inter-correlated predictors. Regression models are generally not intended to be applied to predictor data outside the range encountered in the calibration period (Aiken L. S. et al., 2003).

The model expresses the value of a predictand variable as a linear function of one or more predictor variables and an error term:

$$\mathbf{y = b_0 + b_1 x_1 + b_2 x_2 + \cdots + b_K x_K + e}$$ **Equation 4: Multiple Linear Regression**

x_k – value of k^{th} predictor
b_o – regression coefficient
b_k – coefficient on the k^{th} predictor
K – total number of predictors
y – predictand
e – error term

In NIR spectroscopy there are usually fewer calibration samples compared to the recorded wavelengths. Consequently, MLR often leads to unstable estimates of the response. MLR model could fit the calibration set well, but if the regression vector is unstable, small random errors in future samples could be enlarged. This may result in large prediction error in future samples during routine use of a method.

In case of the applications from the filter-based instruments, where few wavelengths are available, MLR could be a suitable regression method. The same holds for the cases where there are sharp and well defined absorption peaks, e.g., in case of some organic solvents, chemicals or active pharmaceutical ingredients (APIs). In such cases, MLR could perform better compared to more advanced regression methods like Partial Least Squares (PLS) or Principal Component Regression (PCR).

1.3.1.2 Principal Component Regression

Principal Component Analysis (PCA) is a method of data analysis for building linear multivariate models of large amount of data. PCA models are developed using orthogonal vectors (loadings), usually called principal components. PCA aims at eliminating the principal components associated with noise, reducing the dimensionality of complex data sets and minimizing the effect of a random measurement error.

PCA is a chemometric method that explains the covariance structure of a data by a relatively small number of new variables (principal components). These components are linear combinations of the original variables that allow the interpretation and a better understanding of the different sources

of variation in a data set. PCA as a data compression tool is widely used for the analysis of high-dimensional systems which are frequently encountered in chemometrics. PCA is usually the first step in a data analysis, followed by classification, cluster analysis, or other multivariate regression methods.

The most important step in PCA is to select the principal components that carry most of the information relevant to the analysis. The first principal component corresponds to the direction in which the projected observations have the largest variance. The second component is orthogonal to the first one and again maximizes the variance of the data points projected on it. Continuing in this way, PCA produces all the principal components, which correspond to the eigenvectors of the empirical covariance matrix.

This method is sensitive to anomalous observations. The first components are often attracted toward outlying points and thus may not capture the variation of the regular observations which are relevant for the analysis. Therefore, data reduction based on PCA becomes unreliable if outliers are present in the data set (Jolliffe I., 2005).

1.3.1.3 Factor Selection

Selection of the number of principal components in a PCA model is critical because retaining more factors than needed would only add more noise to the model and would deteriorate its predictive ability. On the other hand, if less than optimal number of factors is kept, meaningful information would not be included in the model and that would results in suboptimal model. There are a number of ways to ensure the correct selection of the model dimensionality.

1.3.1.4 Predicted Residual Error Sum of Squares (PRESS)

One of the best ways to determine how many factors to use in a PCR calibration is to generate a calibration for every possible number of factors and use each calibration to predict the property of interest in a set of independent validation samples. The predicted residual error sum of squares, or PRESS, is calculated for each calibration and the calibration that provides the best results is chosen. The number of factors used in that calibration is the optimal number for that system.

1.3.1.5 Cross-validation

Sometimes, a sufficient set of independent validation samples to calculate PRESS is not available. In such cases, the original training set can be used to simulate a validation set. This approach is called cross-validation. The cross-validation is performed in a way that a calibration is calculated using all of the training set samples except for one sample or group of samples. Calibration is then used to predict the concentration of the analyte in the sample that was left out of the training set. In the next step, the sum of squared differences (errors) between the expected and the predicted concentrations for the sample that was left out is calculated. Excluded sample is then returned to the training set, and another sample is left out. New calibration is calculated for the new subset of the original training set. New PRESS value is calculated and added to the one calculated so far. When all `leave-one-out` combinations are computed and overall PRESS value calculated the process is repeated for every possible number of factors. The PRESS is examined for each of the calibrations to choose the one that gives the best results. The number of factors used in that calibration is the rank of the system. This procedure is known as "leave one out" cross-validation. This is not the only cross- validation method, but rather the most popular although it tends to generate the models with unrealistically small model error (Standard Error of Cross Validation), which is not representative of the future predictions. Cross-validation with leaving out the calibration (property) range segments instead of the single samples was used in this work as it is suggested by many authors as the one giving the most realistic models. The calibration range is divided in ten to twenty segments and the segments are left out in iterative cross-validation steps. This method tends to generate the calibration models with higher Standard Error of Cross Validations but is better estimate of the error to be expected in routine analysis (Kohavi R., 1995).

1.3.1.6 Spectra Reconstruction and Model Calculation

By discarding the principal components that carry the noisy information, it is possible to remove a portion of the noise from the spectra. The spectra that are generated after the noise removal are called reconstructed spectra. When principal component regression is applied to the data set, there is not really a separate, explicit data regeneration step. When the PCR model is developed and applied to the unknown data set, the spectra are automatically reconstructed excluding the noise information by using the factors that explain the spectral variation related to the change in the property under study. When the model is applied to an unknown sample, the predicted property is calculated as the product of the measured spectrum of the sample and the calibration matrix.

1.3.1.7 PCA as a Multivariate Data Exploratory Tool

First few principal components usually represent a relevant part of the total data variance. Thus, when plotting pairs of principal component scores, the data structure can be visually inspected in two dimensions in order to identify groups of objects. PCA transforms the data matrix X, containing data for n objects with m variables, into a matrix of lower dimension T. In the matrix T, each object is characterized by a relative small number of PCA scores. Score t_i of the i^{th} object x_i is a linear combination of the variables of vector x_i and the vector components (loadings) of a PCA loading vector p. The score vector t_k of PCA component k contains the scores for all n objects; T is the score matrix for n objects and a components; P is the corresponding loading matrix. PCA is usually the first choice to visualize multivariate data by scatter plots and transform highly correlating variables into a smaller set of uncorrelated variables. Outliers may heavily influence the result of PCA and diagnostic plots help to find outliers (leverage points and orthogonal outliers) falling outside the hyper-ellipsoid which defines the PCA model.

1.3.1.8 Partial Least Squares Regression

PLS is a variation of PCR that takes its concept one step further by using a different way to find a coordinate system that can have advantages over the coordinate system used for PCR. This strategy involves finding factors for both the spectral and the reference data.

The reason behind this approach is the following: First, to utilize the noise removal capabilities of PCA and remove some of the noise from the reference data. Second, and because the noise in the spectral data will deflect each eigenvector slightly out of the plane containing the theoretical, noise-free data in some randomly different direction than the deflection of the corresponding spectral eigenvector (since noise in the reference and spectral data are independent from each other). PLS rotates the vectors back, towards each other until they are aligned and provide better noise removal by bringing the vectors closer to the ideal planes, containing the noise-free spectral and reference data. In addition to the set of new coordinate axes for the spectral data (the x- block), we also find a set of new coordinate axes for the referencing data (the y-block). These reference data are expressed as projections onto the concentration factors in a way similar to expressing the spectral data as projections onto the spectral factors.

Each pair of factors is rotated towards each other on a factor-by-factor basis to maximize the fit of the linear regression between the projections of the spectra onto the spectral factor with the projections of the reference data onto the concentration factor. The calibration (regression) coefficients are then

calculated using linear regression between the projections of the spectra on each individual spectral factor with the projections of the reference data on each corresponding referencing factor of the same order.

The prediction step for PLS is also slightly different than for PCR where it is also performed on a rank-by-rank basis using pairs of spectral and reference factors. Taking predicting concentration as an example, for each component, the projection of the unknown spectrum onto the first spectral factor is scaled by a response coefficient to become a corresponding projection on the first concentration factor. This yields the contribution to the total concentration for that component that is captured by the first pair of spectral and concentration factors. The process is then repeated for the second pair of factors, adding its concentration contribution to the contribution from the first pair of factors, and continued until all of the factors in the basis space have been used.

PLS will search for a single vector, W, that represents the best compromise between the spectral factor and the reference factor, which is not necessarily the factor that lies exactly half-way between them. It is, instead, the factor that maximizes the linear relationship between the projections (scores) of the spectral points onto the factor and the projections (scores) of the corresponding reference points onto this same factor and maximizes the covariance between the two (Geladi P. and Kowalski B. R., 1986).

1.3.2 Spectral Pre-processing

The successful application of multivariate calibration methods is negatively affected by the presence of uninformative variance in NIR spectra. Baseline effects may occur from small changes in sample properties (packing density, surface texture, temperature and humidity, inhomogeneities, etc.). In addition, uninformative variance may be introduced into a data set by changes in the operational parameters of the NIR spectrometer.

One approach to minimize these effects is to apply mathematical pre-treatments to the raw spectra. There are many types of pre-treatments, some of which are commonly indicated for certain conditions (like derivatives to exclude baseline shifts) while in many cases their use is sample- and application-dependent.

1.3.2.1 Mean Centering

Mean centering is applied by subtracting the mean spectrum of the data set from every spectrum in the data set, equation is given below:

$$R_{i,j}^{mc} = R_{i,j} - \left(\sum_{j=1}^{J} \frac{R_{i,j}}{J}\right)$$ **Equation 5: Mean Centering**

R = Spectrum j in an array of J spectra
i = wavelength data point

Mean Centering translates the collection of data to the origin of the multivariate space where analysis will be performed. The practical consequence of mean-centering data is often a more simple and interpretable regression model. In effect, mean centering removes the need for an intercept from the regression model. Consequently, since fewer terms in the regression model may need to be estimated, estimated analyte concentrations may be more precise following mean centering of the data (Seasholtz M. B. and Kowalski B. R., 1992).

1.3.2.2 Smoothing

With smoothing, it is possible to improve the signal-to-noise ratio of a spectrum, for example, as a function of time or more commonly, wavelength.

Caution must be used when smoothing data. Strong smoothing gives better signal-to- noise ratios than weak smoothing, but strong smoothing may adversely reduce the resolution of the signal and hence affects methods involving spectra with sharp peaks or shoulders.

The simplest method of smoothing is to calculate a running average for a narrow window of points. The smoothed spectrum is generated by using the average value from the window. This causes problems at the endpoints of the curve, and numerous authors have described different methods for treating them.

The most commonly used type of smoothing is polynomial smoothing, also called Savitzky-Golay smoothing. Polynomial smoothing works by fitting of a smooth polynomial function to the data in a sliding window of width *w*, where *w* is usually an odd number. Smoothed points are generated by evaluating the polynomial function at its midpoint. The window is moved to the right by dropping the oldest point from the window and adding the newest point to the window until the entire curve has been smoothed. The degree of smoothing is controlled by varying the width of the window, *w*, and by changing the degree of the fitted polynomial function (Savitzky A. and Golay M., 1964).

1.3.2.3 Derivatives

Taking the derivative of a continuous function can be used to remove baseline offsets, because the derivative of a constant is zero. In practice, the derivative of a digitized curve can be closely approximated by numerical methods to effectively remove baseline offsets.

The derivative transformation is linear, and curves produced by taking the derivative retain the quantitative aspects of the original signal. The most commonly used method is based on polynomial smoothing. As in polynomial smoothing, a sliding window is used; however, the coefficients for the smoothing operation produce the derivative of the polynomial function fitted to the data. As in polynomial smoothing, the frequency- response function of these types of filters is not ideal, and it is possible to introduce distortions and artefacts if the technique is misused. Zero crossing points can be used to identify the location of peaks in the original spectra (Faber N. M., 1999).

1.3.2.4 Normalization

Here, each spectrum is normalized to constant area, thus removing the effect of the fluctuating signal. The simplest normalization technique is to simply set the sum of squares for each

spectrum to 1, i.e., each spectrum has unit length. This procedure is similar to variance scaling, except the method is applied to rows in the data matrix rather than columns. Many other normalization schemes can be employed, depending on the needs dictated by the application. Normalisations by height, local band area or largest peak are other methods commonly used in spectroscopy.

1.3.2.5 Multiplicatice Scatter Correction and Standard Normal Variate

MSC is used a method to correct differences in baseline offsets and path length due to differences in particle-size distributions in near-infrared reflectance spectra of powdered samples.

In NIR reflectance measurements, there are two components of reflected light that reach the detector: specular reflectance (light reflected without being absorbed or interacting with the sample) and diffuse reflectance (light that is reflected by the sample after penetrating the sample particles, where some of the light is absorbed by the chemical components present in the particles). Powdered samples with very small uniform particles tend to pack very efficiently compared to samples with large, irregularly shaped particles. Samples with small, efficiently packed particles give a greater intensity of specular reflectance, and after transformation as log (1/reflectance), the higher levels of specular reflectance appear as increased baseline offsets; thus samples with smaller particle-size distributions tend to have larger baseline offsets. Beam penetration is shallow in samples with small, efficiently packed particles; thus these kinds of samples tend to have shorter effective path lengths compared to samples with larger irregularly shaped particles. MSC attempts to compensate these two measurement artefacts by making a simple linear regression of each spectrum against a reference spectrum. The mean spectrum of a set of training spectra or calibration spectra is usually used as the reference. The least-squares coefficients are first estimated and then used to calculate the MSC-corrected spectrum.

MSC has been shown to work well in several empirical studies, which showed an improvement in the performance of multivariate calibrations and a reduction in the number of factors in PCA.

However, in SNV transformation, the mean of each spectrum is subtracted and the length is normalized to 1, and it produces results similar to MSC in many cases, which sometimes makes it difficult to choose between the two methods. In practice, it is best to try both methods and select the pre-processing method that gives superior performance (Isaksson T. and Naes T., 1988; Barnes R. J. et al., 1989).

1.4 Calibration Model Development and Optimization

NIR instruments determine the analytes by measuring the intensity of reflected or transmitted radiation which then needs to be correlated to the amount of the same analyte determined by some other method called a reference or standard method. Establishing this relationship by using a set of samples of known composition is called calibration of an NIR method. The relationship between the NIR radiation intensity and values obtained by reference method always involve certain form of regression equation.

The success and acceptance of NIR analysis depend in large part on the power of the mathematics used in the calculation of the calibration models.

Multivariate calibration methods lead to a generation of a regression model, providing a high dimensional vector of estimated coefficients. The coefficients weigh the spectrum and provide the estimated response. In order to develop a model, a set of calibrated concentrations (response) and the corresponding spectra are collected at discrete intervals. Usually, there are many more regressors than training observations so the classical linear regression can`t be applied and special methods like Principal Component Regression or Partial Least Squares Regression, need to be used.

1.4.1 Data Sets and Representative Sampling

Calibration samples should include representation of every responding chemical species in a system under study. Spectral shifts and changes in instrument response for mixtures due to interactions between components, changes in pH, temperature, ionic strength, and index of refraction are well known. The use of mixtures instead of pure standards during calibration development enables multivariate calibration methods to generate linear models for the estimation of the analyte of interest with the present interactions.

The calibration samples should cover a sufficiently broad range of sample composition. For simple systems, it is usually possible to prepare mixtures according to experimental design, where concentrations for all ingredients are varied over a suitable range. Because it is more desirable to make interpolations rather than extrapolations when making predictions from a calibration model, the range of concentrations in the calibration standards should exceed the working range expected during routine use. Calibration sample compositions should give a fairly uniform coverage across the range of interest. However, if the range is too large, deviations from linearity could begin to appear.

The recommended minimum number of calibration samples is 30 to 50, although this depends on the complexity of the problem.

It is very important that validation sets do not contain samples or subsamples used for calibration development. The validation sample set should be independent from the calibration set. Another important point is that the composition of validation samples should be designed to lie at points in between calibration points and should well represent the future sample profile expected to be analyzed during routine use of the method.

Different validation sets should be prepared to investigate every source of expected variation in the instrument response, operational environment changes, as well as expected sample variability.

Proper design of calibration sets yields calibrations that are performing well in terms of precision and accuracy. The complexity of calibration development has not allowed, yet, completely automated mathematical modeling in any current software. In any case, the most critical step in calibration is the proper collection of samples to represent the population for routine analysis (Shenk J. S. and Westerhaus M. O., 1991).

1.4.2 Developing a Calibration Model

Development of a NIR calibration model depends on the variety and flexibility of the data treatments and experience of the person doing the development.
The first step in the development process is recording the NIR spectra and collecting the reference values on the sufficient number of calibration samples. Number of samples necessary for building the robust calibration model depends on the complexity of the analytical problem and ranges from 30 up to couple of hundreds. The feasibility study , that should be always carried out before the method development, aims at identifying the sources of variability and facilitates the design of the sample sets that will be used for the method development.
The second step is to determine the sampling and reference method errors. Reproducibility or standard error of laboratory (SEL) may include the sampling error and can be determined as the standard deviation (SD) of the differences between reference measurements on duplicate samples. The tests should duplicate both sample preparation and analysis. NIR method can`t correlate to a reference method better than the reference method correlates to itself. That means that the SEL is the lowest achievable limit for the standard error of calibration (SEC) which is the calibration model error.
Third step in the development process would be to choose the chemometric parameters in order to achieve the acceptable SEC which is usually up to two times standard error of laboratory (SEC < 2 X

SEL). After developing the calibration with sufficient SEC it is necessary to validate the develop method to test for *overfitting*, which happens when calibration model approximates non-representative features of the particular samples used for developing the calibration model. Common indicators of the overfitting are:

1. SEC much lower than SEL. It is usually the case when too many principal components/factors were used for building the regression model. The other possibility is that calibration sample set was too small.
2. Validation set BIAS is significant compared to the SEC/SEP
3. BIAS is insignificant but SEP is larger than two times SEL, usually due to significant sampling error

The following important step in calibration model development is to understand why it works. Why certain wavelengths, pretreatments and principal components were chosen. In that step, regression coefficients plots are observed, loading vectors, score plots and various other chemometric inspection tools available in common chemometric software packages. Calibration that has not been justified spectroscopically is very likely to fail when applied in routine analysis even though it has been properly validated.

1.4.3 Model Evaluation

Several parameters are used to judge the calibration performance. Many chemometric software packages offer automatic calibration development with implemented criteria to judge the quality of the developed calibration model. Nevertheless, manual observation of the figures of merit is often needed due to the particular variety and complexity of the analytical tasks.

1.4.3.1 Coefficient of Determination

Also termed total explained variation, this statistic described by equation 6, allows us to determine the amount of variation in the data that is adequately modeled by the calibration equation as a total fraction of 1. Thus $r^2 = 1.00$ indicates the calibration equation models 100% of the variation within the data, while an $r^2 = 0.50$ indicates that 50% of the variation in the difference between the actual values for the data points and the predicted or estimated values for these points are explained by the calibration equation (mathematical model), and 50% is not explained. r^2 values approaching 1.00 are attempted when developing calibration.

$$RSQ = r^2 = \left[\frac{\sum(x-\bar{x})(y-\bar{y})}{\sqrt{\sum(x-\bar{x})^2 \sum(y-\bar{y})^2}}\right]^2$$

Equation 6: Coefficient of Determination

1.4.3.2 Student`s t value

This statistic is used to determine of the correlation between X and Y data. It can be used to determine whether there is a true correlation between an NIR value and the primary chemical analysis for that sample. It is used to test the hypothesis that the correlation really exists and has not happened only by chance. A large t value indicates a real (statistically significant) correlation between X and Y.

When used for residuals, the test allows evaluating criteria for assessing the variation between an NIR value and its primary chemical value, and t values greater than 2.5 are considered significant and such predictions may possibly be outliers. Most often, high t- test values here indicate poor laboratory results or a problem with sample presentation and positioning.

1.4.3.3 Standard Error of Calibration

This statistic described by equation 7, is the standard deviation for the residuals due to differences between actual (primary wet laboratory analytical values) and the NIR predicted values for samples within the calibration set. It is an indication of the total residual error due to the particular regression equation to which it applies. The SEC will generally decrease with higher number of wavelengths (independent variable terms) used within an equation, indicating that increasing the number of terms will allow more variation within the data to be explained, or "fitted".

$$\boldsymbol{SEC} = \sqrt{\frac{\sum_{i=1}^{N}(x_i - y_i)^2}{N-1}}$$

Equation 7: Standard Error of Calibration

The SEC statistic is a useful estimate of the theoretical "best" accuracy obtainable for a specified set of wavelengths used to develop a calibration equation.

1.4.3.4 Standard Error of Prediction

The SEP is also termed the standard error of performance, is the standard deviation for the residuals due to differences between actual (primary wet chemical analytical values) and the NIR predicted values for samples outside of the calibration set. The SEP is calculated from equation 8 using validation instead of calibration samples. It allows for comparison between NIR-observed predicted values and wet laboratory values.

$$SEP = \sqrt{\frac{\sum_{i=1}^{N}(x_i - y_i - Bias)^2}{N-1}}$$

Equation 8: Standard Error of Prediction

The SEP is generally greater than the SEC but could be smaller in some cases due to chance alone. When calculating the SEP, it is critical that the constituent distribution be uniform and the wet chemistry be very accurate for the validation sample set. If these criteria are not met for validation sample sets, the calculated SEP may not have validity as an accurate indicator of overall calibration performance.

1.4.3.5 Root Mean Squared Error of Prediction

Root Mean Squared Error of Prediction is the measure of the total error of NIR method and is described by equation 9. It is the measure of both systematic (Bias) and random (SEP) measurement error. The relation between the RMSEP, Bias and SEP can be expressed by equation 10.

$$RMSEP = \sqrt{\frac{\sum_{i=1}^{N}(x_i - y_i)^2}{N}}$$

Equation 9: Root Mean Squared Error of Prediction

$$RMSEP = \sqrt{BIAS^2 + SEP^2}$$

Equation 10: Relation Between RMSEP, SEP and Bias

1.4.3.6 Standard Error of Cross-Validation

The calculation of SECV is a method for determining the "best" number of independent variables to use i n building a calibration equation. The SECV method is based on an iterative (repetitive) algorithm that selects samples from a sample set population to develop the calibration equation and then predicts on the remaining unselected samples. Some procedures for calculating SECV may calibrate using two-thirds of the samples while predicting on the remaining one-third of the

samples. The SECV is an estimate of the SEP and is calculated as SEP or SECV as the square root of the mean square of the residuals for N - 1 degrees of freedom, where the residual equals the actual minus the predicted value (equation 11).

$$SECV = \sqrt{\frac{\sum_{i=1}^{N}(x_i - y_i)^2}{N-p}}$$

Equation 11: Standard Error of Cross-validation

p - number of PCs

1.4.3.7 Standard Deviation

Standard Deviation is a measure of the dispersion of the population or a sample from an average value. In this work, it was used as a measure of the spread of the prediction residuals or the reference values (equation 12).

$$SD = \sqrt{\frac{\sum_{i=1}^{N}(x_i - \bar{x}_i)^2}{N-1}}$$

Equation 12: Standard Deviation

1.4.3.8 Standard Error of the Predicted y-value from each x in Regression

RSD_{yx} returns the standard error of the predicted y-value for each x in the regression. The standard error is a measure of the amount of error in the prediction of y for an individual x and is calculated according to equation 13.

$$RSDyx = \sqrt{\frac{1}{N-2}\left[\sum_{i=1}^{N}(y_i - \bar{y})^2 - \frac{\left[\sum_{i=1}^{N}(x_i - \bar{x})(y_i - \bar{y})\right]^2}{\sum_{i=1}^{N}(x_i - \bar{x})^2}\right]}$$

Equation 13: Standard Error of the Prediction

1.4.3.9 Ratio of Performance to Deviation

Ratio of performance to deviation (RPD) expresses the ratio of standard error of prediction to standard deviation of the parameter to be predicted (equation 14).

$$RPD = \frac{1}{\sqrt{1-RSQ}}$$

Equation 14: Ratio of Performance to Deviation

1.4.3.10 Predicted Residual Sum of Squares

This statistic calculates the error sum square (between predicted and reference values) as a function of the number of factors (eigenvectors, principal components or principal factors). The optimum number of PC is always given by the smallest number of PC where the PRESS function for the calibration and validation sets is approximately equal and minimal (equation 15).

$$\boldsymbol{PRESS} = \sum_{i=1}^{N}(x_i - y_i)^2$$

Equation 15: Predicted Residual Sum of Squares

1.4.3.11 Consistency

Consistency is described as the ratio of the Standard Error of Calibration and Standard Error of Prediction. SEC much higher than SEP indicates over-fitting of the model to the calibration samples.

1.4.3.12 Bias

This is the average deviation between the calibration and validation predictions, calculated from equation 16.

$$\boldsymbol{Bias} = \frac{\sum_{i=1}^{N} x_i - y_i}{N}$$

Equation 16: Bias

1.4.3.13 Regression Coefficient, Slope and Intercept

Absolute regression coefficient near 1.0 shows that two properties are linearly dependent. Slope should be as close as possible to 1.0 and intercept to 0 (equations 17-19).

$$r = \frac{\sum_{i=1}^{n}(y_i - \bar{y})(\hat{y}_i - \bar{\hat{y}})}{\sqrt{\sum_{i=1}^{n}(y_i - \bar{y})^2 \sum_{i=1}^{n}(\hat{y}_i - \bar{\hat{y}})^2}}$$

Equation 17: Regression Coefficient

$$a = \frac{n\sum_{i=1}^{n}(x_i y_i) - \sum_{i=1}^{n} x_i \sum_{i=1}^{n} y_i}{n\sum_{i=1}^{n} x_i^2 - \left(\sum_{i=1}^{n} x_i\right)^2}$$

Equation 18: Slope of the Regression Line

$$b = \frac{\sum_{i=1}^{n} x_i^2 \sum_{i=1}^{n} y_i - \sum_{i=1}^{n} x_i \sum_{i=1}^{n} (x_i y_i)}{n \sum_{i=1}^{n} x_i^2 - \left(\sum_{i=1}^{n} x_i \right)^2}$$

Equation 19: **Intercept of the Regression Line**

1.4.3.14 Significance of Bias

Standard Student`s t test for checking the significance of Bias calculated for a validation or test set, compared to SEP. If the t calculated is greater than the critical t value at the 95% confidence level, there is evidence that the bias included in the multivariate model is significant compared to SEP (equation 20).

$$\boldsymbol{Tobs\_bias = ABS}\left(\frac{\boldsymbol{Bias}}{\sqrt{\left(\frac{\sum_{i=1}^{N} (x_i - y_i)^2}{N(N-1)} \right)}} \right)$$

Equation 20: **Significance of Bias**

1.4.3.15 Significance of Slope

The test checks if the slope of the regression line is different from 1. It is based on the standard Student`s t test and is calculated according to equation 21.

$$\boldsymbol{Tobs\_slope = ABS(slope - 1)} \sqrt{\left((N-1) \frac{[SD(y_i)]^2}{[RSD_{yx}]^2} \right)}$$

Equation 21: **Significance of Slope**

1.4.3.16 Confidence Interval of Standard Error of Prediction

Test is based on the standard statistical F test and sets the confidence interval for the SEP. The interval is calculated based on the equation 22.

$$F\_sep = \boldsymbol{SEP\ (SECV) \times F_{critical}}$$

Equation 22: **Confidence Interval of Standard Error of Prediction**

1.4.3.17 Durbin-Watson Statistic

This statistic can be used to assess the lack of inter-correlation between data points in the regression. Since the correlation coefficient R only describes the tendency of the line, not the trueness of fit to a linear model. If there is no inter-correlation of the residuals described by the Durbin-Watson statistic, then a linear model is appropriate and may be used. A value closest to 2 indicates good linear correlation referenced and predicted values. The statistic is calculated according to equation 23.

$$\boldsymbol{dw} = \frac{\sum_{i=2}^{n}(e_i - e_{i-1})^2}{\sum_{i=1}^{n}(e_i)^2}$$ **Equation 23: Durbin-Watson Statistic**

1.4.3.18 Predicted Residual Sum Squared Over All Principal Components

X – PRESS - Predicted residual sum of squares expresses the summed up and squared difference between the pretreated spectrum and reconstructed spectrum (equation 24).

$$\textit{X-PRESS} = [\boldsymbol{pretreated\ s.} - (\boldsymbol{mean\ s.} + \boldsymbol{score_1} \times \boldsymbol{PC_1} + \cdots + \boldsymbol{score_i} \times \boldsymbol{PC_i})]^2$$ **Equation 24: X-PRESS**

1.4.3.19 Leverage

The concept of leverage in statistics is comparable to the physical model of a lever. The hinge for the calibration line lies at the center of the x-values. Calibration samples close to the mean of the x-values tend to exert little force on the slope of the calibration curve. Calibration samples farthest from the mean of the x-values can put forth a greater force on the slope of the calibration curve, so that their residuals are made as small as possible. Leverage plots can be used to find optimal factors or to detect outliers.

1.4.4 Method Validation

Validation of a calibration model is a crucial step that should take place prior to implementation of the method in a routine use. Many official monographs, standards, papers and published guidelines exist, directed both to NIR use in general, or specific for pharmaceutical release purposes. Of these, the most notable guidelines are through:

1. USP 30 NF 25, 2007 – Chapter 1119 - Near-infrared spectrophotometry
2. Chapter 1225 - Validation of compendia procedures EP and BP (BP 2007, EP 5.5)
3. Ph. Eur. method 2.2.40 - Near-infrared spectrophotometry
4. SC III F. Validation of analytical procedures
5. EMA - "Note for guidance on the use of near infrared spectroscopy by the pharmaceutical industry and the data requirements for new submissions and variations", 2003.
6. ICH guidelines - Q2 (R1) "Validation of analytical procedures: text and methodology"
7. PASG - Guidelines for the development and validation of near infrared (NIR) spectroscopic methods, 2001

In order to insure the quality and reliability of the data generated by the analytical method the following criteria should be met: validation of the software, validation of the hardware and validation of the NIR spectroscopic method (or any analytical method). NIR software and hardware manufacturers provide automated suitability tests using approved standards in order to validate NIR software and hardware.

The purpose of method validation is to determine the reproducibility of the developed calibration, its bias against a known method or target values and its long-term ruggedness (robustness). Although many guidelines and standards on the method validation exist, multivariate calibration model validation is still very complex task.

Method validation refers to the establishment of appropriate data and documentation to certify that the NIR multivariate method performs as intended. Once the instrument and software validation have been established, NIR method validation can be achieved by observing the points outlined below.
(FDA, 2005; European Medicines Agency, 2012; PASG NIR Subgroup, 2001).

1.4.4.1 Specificity

Specificity is the ability to assess unequivocally the analyte in the presence of components that are present in a sample/matrix. One of the difficulties in analysis of solid dosage forms by NIR spectroscopy is the fact the analysis is performed without extracting the analyte from the matrix. On the other hand, this fact makes NIR attractive because the dissolution/extraction step is not necessary.

NIR spectra represent all chemical species present in the formulation, including the sample physical attributes such as density, particle size, particle shape etc. This makes specificity one of the major validation issues to be overcome.

In the common chemometric software packages, there are various tools that could help in judging the specificity of the developed calibration model such as regression coefficient plots, loading plots, score plots, spectral residuals, etc.

1.4.4.2 Linearity

Linearity of NIR spectroscopic method is determined by calculating the correlation coefficients (r) of the NIR predicted values of the calibration or validation set with respect to reference values. Linearity assessment with r as single figure of merit is usually insufficient. Other supporting statistics is needed.

Durbin-Watson statistic can be used to assess the inter-correlation between data points in the regression. The Durbin-Watson statistic is checking if there are signs of nonlinearity, calculated from residuals obtained from fitting a straight line.

If successive residuals are positively serially correlated, that is, positively correlated in their sequence, d will be near zero. If successive residuals are negatively correlated, d will be near 4, so that 4 - d will be near zero. The distribution of d is symmetric around 2.

1.4.4.3 Range

The ICH guidelines recommend a minimum range of 80% to 120% of the nominal/target value for the assay of a drug substance or a finished product and 70% to 130% of the test concentration for content uniformity.

Production samples are spanning normally very narrow drug content range which brings the need for out-of-specification samples to extend the range to the requited one. The major problem is the fact that it is very difficult if not impossible, to provide out-of-specification products in the production environment. Out-of-specification samples could be manufactured in laboratory or pilot plant. Although the identical raw materials are used, the process signature is often significantly different from laboratory to pilot scale to production that significant calibration model errors will arise.

1.4.4.4 Robustness

The robustness of an analytical method is its ability to perform without significant changes when the small, deliberate variations in the environmental, instrumental, or procedural conditions as well as sample changes are introduced. Method developers should consider tests to evaluate the method/model stability during the development and validationprocess.

In case of NIR analysis of solid dosage forms, this issue is of prime importance. The variation in physical parameters as a result of small process variability, e.g., change in pre-compression, compression force or tableting speed, can introduce significant prediction errors if not considered during method development phase.

The evaluation of robustness should be considered during the development phase and depends on the type of procedure. It should show the long-term reliability of a method with respect to deliberate variations in method parameters.

1.4.4.5 Accuracy

The accuracy of an analytical procedure expresses the closeness of agreement between the values which are accepted either as true values or reference values and the values found (trueness). There are several methods of determining accuracy (ICH 2005):

1. Application of the analytical procedure to synthetic mixtures of the drug product components to which known quantities of the drug substance to be analyzed have been added.
2. Comparison with the results obtained from a second, standard analytical method whose accuracy is defined.
3. Accuracy may be inferred once precision, linearity and specificity have been established.

1.4.4.6 Precision

Precision of analytical procedure describes how close is the agreement between a series of measurements obtained from multiple sampling of the same homogenous sample under the prescribed conditions. The precision of an analytical procedure is usually expressed as the variance, standard deviation or coefficient of variation of a series of measurements and can be described in terms of:

1.4.4.6.1 Repeatability

This is precision under the same operating conditions over a short interval of time. Repeatability is assessed using minimum of 9 determinations covering the specified range for the procedure,e.g., 3 concentrations with 3 replicates each or minimum of 6 determinations at 100% of the nominal content.

1.4.4.6.2 Intermediate precision

Intermediate precision expresses within-laboratories variations and reflects the effects of random events on the precision of the analytical procedure. Typical variations to be studied include days, analysts, equipment, etc.

1.4.4.6.3 Reproducibility

Reproducibility describes the precision between laboratories usually applied in order to standardize the analytical procedure/method.

1.4.4.7 Detection and quantification limits

The detection limit of an individual analytical procedure is the lowest amount of analyte in a sample which can be detected but not necessarily accurately quantified, while the quantification limit is the lowest amount of analyte in a sample which can be quantitatively determined with suitable precision and accuracy.

1.5 Sources of Error in NIR Spectroscopy

Error in NIR measurements comes from various different sources which could be assigned to three main categories:

1. Sampling Error
2. Reference Method Error
3. NIR Method Error

1.5.1 Sampling Error

Sampling error is usually the biggest source of error in NIR measurements. This is especially true due to the fact that the instrumentation today is very advanced, allowing very accurate and precise measurements. Sampling error is caused by the lack of homogeneity of the analyzed material. If the three powder subsamples are withdrawn from one kilogram of the well mixed powder, the amount of moisture that is measured by some analytical technique will differ between the subsamples. The difference comes from the error associated with the analytical technique but, as well, from the differences in the subsamples themselves. The actual difference between the subsamples will dictate the lower limit that could be reached for the SEC of the NIR calibration model developed on these samples (subsamples). Sampling errors occur at several steps of the calibration or validation process:

- Reference and NIR method usually analyze different subsamples
- The methods are usually looking at the different amounts of material. If one method is using four times more material than the other method, it will have around half of the sampling error of the second method.
- The NIR measurement can introduce a sampling error due to the fact that only up to 2 mm of the samples is scanned in the diffuse reflectance measurement mode whereas, in diffuse transmittance, the light penetrates throughout the whole sample (assuming that the samples is transparent for NIR light). The difference in the predicted values in this case could be considered primarily as a sampling error.

It is usually very difficult to measure accurately all the sampling errors in one analytical procedure but it is certainly very important to know in which steps of the procedure the sampling error is significant and to which extent it contributes to the overall sampling error. With this knowledge, one can know where in the procedure to repeat the sampling.

1.5.2 Reference Method Error

Every reference method has certain measurement error. The error of the reference method is commonly called Standard Error of Laboratory (SEL). It is defined as the standard deviation of the differences between measurements of duplicate samples. It can be determined as intermediate precision or reproducibility. If this is not possible, the repeatability of the reference method could be useful estimation as well. SEL is used for comparison and evaluation of the precision of the NIR method. SEL is compared with SEP of the validation or test set. The precision of the developed NIR calibration model is acceptable if the SEP is 1.4 – 2.0 times higher than SEL. This is, of course, the empirical rule that could be found in literature but should not limit the use of NIR, i.e., if the SEP is more than 2 times larger than SEL, the developed NIR calibration model could be still used if the magnitude of the SEP fulfills the requirements/specifications of the user for particular application.

1.5.3 NIR Method Error

This type of error is caused by the spectral measurement errors, lack of intrinsic correlation between NIR and reference method data and finally, from the poor or wrong choice of the data treatments (spectral pretreatments, regression methods, selection of factors and variables, etc.). NIR Instrument related errors are usually far below the sampling error level. Still, there is certain error contribution from the spectral noise that could originate from the imperfections in the detector response or the suboptimal NIR sampling geometry. NIR instrumentation design has advanced in the last few decades but the errors originating from x axis instability (repeatability/reproducibility of the wavelength) and the y axis instability (variations in the detected light intensity) could be significant in comparison to the sampling error. Rounding error and error associated with the use of smoothing algorithms in the commercially available chemometric software packages could contribute to the overall error as well (Shenk J. S. et al., 2001).

1.6 Design of Experiments Methodology

1.6.1 Experimental Design

Experimental design is how to conduct and plan experiments in order to extract the maximum amount of information from the collected data in the presence of noise. The basic idea is to vary all relevant factors simultaneously, over a set of planned experiments, and then connect the results by means of a mathematical model. This model is then used for interpretation, predictions and optimization.

1.6.2 Objectives of Experimental Design

During the investigation the following questions need to be answered:
Which factors have a real influence on the responses (results)?
Which factors have significant interactions (synergies or antagonism)?
What are the best settings of the factors to achieve optimal conditions for best performance of a process, a system or a product?
What are the predicted values of the responses (results) for given settings of the factors?
An experimental design can be set up to answer all of these questions.

1.6.3 Screening Designs

Screening is the first stage of an investigation where the goal is just to identify the important factors. An important factor is a factor that causes substantial changes (effects) in the response when it varies. In the screening stage one uses simple models (linear or linear with interactions), and experimental designs that allows the identification of the factors with the largest effects in the fewest possible number of experimental runs.

Examples of such designs supported by *MODDE* software that was used in this research are: Full Factorial, Fractional factorial, L-designs, Plackett Burman, Rechtschaffner, Onion, and D-optimal designs for screening experiments.

1.6.4 Response Surface Modeling

After screening, the goal of an investigation is usually to approximate the response by a quadratic polynomial (model) in order to:

- Understand in more detail how the factors influence the response; get a map of the system.

- Make predictions, optimize or find a region of operability.

Examples of such designs are*:* Three-level full factorial, central composite, (CCC and CCF), Box Behnken, Rechtschaffner, Doehlert, Onion, and D-optimal designs for RSM investigations.

1.6.5 Fit Methods

The data collected by the experimental design is used to estimate the coefficients of the model. The model represents the relationship between the response Y and the factors X1, X2, etc.

MODDE software uses multiple linear regression (MLR) or Partial Least Squares (PLS) to estimate the coefficients of the terms in the model. PLS is suggested when the investigation has a high condition number.

1.6.5.1 Multiple Linear Regression

With Multiple Linear Regression the coefficients of the model are computed to minimize the sum of squares of the residuals, i.e. the sum of squared deviations between the observed and fitted values of each response. The least squares regression method yields small variances for the coefficients and small prediction errors. It is important to note that MLR separately fits one response at a time and hence assumes them to be independent.

1.6.5.2 Partial Least Squares

PLS deals with many responses simultaneously, taking their covariances into account. This provides you with an overview of how all the factors affect all the responses.

PLS contains the multiple regression solution as a special case, i.e. with a single response or different models, and a given number of PLS dimensions, the PLS regression coefficients are identical to those obtained by multiple regression.

PLS finds the relationship between a matrix Y (response variables) and a matrix X (model terms).

The PLS model consists of a simultaneous projection of both the X and Y spaces on a low dimensional hyper plane with new coordinates T (summarizing X) and U (summarizing Y), and then relating U to T.

This analysis has the following two objectives:

1. To well approximate the X and Y.
2. To maximize the correlation between X and Y in the projected space (between u and t).

The dimensionality, number of significant PLS components, is determined by cross validation (CV), where PRESS (Predictive Residual Sum of Squares) is computed for each model dimension. Software MODDE selects automatically the number of PLS dimensions that give the smallest PRESS. PRESS is then re expressed as $Q^2 = (1 - PRESS/SS_Y)$, where SS_Y is the sum of squares of Y.

1.6.6 Results

Both MLR and PLS computes regression coefficients for each response. Thus Y is expressed as a function of the X's according to the selected model (i.e. linear, linear plus interactions, or quadratic).

1.6.7 D-Optimal Designs

D-Optimal designs are computer generated designs, tailor made for a specific problem. They allow great flexibility in the specifications of the problem. They are particularly useful when one wants to constrain the region and no classical design exists.

"D-Optimal" means that these designs maximize the information in the selected set of experimental runs with respect to a stated model.

D-Optimal designs are constructed by selecting N runs from a candidate set. This candidate set is the discrete set of "all potential good runs".

Software MODDE generates the candidate set as follows:

For a regular process region, the candidate set consists of one or more of the following sets of points (depending on your model and the number of factors):

- The full factorial for up to 10 factors, reduced factorial for up to 32 factors.
- Centers of edges between hyper-cube corners
- Centers of the faces of the hyper-cube.
- Overall centroid

For constrained regions of mixture and/or process factors, the candidate set consists of one or more of the following set of points:

- The extreme vertices of the constrained region
- The centers of the edges
- The centers of the various high dimensional faces
- The overall centroid.

MODDE has implemented an algorithm to compute the extreme vertices, center of edges, center of faces etc. as described by Piepel (1988).

1.6.8 Model Evaluation

1.6.8.1 Variation Explained by the Model

R^2 is the percent of the variation of the response explained by the model. R^2 is a measure of fit, i.e. how well the model fits the data.
A large R^2 is a necessary condition for a good model, but it is not sufficient. One can have poor models (models that cannot predict) with a large R^2. This is particularly true when you have few degrees of freedom for the residuals.
R^2 is usually poor when the reproducibility is poor (poor control over the experimental error) or poor Model validity (the model is incorrect).

1.6.8.2 Response Variation Predicted by the Model

Q^2 is the percent of the variation of the response predicted by the model according to cross validation. Q^2 tells how well the model predicts new data. A useful model should have a large Q^2
Q^2 is usually poor when the reproducibility is poor (poor control over the experimental error) and/or poor Model validity (the model is incorrect).
When the R^2 is good, model validity moderate, and a design with many degrees of freedom of the residuals, then a poor Q^2 is usually due to insignificant terms in the model.
If there are many correlated Y's (responses), one should only remove the terms insignificant to all the Y's.

1.6.8.3 Model Validity

This is a measure of the validity of the model. When the Model Validity is larger than 0.25, there is no lack of fit of the model (the model error is in the same range as the pure error).
A Model Validity of 1 represents a perfect model.
When the Model Validity is less than 0.25 there is a significant lack of fit and the model error is significantly larger than the pure error (reproducibility).

1.6.8.2 Reproducibility

This is the variation of the response under the same conditions (pure error), often at the center points, compared to the total variation of the response.
Reproducibility = 1 - (MS (Pure error) / MS (total SS corrected))

MS = Mean squares, or Variance.

When the Reproducibility is 1, the pure error is 0. This means that under the same conditions the values of the response are identical.

When the Reproducibility is 0, the pure error equals the total variation of the response.

If the reproducibility is below 0.5, there is a large pure error, poor control of the experimental set up (the noise level is high), and the validity of the model needs to be assessed. This results in low R^2 and Q^2.

1.6.9 The Coefficient Plot

It displays the regression (MLR) or PLS coefficients with confidence intervals.

MODDE software displays the coefficient plot with centered and scaled data. The scaling of the data makes the coefficients comparable. The size of the coefficient represents the change in the response when a factor varies from 0 to 1, in coded units, while the other factors are kept at their averages.

The coefficient is significant (different from the noise), when the confidence interval does not cross zero (Eriksson L., 2008)

1.7 Pharmaceutical Tableting

Tablets are solid preparations containing a single dose of one or more pharmaceutical active ingredients (APIs) and obtained by compressing powders or granulated materials. One of the definitions of the tablets stated by British Pharmacopoeia is: "Tablets are solid dosage forms circular in shape with either flat or convex faces and prepared by the compression or compaction of suitably prepared medicament by means the tablet machine". Tablets are intended for oral administration. They are usually swallowed as a whole, some are chewable, some dissolved or dispersed in water before being applied and some are retained in the mouth where the $API_{(s)}$ is released.

Tablets are the most common and inexpensive dosage forms. They are prepared by forcing particles into close proximity to each other by compaction process, which enables the particles to cohere into a solid specimen. The compaction process takes place in a die of the tablet press, whereby upper and lower punches are applying compressive force on the powder bed or granulated material. Intermolecular bonds are formed between the particles when the compression force is applied and this provides the coherence to the powder, i.e., tablet is formed.

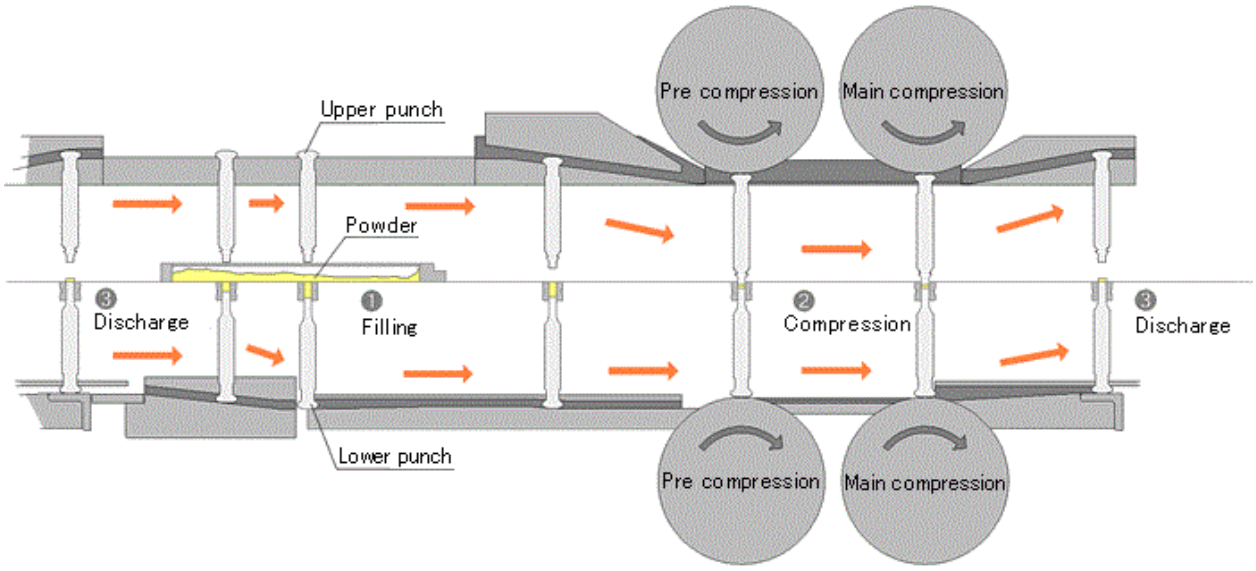

Figure 9: Stages of tablet manufacture

Irrespective of the press type used, a complete tablet manufacturing cycle occurs in the following steps described in figure 9: (i) the die is filled and adjusted (scraped), (ii) the tablet is compacted, and (iii) the tablet ejected from the die. (Levin M., 2001; Sinka I. C. et al., 2009; Marshall K., 1963).

1.7.1 Compaction Mechanisms

The compaction process consists of a series of phases starting from particle rearrangement, particle deformation and finally formation of inter-particulate bonds. When the compression force is applied to the powder bed, the volume of the powder in a dye is being reduced. The particles become closer to each other. At certain point, further reduction in compact volume results in deformation of the particles. Particle deformation can be elastic, viscoelastic, plastic or brittle. Elastic deformation has reversible character whereas plastic deformation is irreversible. Particle fragmentation characteristic for brittle substances results in smaller particles which further decreases the compact volume. As a consequence of the particles being in closer proximity, inter-molecular bonds will be formed. Three types of bonds could be formed between the particles during the compaction process: mechanical interlocking between particles with irregular shape, inter-particulate attraction forces (Van der Waal forces, hydrogen and electrostatic forces) and melting solid bridges. It should be bear in mind that all materials show certain degree of elastic, plastic or brittle behavior. Which deformation behavior will predominate depends on the parameters such as temperature or compaction rate (Sheikh-Salem M. and Fell J. T., 1981).

1.7.2 Tablet Formulation

Excipients as inactive substances play a major role in formulation development apart from active pharmaceutical ingredients (table 1). Pharmaceutical excipients are substances other than the pharmacologically active drugs or pro-drugs which are included in the manufacturing process or are contained in a finished pharmaceutical dosage form.

In addition to transporting the API to the site in the body where the drug is intended to exert its action, excipients play an important role in the manufacturing process. They may also be important for keeping the drug from being released in places in organism where it could damage the sensitive tissue and create gastric irritation or stomach upset.

Other excipients promote the tablet disintegration into particles small enough to reach the blood stream more quickly and some are increasing the API stability. In addition, some excipients are used to aid the identification of a drug product.

Some excipients are used to improve the product taste and appearance. This improves patient compliance, especially in case of children. Although excipients are pharmacologically inactive, they are essential components of a modern drug product. In many products, excipients make up the bulk of

the total dosage form. Apart from the API, other essential components include diluents or fillers, binders, disintegrants, lubricants and coloring agents. Diluents or fillers are inert ingredients that can significantly affect the chemical and physical properties of the final tablet thus affecting the biopharmaceutical profile (Kesavan J. G. and Peck G. E., 1996).

Table 1: Common Excipients used in Tablet Formulations

Common excipients used in tablets		
Excipient	**Function**	**Examples**
Diluents	Provide bulk and enable accurate dosing of potent ingredients	Sugar compounds e.g. lactose, dextrin, glucose, sucrose, sorbitol Inorganic compounds e.g. silicates, calcium and magnesium salts, sodium or potassium chloride
Binders, compression aids, granulating agents	Bind the tablet ingredients together giving form and mechanical strength	Mainly natural or synthetic polymers e.g. starches, sugars, sugar alcohols and cellulose derivatives
Disintegrants	Aid dispersion of the tablet in the gastrointestinal tract, releasing the active ingredient and increasing the surface area for dissolution	Compounds which swell or dissolve in water e.g. starch, cellulose derivatives and alginates, crospovidone
Glidants	Improve the flow of powders during tablet manufacturing by reducing friction and adhesion between particles. Also used as anti-caking agents.	Colloidal anhydrous silicon and other silica compounds
Lubricants	Similar action to glidants, however, they may slow disintegration and dissolution. The properties of glidants and lubricants differ, although some compounds, such as starch and talc, have both actions.	Stearic acid and its salts (e.g. magnesium stearate)
Tablet coatings and films	Protect tablet from the environment (air, light and moisture), increase the mechanical strength, mask taste and smell, aid swallowing, assist in product identification. Can be used to modify release of the active ingredient. May contain flavors and colorings.	Sugar (sucrose) has now been replaced by film coating using natural or synthetic polymers. Polymers that are insoluble in acid, e.g. cellulose acetate phthalate, are used for enteric coatings to delay release of the active ingredient.
Coloring agents	Improve acceptability to patients, aid identification and prevent counterfeiting. Increase stability of light-sensitive drugs.	Mainly synthetic dyes and natural colors. Compounds that are themselves natural pigments of food may also be used.

1.7.3 Factors Affecting Tableting Process

Compaction process is affected by numerous factors. Factors can be related to formulation of the product, equipment/process or to the environment. Below are listed and briefly explained the most significant factors affecting compressibility and compactibility of the granulated materials.

1.7.3.1 Crystalline Form

Polymorphism, pseudo-polymorphism, and the crystal ordering of APIs and excipients are affecting their densification behavior and the final compact attributes. Crystalline materials usually undergo brittle fragmentation whereas amorphous materials undergo plastic deformation (Sun C. and Grant D. J. W., 2001).

1.7.3.2 Porosity and Bulk Density

The relative density and porosity vary largely among pharmaceutical materials. These factors may change significantly during processing. The initial porosity determines the extent to which the porosity can be reduced during compression step in a certain tablet press. Porosity of the granules themselves also influences the compressibility behavior. Increase in granule porosity results in increase of the compressibility (Berggren J. and Alderborn G., 2001).

1.7.3.3 Particle Size and Shape

Particle size, shape and particle size distribution are important determinants of the deformation behavior of pharmaceutical granulated materials. Increasing the irregularity and roughness of granules changes the compaction behavior from plastic deformation towards a more complex process including fragmentation and attrition of the particles. Compressibility is generally better if the particle size is larger due to a greater degree of densification. This is attributed to increased frictional and cohesive forces associated with the smaller size range; which tends to restrict particle flow and thus reduce densification (Sun C. and Grant D. J. W., 2001).

1.7.3.4 Pre-compression and Compression Force

Compression force is the major factor influencing densification process. The compression force rate affects the way particles deform and also determines to high extent the integrity (crushing strength) of the formed compact. There is a positive correlation between compression force and compactibility

of the granulated material up to a certain threshold beyond which either the crushing force of the compact remains unchanged, decreases or results in manufacturing problems like capping or lamination. Pre-compression force usually increases the integrity of the compact by promoting the particle rearrangement and excluding the entrapped air in the powder bad. The effect of the pre-compression force on the mechanical properties of the final compact is formulation dependent (Stiel D. M, 1978; Vezin W. R. et al., 1983).

1.7.3.5 Tableting Speed

Some pharmaceutical materials show time-dependent compaction properties and the nature of this time dependency is related to the compaction mechanism of a given material. Viscoelastic or viscoplastic materials show higher speed sensitivity (time dependent compaction properties). Brittle materials are much less speed dependent. Particle size and particle size distribution of the powders or granules have also an important role in the speed sensitivity due to their effect on the deformation mechanism. Speed sensitivity of pharmaceutical materials effects significantly final tablet attributes. The effect of punch velocity is particularly significant when the tableting process is transferred from single punch laboratory tablet press to pilot or production rotary tablet press. Materials that exhibit plastic deformation upon compaction tend to show decrease in tablet crushing strength when the tableting speed is increased. Capping or lamination might occur as well (Tye C. K. et al., 2005).

1.7.3.6 Formulation Factors

Fillers, compression aids or binders bind the tablet ingredients together giving form and mechanical strength to the compact. These substances are mainly natural or synthetic polymers e.g. starches, sugars, sugar alcohols and cellulose derivatives. The development of direct compression as an alternative method to wet granulation has stimulated the development of the fillers and binders used in direct compression tableting. Addition of compression aid component to a tablet formulation changes the surface properties of the coarse compound particles as they are covered by the small compression aid particles. It was proposed that this surface coverage increases the surface area available for inter-particulate bonding, thus increasing the number of bonds and also possibly creating stronger bonds, with a subsequently increased mechanical strength.

Lubricants are added to tablet formulations to reduce die-wall friction but are also improving flow properties of the granulated materials. The amount of lubricant in formulation and the duration of mixing a lubricant are affecting flow properties, deformation behavior, crushing strength and drug release properties. It is well known that increase in lubricant concentration in a tablet formulation

results in tablet crushing strength decrease. This effect is attributed to a decrease in the degree of cohesiveness between the particles as well as decrease of friction effects at the punch faces and die-wall.

Glidants are improving the flow properties of granulated materials by decreasing surface roughness of the particles by forming a uniform coating around them. Some glidants are acting as physical barrier between particles which reduces attractive forces between them. Finally, some glidants are absorbing moisture from the surface of the particles and improving the flow properties in that way (Lin S. Y., 1988).

1.7.3.7 Moisture

Moisture affects powder flow and compactibility as well as physical - chemical and microbiological stability of the pharmaceutical powders and granules. Water molecules can form hydrates or pseudo-hydrates when they are incorporated into the solid`s crystalline structure. The other way of interacting with solids is when the water is absorbed at the surface of the solid or into the material acting as a plasticizer which is common in case of amorphous or semi-crystalline substances. Absorbed moisture increases the compactibility especially in case of polymeric substances by facilitation of the temporary transition of material from glass to rubbery state (Sebhatu T. et al., 1994).

1.7.4 Tablet Presses

1.7.4.1 Eccentric tablet presses

Eccentric tablet presses use an eccentric shaft connected to a rotating wheel to control the displacement of the upper punch (figure 10). Displacement rate is controlled by adjusting the rotation rate of the eccentric wheel. Lower punch is stationary during the compaction and has the function to enable uniform die filling with the granulated material and ejection after the compact is formed. In case of eccentric tablet presses compaction process is single-sided whereas with rotary presses it is double-sided.

Figure 10: Eccentric tablet press

1.7.4.2 Rotary Tablet Presses

Rotary presses have high output rate of tablet production (figure 11). They operate with a number of sets of dies and punches. The dies are mounted on the die table and both rotate together during operation of the tablet machine. Punch movement is controlled by tracks that pass over cams and rolls are controlling the volume of powder that is fed into the die and the pressure applied during compaction. Powder is stored in a hopper whose lower opening is located right above the die table.

The powder flows freely and is fed into the die by a feed frame. Both punches are involved in compaction process.

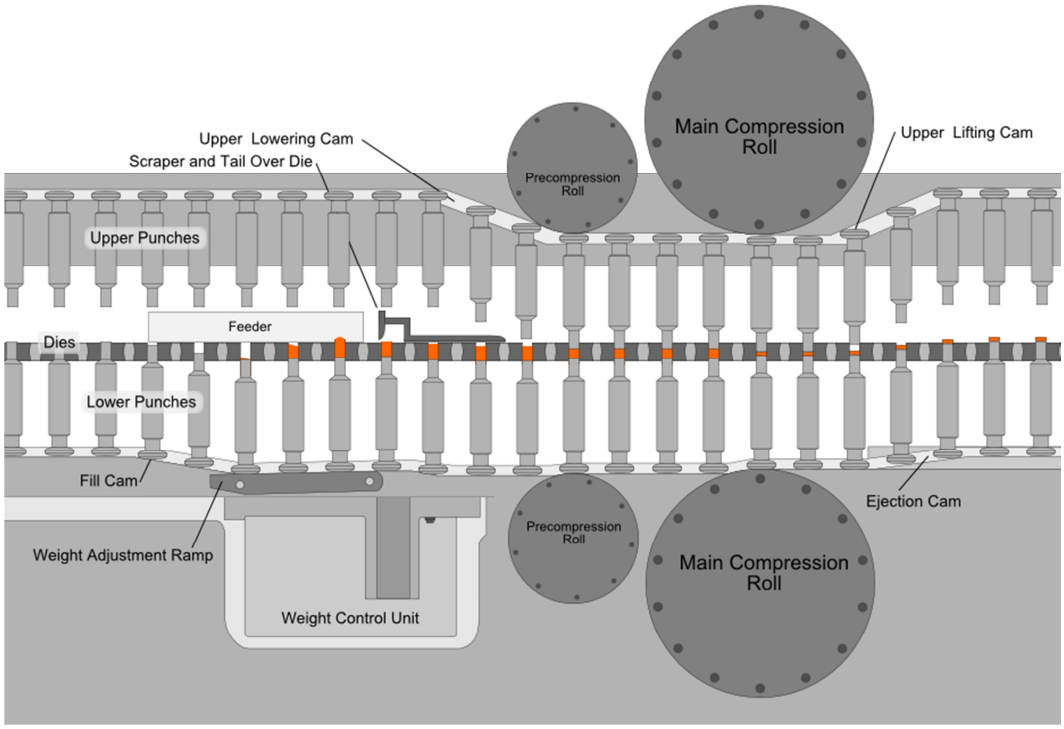

Figure 11: Rotary tablet press

1.7.5 Direct - compression Tableting

Direct compression, in contrast to tableting process which involves granulation as a unit process, consists of fewer operations of the powder treatment. Direct compression tableting involves two operations, powder mixing and tableting. Direct compression reduces the production costs in comparison to the process that involves granulation. Direct compression formulations require the use of fillers and binders with special properties compared to traditional ones. Stability of the tablets manufactured by direct compression method is usually better since heating and water are not involved in production process. Release of the drug substance from the direct compression formulations is generally faster since the tablets disintegrate into primary particles.

In order to apply direct compression a powder needs to have acceptable flowability and bulk density as well as large enough particles which could be a technological problem. Large particles could be difficult to mix to acceptable homogeneity and such particulate systems may be prone to segregation. Compactibility of the powder mixture is certainly the critical characteristic which highly depends on the drug load since the APIs are usually poorly compactible. When simplicity of the formulation and processing is taken into account, direct compression tableting is certainly the tableting method of choice and is applied as well in this research (Kanig J. L., 1975).

1.7.5.1 Powder Compressibility Assessment

In the third project of the thesis, the compaction results have been fitted using Heckel-Plot (Heckel, 1961; Heckel, 1961), the modified Heckel-Plot (Kuentz, et al., 2000) and the Leuenberger equation (Leuenberger et al., 1984; Leuenberger, 1982).

Heckel- Plot

Heckel – Plot is the most commonly used equation in the pharmaceutical compaction studies. It was published by R.W. Heckel in 1961 (Heckel, 1961; Heckel, 1961). In this equation, the first-order kinetics type of reaction behaviour of the voidage reduction with applied pressure has been explained.

$$\ln\frac{1}{1-D}=k\cdot P+A \qquad 1$$

where D is the relative density of a powder compact at pressure P. Constant k is a measure of the plasticity of a compressed material. The Constant A is related to the die filling and particle rearrangement

before deformation and to a bonding of the discrete particles.

Modified Heckel- Plot

The pressure susceptibility (χ_p) is defined as the decrease of porosity under pressure. This term is assumed to be constant in Heckel-Plot. Kuentz and Leuenberger (Kuentz, et al., 2000) incorporated the pressure susceptibility term in the equation and developed a modified Heckel-Plot:

$$\sigma = \frac{1}{c}\left[\rho_c - \rho - (1-\rho_c)\cdot \ln\left(\frac{1-\rho}{1-\rho_c}\right)\right]$$

Where ρ is the relative density, σ is the pressure, ρ_C is the critical density and C is a constant, which represents the compressibility of a powder.

For the powder compressibility calculation, the constant K from Heckel equation and the constant C from the modified Heckel equation can be determined.

Well compressible, ductile and soft powders have higher C and K values compared to poorely compressible, brittle and hard powders.

The parameter ρ_c is defined as rigidity threshold. It represents the critical relative density, producing a negligible mechanical resistance between the punches. With a geometrical focus, this threshold represents the transition point between dispersed solid in air and voids in a solid matrix.

Leuenberger Equation

This equation was developed and published in the early 1980s by H. Leuenberger (Leuenberger, et al., 1984; Leuenberger, 1982).

$$\sigma_t = \sigma_{t\max}\cdot(1-e^{-\gamma\sigma p_r})$$

σtmax is the tensile strength (kg/cm^2) when P (compression pressure) $\rightarrow \infty$, ρr $\rightarrow$ 1, and γ is compression susceptibility, characterizing the compressibility of the powder.

This equation describes the powder compressibility and in a second step the compactibilty, defined as the ability of the powder to be compressed to a tablet of a specific strength. Each of the three equations contain a factor which characterizes the compressibility of the powder. By fitting the measured and calculated compaction data to the three equations, the above mentioned technical factors (k, C, γ) can be calculated and evaluated.

1.7.6 Compaction simulators

Besides instrumented tablet presses, compaction simulators can be used for the investigation of the compaction process. All compaction simulators have load frame, hydraulic unit and data acquisition system. There are many variables of a tableting process which could be simulated. Compaction forces, punch velocity, tableting speed, dwell time, relaxation, etc. Usually small amount of powder is used for investigation of the feeding setup in a compaction simulator which makes it difficult to simulate the powder supply in an industrial press (Celik M. and Marshall K., 1989).

1.7.6.1 Presster™

Presster is a linear tablet press simulator. It offers many advantages of a conventional compaction simulator such as ease of use and flexibility. Presster was developed by Metropolitan Computing Corporation Inc. NJ, USA in the late 1990s and has the ability to simulate almost all commercially available rotary tablet presses (figure 12). The main feature of the Presster is that it uses the compression rolls of the same dimensions as those of the simulated tablet press. In that way, the compression profiles resemble closely those of the simulated tablet press.
The design resembles a single station rotary press with all its parts with the difference that the movement of the single station is not circular but linear instead. Main instrumentation sensors are on the pair of punches and one die. A turret-analogue carriage with the tooling set is the central part of the machine. This carriage is driven horizontally through the machine. It passes the dosing cam, the upper and lower rollers of the pre-compaction, the roller set of the main compaction station, ending at the ejection cam and the take-off bar. The instrument functions by measuring the position of a core rode inside the cylinder relative to a predefined position. The resulting voltage is proportional to the object displacement.

Presster is connected to an electronic data acquisition system governed by the software which allows all the experimental parameters to be set on a personal computer. In this way, parameters like gap, compaction force, dwell time, ejection angle, could be adjusted fast and easy, allowing the operator to investigate the influence of these parameters on the resulting tablet (Neuhaus T., 2007).

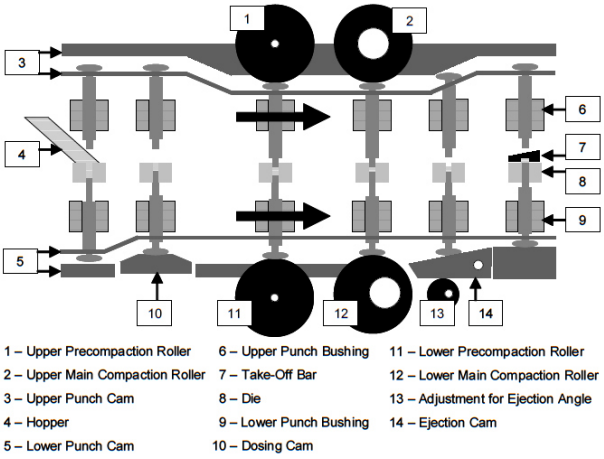

Figure 12 : Schematic view of the Presster™

2. Results and Discussion

2.1 Research Project I: Effect of Simulated Precompression, Compression Pressure and Tableting Speed on an Offline Diffuse Transmittance and Reflectance Near-infrared Spectral Information of Model Intact Caffeine Tablets

2.1.1 Introduction

Near infrared Spectroscopy (NIRS) is fast and non-destructive analytical technique based on the measurements of the absorbed radiation spanning the spectral range of $780 - 2500\ nm$ ($12{,}800 - 4000\ cm^{-1}$). NIRS is used in the cases where multicomponent analysis is required in the presence of interfering substances. The near infrared spectra consist of overtones and combination bands of the fundamental molecular absorptions found in the mid infrared spectral range. Near infrared spectra consist of overlapping vibrational bands that may appear non-specific and poorly resolved and for that reason, chemometric data processing methods are commonly applied to calibrate for qualitative or quantitative analysis. Ease of use, speed and no requirement for sample preparation make this technique an excellent process analytical technology (PAT) tool. In line with the quality by design (QbD) concept, NIRS as one of the major PAT tools, plays an important role in real-time release testing and in that way minimizes the overall drug product quality risk and increases the productivity by shortening the production cycles.

Q8 guideline on pharmaceutical development from International Conference on Harmonization (ICH) suggests a careful risk assessment of the variables such as raw material attributes, process parameters, environmental conditions, analytical method characteristics, etc., on the critical to quality attributes (CQAs) of the final drug product (figure x). As analytical method being one of the important variables of the overall quality risk assessment matrix, it is important to insure the complete understanding of the factors influencing its performance. NIRS applications in pharmaceutical industry are most often based on the statistical correlations and predictions of the parameters of interest rather than on direct determination. Another feature of the NIRS analysis of the solid dosage forms is the fact that the physical attributes of the sample such as particle size, density, hardness, or porosity, dominate the NIR spectrum. Physical attributes of the sample are determined by the formulation and the manufacturing process factors. Formulation of the drug product is mostly constant over time but the

manufacturing process factors and its effect on the NIR spectrum of the drug product need to be well understood and controlled.

Specificity of analytical method is a characteristic and a validation parameter determined at the onset of method development process in the course of a feasibility study. It needs to be demonstrated that the signal that originates from the analyte can be distinguished from the matrix and that the analytical technique is adequate for the intended purpose. The other critical validation parameter is the analytical method robustness. Robust method needs to be able to provide stable measurements over extended period of time with all possible variations of environmental and process conditions as well as small, deliberate changes in the analytical procedure itself. Robustness needs to be inherently built into an NIR method during the development phase. Systematic and science-based study of the factors influencing NIR spectral response and performance of the NIRS method at the onset of the development phase is critical to enable long-term stability of the method and to lower-down the overall risk to the drug product quality. In the development of the robust calibration models, in this study, the global calibration model approach was accepted. In the case of conventional method development and validation, robustness is frequently assessed after the method has been developed, and may not be built in during method development (PASG NIR Subgroup, 2001). This may increase the overall risk to the drug product quality.

Instead of most frequently used empiric approach to defining the critical factors affecting NIR spectral response and calibration model performance, systematic and science-based approach such as design of experiments (DoE) is suggested to be used at the onset of method development in accordance with the ICH Q8 and Q9 guidelines. All the process, formulation, environmental and NIR acquisition parameters that affect the NIR method performance should be identified and included in the NIRS method development from the outset. These factors should be treated as a potential risks to the quality of the final drug product and as such, included in the quality risk assessment matrix (figure 13).

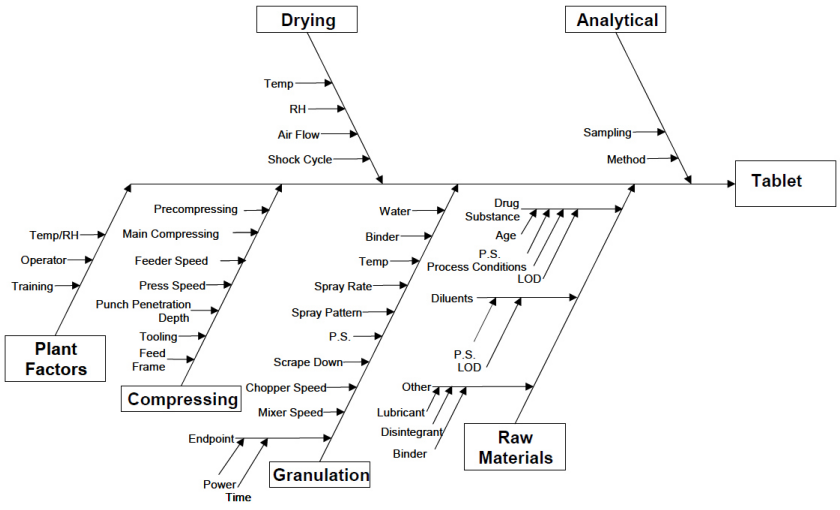

Figure 13: Fishbone diagram with the variables influencing the quality of a tablet

2.1.2 Reports - NIRS Applications in Pharmaceutical Industry

Near-infrared spectroscopy has gained a lot of attention in the pharmaceutical industry in the last two decades (Luypaert, J. et al., 2007). Numerous applications have been reported among which identification of raw materials is the most common one (Gemperline et al., 1987; Candolfi, A., et al., 1999; Blanco M. et al., 2001). Quantification of pharmaceutical active ingredients in different pharmaceutical products has proven its usefulness in the latest decade (Blanco M. et al., 2006; Blanco M. et al., 1996; Chalus P. et al., 2007; Mantanus, Jérôme, et al. 2010). NIRS in monitoring powder blending process is becoming an efficient PAT tool to ensuring solid dosage form uniformity in pharmaceutical industry (Moes, J. et al., 2008; Sulub Y. et al., 2009; Lyon, Robbe C., et al., 2002; Ely D. et al., 2006). Determination of tablet hardness by NIR spectroscopy was shown to be an alternative to conventional tablet hardness testing (Morisseau K. M. et al., 1997; Donoso M. et al., 2003). NIRS coupled with PLS and artificial neural networks, was proven be a useful tool to monitor average particle size in real-time (Santos A. F. et al., 1998). Prediction of moisture content in different pharmaceutical drug products is quite frequently applied in drug product quality control (Zheng Y. et al., 2008) as well as a process monitoring tool (Rantanen J. et al., 1998). Diffuse reflection NIRS studies of film coating process in fluidized bed and pan coater were reported by several authors (Andersson M. et al., 2000; Pérez-Ramos, D., et al., 2005; Roemer M. et al., 2008; Lee M. J. et al., 2011). NIRS studies on crystalline structure and polymorphic forms of APIs and excipients are quite common in pre-formulation stage of the drug product development. Several studies on this topic were reported in literature (Aldridge K. et al., 1997; Blanco M. et al., 2005; Otsuka M. et al., 2001).

2.1.3 Reports - API Content Prediction in Tablets by Diffuse Reflection NIRS

Prediction of content of active pharmaceutical ingredients in intact tablets is one of the most frequently reported applications of NIRS in pharmaceutical industry apart from raw material identification. Silvia S. Rosa et al. (Silvia S. Rosa et al., 2007) has described the strategy for development and validation of NIRS calibration model for Ranitidine content in tablets in diffuse reflectance measurement mode. The authors stressed the necessity for suitability test at the onset of method development in order to find out if the NIRS analysis of the parameter of interest is feasible. Schneider C. et al. have analyzed the ecstasy tablets with NIR diffuse reflectance and transmittance measurement mode (Schneider C. et al., 2003). Transmittance mode was shown to perform better. Trafford D. et al. have developed NIRS model for paracetamol content prediction in tablets by using MLR algorithm (Trafford D. et al., 1999). Validation results indicated the performances comparable to UV spectroscopic assay procedure from British Pharmacopoeia 1993. Chalus P. et al. have studied

the influence of different spectral pretreatments and regression methods on the accuracy of the NIR method for the API content prediction in intact low dose tablets. SNV and second derivative spectral pretreatments together with PLS regression method provided the best results (Chalus P. et al., 2005). Feng, Y. et al. developed universal quantitative models for the analysis of two APIs in tablets from different Chinese manufacturers (Feng, Y. et al., 2006). The models were validated according to ICH guidelines.

2.1.4 Reports - API Content Prediction in Tablets by Diffuse Transmission NIRS

Dyrby M. et al. have developed quantitative calibration models based on transmittance NIR and Raman spectroscopy (Dyrby M. et al., 2002). The authors have applied PLS algorithm for creation of the calibration model of the API which contains C≡N functional group. NIR diffuse transmittance sampling has proven its effectiveness compared to (microscopic) surface sampling of the Raman procedure. Gottfries J. et al. compared the NIRS models for metoprolol content predictions developed in diffuse reflectance and transmittance measurement mode (Gottfries J. et al., 1996). NIRS reflectance has shown to be more sensitive to inhomogeneity whereas diffuse transmittance mode scans larger portion of the tablet. The study indicated that the diffuse transmittance mode is more suitable for NIRS tablet analysis. Meza C. P. et al. developed an NIR calibration model for prediction of API content present in less than one percent in tablet formulation (Meza C. P. et al., 2006). Mark H. et al. have developed the strategy to successfully validate the NIR transmittance spectroscopic procedure according to ICH guidelines with special attention to the relevant statistical figures of merit (Mark H. et al., 2002).

2.1.5 Reports - Factors Affecting NIR Spectra of the Tablets

Laasonen M. et al., developed a NIRS model for caffeine content determination in intact tablets (Laasonen M. et al., 2003). Authors have found that there was non-uniformity of caffeine repartition within each tablet. Tablets were scanned on both sides to account for that phenomenon. Method was found to be unaffected by the light source replacement but the positioning of the tablet in the sample holder was shown to have significant influence on the results. Abrahamsson C. et al. have applied time-resolved transmission NIR spectroscopy for the analysis of intact tablets in order to overcome the disadvantage of conventional NIR transmission spectroscopy being sensitive to physical attributes of the sample (Abrahamsson C. et al., 2005). The applied technique separates the absorption properties of the sample from the scattering properties. Saeed M. et al. assessed the effect of the compression force on the accuracy of the developed NIRS calibration model for API content

prediction of intact tablets (Saeed M. et al., 2009). The authors stressed the need for the careful design of the calibration sample set for the successful NIRS model development. Ito M. et al. developed the calibration models for the acetaminophen and caffeine content in intact bilayer tablets (Ito M. et al., 2010). The initially developed models exhibited poor performances because the tablet thickness varied excessively. The proper control of the tablet thickness led to NIR models with satisfying accuracy and linearity. Unlike Laasonen M. et al., the authors have shown that the control of the irradiated side of the tablet was not necessary. Xiang D. et al. developed a robust method for content uniformity test of complex tablet formulation (Xiang D. et al., 2009). Robustness assessment involved challenging the model with tablets that varied in hardness, excipient vendor, excipient content and particle size. Xiang D. et al., assessed different measurement modalities, namely diffuse reflectance, diffuse transmittance and diffuse reflectance with fiber optic probe to analyze intact tablets (Xiang D. et al., 2009). Diffuse transmittance mode exhibited the best performances due to larger illumination spot. Diffuse reflectance mode have shown the sensitivity to tablet engraving. Ito M. et al. developed a NIRS calibration model for caffeine content prediction in intact tablets, robust towards the variation in tablet design, namely tablet thickness, shape, scored line and embossing. Analysis was done in diffuse reflectance and transmittance mode. The global calibration model approach was adopted for development of robust method, namely, the sources of variance were included in the model and that resulted in increase of the predictability of the models. Transmittance model exhibited better performances compared to reflectance model. Borer M. et al. assessed the potential sources of variability in the measurement of solid oral drug products in diffuse reflectance mode, using design of experiment (DoE) methodology (Borer M. et al., 1998). The authors stressed out the need of the careful construction of the calibration set and the control or inclusion of all significant sources of variability. The parameters that were evaluated in this study were number of scans averaged per spectra, data treatment settings such as the segment used for second derivative calculation, design of the library such as the number of dose units scanned, position of the iris i.e. the position of the aperture used to center the samples on the platform of the analyzer used in the study and to control the level of stray light, orientation of the sample platform, number of days and reference spectrum collection frequency. The authors reported some of the major influential factors that were not included in the study, namely, lot-to-lot variability in manufacturing, within-lot variability and temperature. Plackett - Burman design was applied. The studied responses reflected the ability of the library to differentiate the different strengths of the studied tablets, i.e. the performances of the library. Wu W. et al. have studied the effect of different design of the training set for artificial neural network classification modeling (Wu W. et al., 1996). Four different designs were compared. The presented results demonstrated that selection methods based on Kennard-Stone and D-optimal designs showed better performances compared to the designs based on Kohonen self-organized mapping and on random selection methods. Rutan S. et al. have assessed the influence of different sources of variability on the quantitative predictions, combining design of experiments and principal component

analysis (Rutan S. et al., 1998). The study was accomplished by comparing the variations in a set of the measured, replicate spectra to the spectra with simulated variations. The three-level factorial design was applied. The results indicated that the most significant sources of variation were due to variable cell path length and a variable curved background. Correction of these errors resulted in 58% reduction in SD of the predictions. Blanco M. et al. have studied the influence of physical factors on the accuracy of NIRS calibration models (Blanco M. et al., 2010). The authors have evaluated the effect of compression force, particle size, galenic form and coating thickness on the accuracy of the developed calibrations. The authors have used weight values as reference values to build the calibrations. Principal component analysis and cluster analysis was applied to classify the samples according to the stage of the manufacturing process and the physical attributes. The models were built with laboratory samples and tested with production samples. The factors shown to have significant effect on the NIR predictions were included in the initially developed models to improve the predictive ability.

2.1.6 Study Aims

The aim of this study was to systematically assess the influence of the main parameters of the tableting process, namely, pre-compression pressure, compression pressure and tableting speed on the near infrared spectra and performance of the developed calibration models for the prediction of caffeine content in intact tablets. Study was performed in diffuse reflection and diffuse transmission measurement mode. Design of experiments methodology was applied as a science - based approach to studying the effects of the above mentioned tableting parameters on the spectral features represented by the response Average Euclidean Distance (AED) and the performance of the developed NIRS calibration models represented by the response root mean squared error of prediction (RMSEP). The conclusions of the DoE study were challenged by testing the developed calibration models with the tablet test sets that included the variability of the three studied tableting factors. The tableting factors shown to have a significant influence on the studied responses in the DoE study were considered in the development of the robust calibration models towards the three studied factors by following the global calibration model approach.

Research Project I is summarized in a manuscript titled "Effect of simulated precompression, compression pressure and tableting speed on an offline diffuse transmittance and reflectance near-infrared spectral information of model intact caffeine tablets" published in the Journal of Pharmaceutical Development and Technology (DOI: 10.3109/10837450.2014.949267).

Pharmaceutical Development and Technology

http://informahealthcare.com/phd
ISSN: 1083-7450 (print), 1097-9867 (electronic)

Pharm Dev Technol, Early Online: 1–9
 DOI: 10.3109/10837450.2014.949267

informa
healthcare

RESEARCH ARTICLE

Effect of simulated precompression, compression pressure and tableting speed on an offline diffuse transmittance and reflectance near-infrared spectral information of model intact caffeine tablets

Branko Z. Vranic[1,2] and Thierry F. Vandamme[3]

[1]Department of Pharmaceutical Sciences, University of Basel, Basel, Switzerland, [2]BÜCHI Labortechnik AG, Postfach, Switzerland, and [3]CNRS 7199 Laboratoire de Conception et Application de Molécules Bioactives, Équipe de Pharmacie Biogalénique, Faculté de Pharmacie, Université de Strasbourg, Illkirch Cedex, France

Abstract

Near-infrared spectroscopy (NIRS) is used in the pharmaceutical industry for monitoring drug content during the tablet manufacturing process. It is of critical importance to understand the effect of process factors on NIRS performance. Design of Experiments (DoE) methodology was applied in this work for the systematic study of the effects of compression pressure, precompression pressure and tableting speed on an average Euclidean distance (AED), which reflects spectral features of the tablets, and root mean-squared error of prediction (RMSEP) as key performance indicator of NIRS calibration models. Caffeine tablets were manufactured in 17 experimental runs in accordance with D-optimal design. Developed diffuse transmittance (DT) and diffuse reflectance (DR) calibration models were tested on five independent test sets to confirm the conclusions of the DoE. Compression pressure and tableting speed have shown significant effect on the studied responses in DT mode, whereas all three studied factors have shown a significant effect in DR mode. Significant factors were considered in the development of the global calibration models. The authors suggest further study of RMSEP and AED responses to draw reliable conclusions on the effects of tableting process factors. The global calibration model in DT mode has shown superior performance compared to DR mode.

Keywords

Compression pressure, diffuse reflectance, diffuse transmittance, precompression pressure, tableting speed

History

Received 25 November 2013
Revised 23 July 2014
Accepted 24 July 2014
Published online 14 August 2014

Introduction

The Q8 guidance on pharmaceutical development from the International Conference on Harmonization (ICH) suggests a careful risk assessment of variables (such as raw material attributes, process parameters, environmental conditions, analytical method characteristics and so on) on critical to quality attributes (CQAs) of a final drug product[1]. As the analytical method is one of the most important variables of an overall quality risk assessment matrix, it is important to ensure the complete understanding of factors influencing its performance. The physical attributes of a sample are determined by both formulation and manufacturing process factors. Formulation of a drug product is generally constant over time but manufacturing process factors may change; these changes and their effect on the NIR spectra of a drug product need to be well understood and controlled.

Rather than the more commonly used empirical approach to defining critical factors affecting NIR spectral response and calibration model performance, the ICH Q8 and Q9 guidelines suggest that a systematic and science-based approach such as design of Experiments (DoE) should be used from the start of method development where all process parameters that affect NIR method performance should be identified and included in the model[1,2]. These factors should be treated as potential risks to quality of a final drug product and as such, included in a quality risk assessment matrix.

The aim of this study was to systematically assess the influence of precompression pressure (p.p.), compression pressure (c.p.) and tableting speed (t.s.), on near-infrared spectra (NIRS) and the performance of the developed NIR calibration models for the prediction of caffeine content in intact tablets. The secondary aim was to compare diffuse transmittance (DT) and diffuse reflectance (DR) measurement modes in terms of suitability for tablet analysis.

Materials and methods

Materials

Caffeine anhydrous was supplied by BASF AG (Ludwigshafen, Germany), with a mean particle size of $76 \pm 1.4\,\mu m$ and moisture content of $0.42 \pm 0.1\%$. Microcrystalline cellulose (Avicel® PH 102) was purchased from FMC BioPolymer, Philadelphia, PA; the mean particle size was $111.6 \pm 0.7\,\mu m$ and moisture content $4.8 \pm 0.2\%$. Magnesium stearate with a mean particle size of $27 \pm 6.3\,\mu m$ and moisture content of $2.3 \pm 0.4\%$ was supplied by Sandoz AG, Risch, Switzerland. Sodium starch glycolate (mean particle size $47 \pm 2.3\,\mu m$) was supplied by DMV-Fonterra Excipients GmbH, Germany.

Address for correspondence: Branko Z. Vranic, Department of Pharmaceutical Sciences, University of Basel, Klingelbergstrasse 50, CH-4056 Basel, Switzerland. Tel: + 41 762739727. E-mail: branko.vranic@unibas.ch

Equipment

An XS 204 Analytical Balance (Mettler Toledo AG, Greifensee, Switzerland) was used for weighing the powder components. Powders were mixed in a tumbling mixer, a Turbula T2A (Willy A. Bachofen AG Maschinenfabrik, Basel, Switzerland). A Malvern Mastersizer X (Malvern Instruments, Worcestershire, UK) was used to determine average particle size. The infrared balance used to determine moisture content was an LP 16 M (Mettler Toledo AG, Switzerland). Direct compression tableting was done on Presster™ tablet press simulator (Metropolitan Computing Corporation, East Hanover, NJ). A NIRFlex N-500 FT-NIR spectrometer (BÜCHI Labortechnik AG, Flawil, Switzerland), with DT and DR measurement cells, was used for spectra acquisition. Reference analysis was performed on a Beckman DU530 UV-Vis spectrometer. BUCHI NIRCal 5.4 chemometric software was used for generating the PLS calibration models, and MODDE 9.0 software was used for DoE.

Methods

Preparation of powder and tablet samples

Tablet formulations covering the caffeine content range of 82.4–122.0% of the nominal caffeine content (where 100% was 50 mg) were manufactured by direct compression method. Sodium starch glycolate and magnesium stearate were constant in the studied formulations at 3% and 1%, respectively. The amount of microcrystalline cellulose was added to each formulation to the constant tablet weight of 200 mg. Formulation components without added magnesium stearate were accurately weighed on the analytical balance and then transferred to a glass jar to be mixed for 5 min in a tumbling mixer. After a first mixing cycle, the powder mixture was screened through a 0.125-mm sieve, 1% of magnesium stearate added to the mixture and a second mixing cycle lasting 2 min was performed. About 200 mg of the final powder mixture was accurately weighed on the analytical balance and manually fed into the single die of the tablet press simulator. Direct compression tableting was done on a Presster™ tablet press simulator, which was used to simulate an industrial rotary tablet press (Korsch PH336 with 36 stations) by replicating the tableting speed, precompression and compression pressure. Tableting speed was simulated by replicating tablet punch speeds at a given rates expressed as tablets per hour where precompression and compression force were adjusted indirectly through setting the gap between upper and lower punch of Presster™ single tableting station. A set of flat face punches with 10 mm diameter were used, and the weight of the tablets was kept constant at 200 mg.

For the DoE study, one batch of the powder mixture was prepared with a total weight of 200 g. Tablets were manufactured in 17 experimental runs in accordance with the DoE model. For each of the 17 DoE runs, 20 tablets were produced (340 tablets in total) following tableting factor adjustments suggested by the DoE.

For the development of the local NIR calibration models for the prediction of caffeine content in intact tablets, 11 concentration levels were prepared covering the nominal caffeine content range of 80–120%. Tablet weight was 200 mg. Total weight was 50 g per concentration level. About 220 tablets were produced, 196 were used to build the local calibration models and 24 tablets were excluded due to cracks, picking, coloration or erroneous UV reference measurements. Tablets were manufactured using target tableting parameters, i.e. 76 MPa compression pressure, 25 MPa precompression pressure and tableting speed of 100 000 tablets per hour (tph). Tablets were stored for 24 h in the desiccator before the NIR and reference analysis by UV-spectrophotometry were performed.

For the extension of the local calibration model, (that is for the development of a global model), 80 additional tablets were manufactured. Five different concentration levels were prepared covering the nominal caffeine content range of 84–116%. Compression pressure ranged from 38 to 114 MPa, precompression pressure from 13 to 38 MPa and simulated tableting speed from 10 000 to 200 000 tph.

Testing of the developed calibration models was done by manufacturing five tablet test sets. Each test set was composed of 30 tablets. Nominal caffeine content in the tablets spanned the range of 88–112%.

Test set 1 was manufactured with the target tableting parameters. In case of the other four test sets, two out of three tableting factors were kept at the target values while the third one was varied. Test set 2 had higher (95 MPa) and test set 3 had lower (57 MPa) compression pressure. With test set 4, precompression pressures of 13, 18, 25, 32 and 38 MPa were used to manufacture the tablets. Six tablets for each of the five precompression pressures were prepared. The tablets of test set 5 were manufactured by simulating the tableting speeds of 10 000, 50 000, 100 000, 150 000 and 200 000 tph. Six tablets were produced for each tableting speed.

Acquisition of NIR spectra

The NIRFlex N-500 FT-NIR spectrometer with DT and DR measurement cells was used for spectra acquisition. DT measurements were done with spectral resolution of 16 cm^{-1}. Digital resolution was 4 cm^{-1}. The wavenumber range was 11 520–6000 cm^{-1}. Each spectrum was the average of 64 scans. Ambient air was measured as a background for calculating the spectra. DR measurements were carried out with 8 cm^{-1} optical resolution, and digital resolution was 4 cm^{-1}. The wavenumber range was 10 000–4000 cm^{-1}. Each spectrum was average of 32 scans. Spectralon® was used as an external reference.

Diffuse reflectance measurements require shorter acquisition times compared to DT mode but probe only the tablet surface, whereas DT mode probes larger portion of the tablet but is more sensitive to variations in tablet physical properties. The comparison between the two measurements mode has been carried out.

UV spectrophotometric reference analysis

Distilled water was used to dissolve each tablet and the filtered solution was measured in a 10-mm cell at 273 nm. The UV calibration line was obtained in the same medium with a coefficient of determination of 0.993. Obtained standard error (SE) was 0.5 mg which corresponds to 1% of the nominal caffeine content, thereby validating the UV spectrophotometric method.

NIR method development

Calibration models for the prediction of the caffeine content in intact tablets were developed using the PLS method. Available data were divided into calibration and validation sets, where two-thirds were used to develop the NIRS model and one-third to validate it. The number of principal components was chosen based on the sum of squares of the spectral residuals (X-PRESS), assuring an adequate reconstruction of spectra by the model and, additionally, predicted residual error sum of squares based on a validation set (V-set PRESS). The developed NIRS models were judged based on coefficient of determination (RSQ), standard error of calibration (SEC), validation set Bias and standard error of prediction (SEP). Linearity was assessed by evaluating the slope and the intercept of the calibration line and by calculating the RSQ. Bias and slope of the validation and test sets were tested for significance based on Student's *t*-test. The Durbin–Watson test was applied to the prediction residuals to check for evidence of

serial correlations between them. Every model was tested for outliers in both the calibration and validation sets by visual inspection of the scatter plot of the reference against NIR predicted values, scores plot, leverages and spectral residuals. The ultimate performance indicator of the developed models was the root mean squared error of prediction (RMSEP) of the test set, and the ratio of performance to deviation (RPD).

Local NIR calibrations were developed with 196 spectra of the tablets manufactured with the target tableting parameters (76 MPa compression pressure, 25 MPa precompression pressure and simulated tableting speed of 100 000 tph). An additional 79 spectra of the tablets, prepared with variable compression pressure, precompression pressure and simulated tableting speed were added to extend the local models, i.e. to develop the global calibration models. Local and global calibration models were tested with five independent test sets, each composed of 30 tablet samples.

Design of experiments

Compression pressure, precompression pressure and tableting speed were studied to examine the effect on NIRS and the subsequent predictions of the developed calibration models. The tableting process factors to be studied by the DoE were chosen based on the screening experiments DoE is summarized in Tables 1 and 2.

The variability of the three studied tableting factors was beyond the normal variability of the tableting process. This was done intentionally to highlight the inefficacy of the currently available spectral pretreatments to completely remove non-linear spectral scaling effects, and to emphasize the need for careful design of the calibration data set.

The aim of studying the effects of these tableting parameters on NIR spectra was to evaluate their effect on the prediction performance of an NIR calibration model. The most appropriate figure of merit used to judge the performance of NIR calibration models is the RMSEP, as shown in equation (1). It is a measure of a total NIR error incorporating both systematic (Bias) and random error (SEP):

$$RMSEP = \sqrt{\frac{\sum_{i=1}^{N} (x_i - y_i)^2}{N}} \quad (1)$$

where N is the number of samples, x_i is the reference value and y_i is the NIR predicted value. RMSEP was selected as the first

Table 1. Design of experiments – diffuse transmittance study.

Experiment no.	Run order	Compression pressure [MPa]	Precompression pressure [MPa]	Tableting speed [tph]	RMSEP [%]	AED
4	1	38	38	10 000	2.41	0.068065
2	2	114	13	10 000	2.02	0.254038
16	3	114	38	200 000	2.11	0.235421
17	4	114	38	200 000	2.06	0.213638
12	5	76	25	200 000	1.04	0.140521
7	6	76	13	100 000	0.96	0.152458
13	7	38	38	200 000	2.58	0.050159
15	8	114	38	200 000	2.17	0.229461
9	9	114	38	100 000	1.96	0.235979
5	10	76	38	10 000	0.94	0.162516
14	11	114	38	200 000	2.17	0.232987
11	12	114	13	200 000	2.31	0.21575
3	13	114	25	10 000	2.09	0.254562
8	14	38	25	100 000	2.51	0.06223
6	15	114	38	10 000	2.01	0.260523
1	16	38	13	10 000	2.47	0.057639
10	17	38	13	200 000	2.56	0.056411

RMSEP, root mean squared error of prediction; AED, average Euclidean distance.

Table 2. Design of experiments – diffuse reflectance study.

Experiment no.	Run order	Compression pressure [MPa]	Precompression pressure [MPa]	Tableting speed [tph]	RMSEP [%]	AED
4	1	38	38	10 000	2.21	0.003316
2	2	114	13	10 000	2.06	0.011902
16	3	114	38	200 000	2.17	0.010305
17	4	114	38	200 000	2.24	0.010043
12	5	76	25	200 000	1.48	0.005643
7	6	76	13	100 000	1.39	0.005551
13	7	38	38	200 000	2.27	0.004691
15	8	114	38	200 000	2.17	0.011557
9	9	114	38	100 000	2.12	0.011169
5	10	76	38	10 000	1.52	0.007444
14	11	114	38	200 000	2.13	0.011205
11	12	114	13	200 000	1.84	0.008277
3	13	114	25	10 000	1.92	0.012509
8	14	38	25	100 000	2.19	0.004032
6	15	114	38	10 000	2.05	0.012065
1	16	38	13	10 000	2.08	0.003529
10	17	38	13	200 000	2.00	0.002271

response in the DoE study. For obtaining the RMSEP response values, two local calibration models were developed for caffeine content prediction in DT and DR measurement mode. Seventeen test sets manufactured according to DoE (composed of 20 tablets each) were predicted by the developed local calibration models, and RMSEP response values were calculated to provide the inputs for response surface modeling (RSM).

Average Euclidean distance (AED) was introduced as a second response for the DoE study[3–5]. It is not dependent on calibration model parameters, i.e. on the selected pretreatments but rather reflects the effect of the studied factors on the spectral features since the spectral pretreatments were not included in the calculation. Equation (2) shows how the AED was calculated:

$$d(a,\ b) = \sqrt{[(x_1 - y_1)^2 + (x_2 - y_2)^2 + \cdots + (x_n - y_n)^2]} \quad (2)$$

where x_n is a single wavelength of spectrum a, y_n single wavelength of spectrum b, a – spectrum ''a'' composed of n wavelengths, b – spectrum ''b'' composed of n wavelengths and $d\ (a,\ b)$ is Euclidean distance between the spectrum a and b.

Average Euclidean distance was introduced as a distance between the average spectrum of the 20 tablets of the test set manufactured according to DoE, and the reference spectrum which was the average spectrum of the 20 tablets manufactured using the ''target'' tableting parameters (Figure 1). Here, target parameters correspond to the mean of the design space, and were defined with a compression pressure of 76 MPa, precompression pressure of 25 MPa and tableting speed of 100 000 tph. AED response values were calculated for both studied NIR measurement modes.

Target values of the studied tableting parameters were chosen based on the recommendations of the United States Pharmacopeia (USP) and the European Pharmacopoeia (EP)[6,7]. USP chapters <1216> and <1217> and EP chapter <2.9.8>, which refer to the mechanical properties of tablets, were considered when developing the experimental design space. A tableting speed of 100 000 tph was set as a target parameter to be simulated. The selected target parameters resulted in tablets with appropriate mechanical properties, with no signs of capping, lamination, cracking or chipping.

The two chosen responses were approximated by quadratic polynomial models in order to understand how the tableting factors influence them. Response surface modeling was applied for evaluating the effects of precompression pressure, compression pressure and tableting speed on the RMSEP and AED responses. D-Optimal design (chosen for its flexibility and ability to target a specific problem), used with a quadratic model and 17 experimental runs, was chosen to model and optimize the effects of the three tableting factors on the two responses in both studied measurement modes. Multiple linear regression (MLR) was used to fit the data. The models that were developed were assessed based on the variation expressed by the coefficient of determination (R^2), the response variation predicted by the model (Q^2), the model validity and the reproducibility.

Results and discussion

Local NIR calibration models

The local calibration models in DT and DR measurement mode were developed using 196 tablet samples manufactured with the target tableting conditions. The aim was to have optimized calibration models which would be used to obtain the RMSEP response values for the DoE study. The test set tablet samples, manufactured in accordance with DoE, were predicted by the local calibration models and the RMSEP was calculated for each

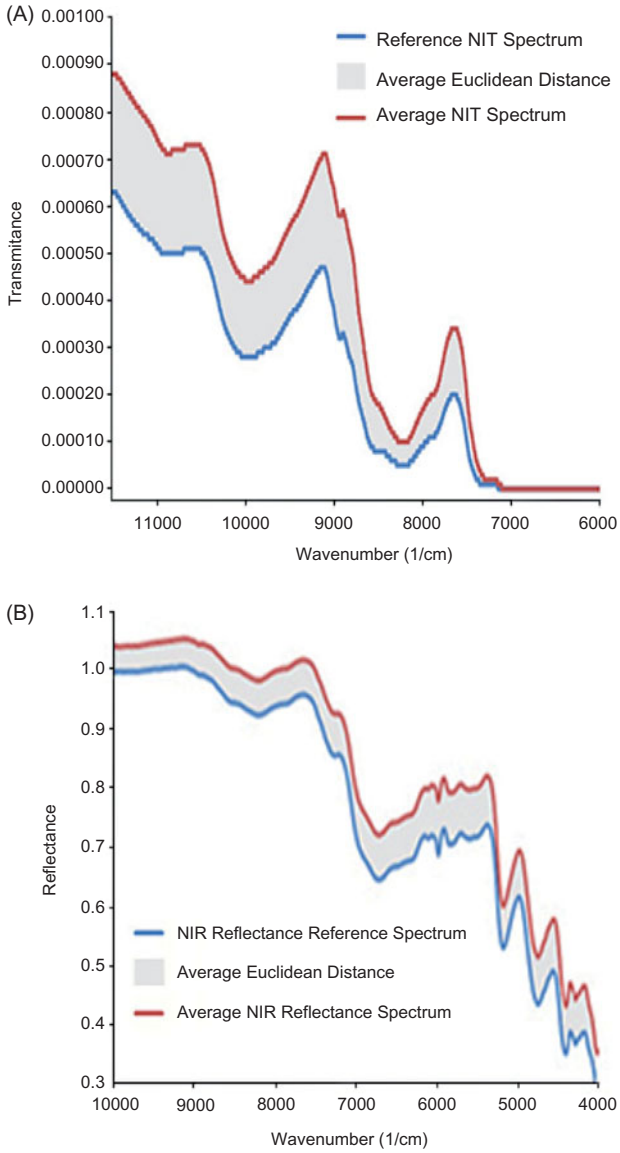

Figure 1. Average Euclidean distance in DT and DR measurement mode.

test set for both measurement modes. PLS regression was used to calculate the model. SNV spectral pretreatment was used to reduce the path length differences in both measurement modes. The wavenumber range 7000–11 520 cm^{-1} was used for the calculation in DT mode and 4000–10 000 cm^{-1} in DR mode. Spectra were divided into calibration and validation sets, where two-thirds of the data were assigned to a calibration and the remaining third to a validation set. Four principal components were selected to build the calibration models in both measurement modes. The property range covered was 82.4–122.0% and 81.4–123.5% of the nominal caffeine content for DT and DR mode, respectively. Both local models exhibited an RSQ of 0.99 and an SEC of 1.07% and 1.55% for DT and DR mode, respectively. The local calibration models were validated and a summary of the figures of merit is shown in Table 3. The validated local calibration models were tested on a set of independent test samples. Test set 1, made up of 30 tablet samples manufactured using the target tableting parameters, was used for testing the model. NIR predictions were plotted against reference values and the RSQ was 0.92 and 0.84 for DT and DR mode, respectively. Slope and bias of the regression lines were tested for significance using Student's t-test and were shown to be not significant (the significance level was 0.05). The RMSEP for DT mode was

Table 3. Validation statistics – local diffuse transmittance (DT) and reflectance (DR) models.

NIR % nominal = *f* (Reference % nominal)											
NIR % nominal				Reference % nominal			**DT**	**DR**			
N	**DT** (58)	**DR** (63)		**DT** (58)	**DR** (63)	Alpha	0.05	0.05			
Average	101.52	101.63		101.45	101.56	*T* value	2.00	2.00			
Min	83.36	82.56		82.56	81.82	*F* value	1.57	1.54		**Probability**	
Max	121.79	121.88		121.88	122.79					**DT**	**DR**
SD	13.13	12.75		13.03	12.92	Tobs_Bias	0.52	0.43	ns	0.608	0.671
			DT	**DR**							
RMSEP			0.998	1.382		F_sep	1.57	2.14	ns		
BIAS			−0.068	0.075							
SEP			1.004	1.391		Tobs_slope	0.45	0.56	ns	0.653	0.573
RSDyx			1.011	1.399							
Slope			1.005	1.008		MAE	0.69	0.89			
Intercept			−0.403	−0.877							
RSQ			0.994	0.988		Quartile75	1.16	1.66			
RPD			13.098	9.311							

N, number of samples; **DT**, diffuse transmittance; **DR**, diffuse reflectance; SD, standard deviation; RMSEP, root mean squared error of prediction; SEP, standard deviation of the prediction residuals; RSDyx, standard error of the predicted *y* value for each *x* in regression model; RSQ, coefficient of determination; RPD, ratio of performance to deviation; Alpha, significance level; *T* value, *T* critical value of the Student's *T* test; *F* value, *F* critical value of the *F* test; Tobs_Bias, *T* observed value returned from the BIAS significance testing according to ISO 12099; F_sep, SEP (SECV) of the validation set multiplied with *F* critical value for SEP (SECV) confidence limits estimation according to ISO 12099; Tobs_slope, *T* observed values returned from slope significance testing according to ISO 12099; probability: probability for the Student's *T* distribution calculated for the *T* observed values; MAE, mean of absolute errors; Quartile75, third quartile value for the absolute errors; ns, non-significant.

0.92% and 1.43% for DR mode. Exhibited performance was comparable to the validation results.

The observed performance indicated that the developed local calibration models in DT and DR measurement modes were optimized and suitable for obtaining the NIR predictions necessary for calculating the RMSEP response values for the DoE study.

Diffuse transmittance DoE study – response RMSEP

The obtained model with the stated RMSEP had nine terms. Each term was analyzed and the fact that the confidence interval had not crossed the zero line indicated that the term was statistically significant. The fitted model has shown a high level of prediction performance and validity. The model exhibited R^2 of 0.99 and Q^2 of 0.94. The validity of the model was found to be 0.76 and reproducibility 0.99. The high R^2 value indicated a high percent of variation of the response explained by the model; the Q^2 was also fairly high. The presence of insignificant model terms was shown by the moderate model validity; removing these terms would increase the prediction ability of the model as initially calculated. The high levels of model reproducibility were due to the low variation of the responses under the same experimental conditions. All insignificant equation terms were kept in the model in order to facilitate the physical interpretation of the model; this was acceptable since the aim was not to optimize the predictive ability of the model.

Compression pressure (c.p.), tableting speed (t.s.) and squared compression pressure (c.p.^{2}) have shown significant effect (confidence level 0.95) on the response RMSEP. Figure 2 shows the MLR regression coefficients with the confidence intervals of the model for the response RMSEP. Coefficients were scaled and centered in order to make them comparable. The size of the coefficient represents the change in the response when a factor varies from zero to one, in coded units, while the other factors are kept at their averages.

The compression pressure and RMSEP have shown squared dependency. An increase or decrease of a compression pressure, as compared to the target compression pressure value, led to increase of RMSEP (Figure 3). The tablets manufactured using

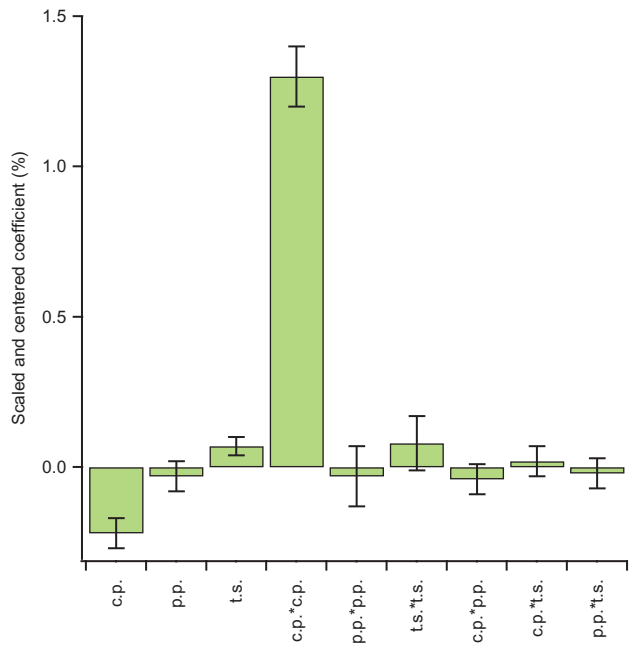

Figure 2. Scaled and centered coefficients of the model for the response RMSEP – diffuse transmittance.

higher or lower compression pressure as compared to the target value, resulted in a higher RMSEP due to the fact that the respective physical variability was not included in the NIR calibration model which was used to generate the caffeine predictions and RMSEP values. Tableting speed has shown a positive correlation with the response RMSEP, where increase in tableting speed led to increase of RMSEP (Figure 3). This phenomenon could be attributed to the fact that increase of tableting speed changes the structural properties of a tablet which consequently affects scattering and the optical path length in the tablet precompression pressure (p.p.) has shown no significant effect on RMSEP response.

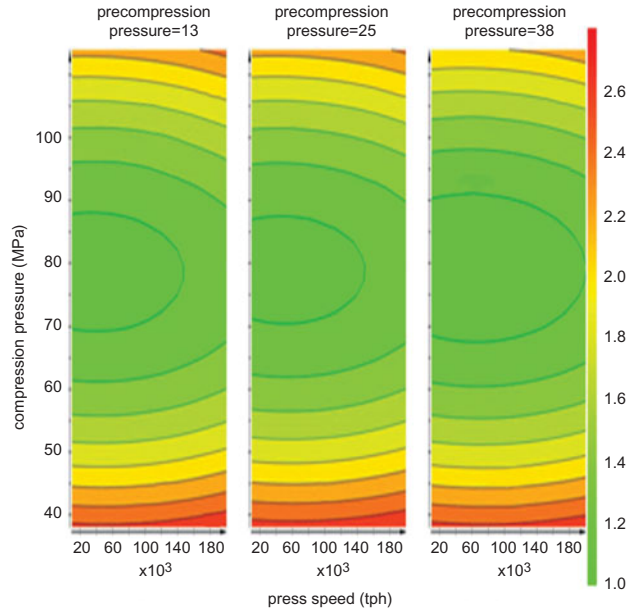

Figure 3. Contour plots for the response RMSEP – diffuse transmittance.

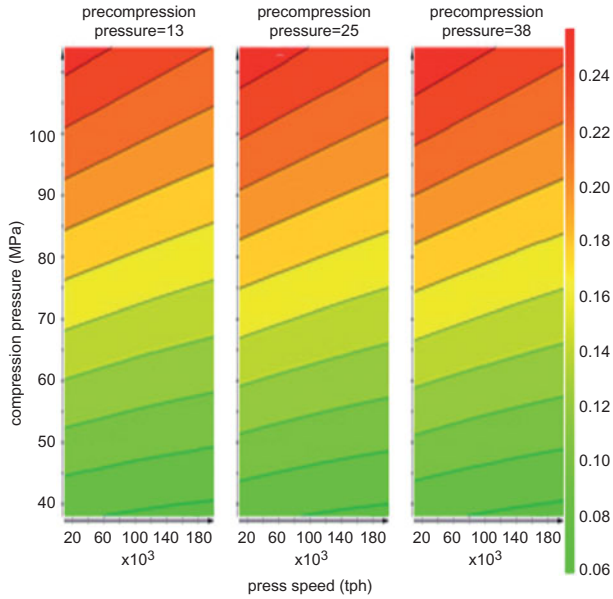

Figure 5. Contour plots for the response AED – diffuse transmittance.

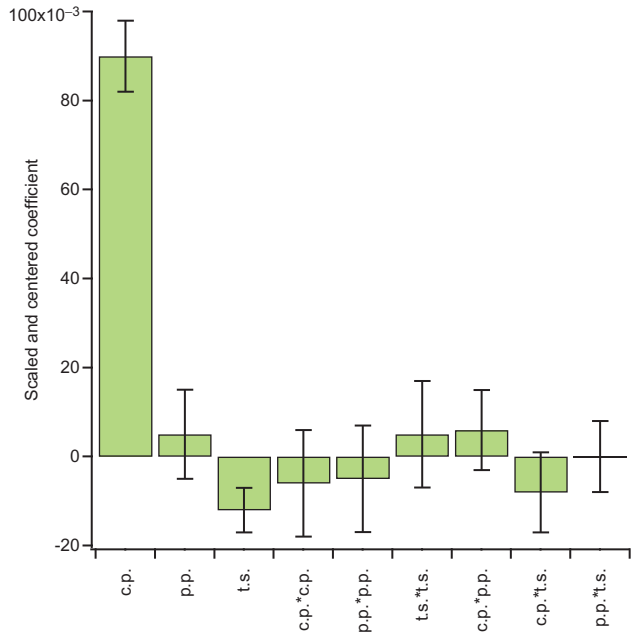

Figure 4. Scaled and centered coefficients of the model for the response AED – diffuse transmittance.

Diffuse transmittance DoE study – response AED

The model for AED also had nine terms. Compression pressure and tableting speed showed a significant effect (confidence level 0.95) on the response AED (Figure 4). The fitted model has shown a high degrees of both accuracy of prediction and validity. The model for the response AED was characterized by an R^2 of 0.99, a Q^2 of 0.97, a model validity of 0.94 and reproducibility of 0.99.

Figure 5 shows the main effects on the studied response and the interdependency of the studied factors. The positive linear correlation between compression pressure and AED could be explained by the fact that an increase of compression pressure results in a decrease in the thickness of the tablet, and an optical path length which is reflected as spectra up-scaling relative to the intensity of diffusely transmitted NIR light. There was a negative linear correlation between the tableting speed and the response AED, which could be explained by the fact that an increase of tableting speed decreases particle bonding in the powder bed, which makes it less dense and therefore increases the optical path length.

Diffuse reflectance DoE study – response RMSEP

The model for the response RMSEP had nine terms, three of these were single factor effects, three were squared effects and three were interaction effects. Four of the nine terms have shown a significant effect on the response, with a confidence level of 0.95. The most significant model terms were compression pressure (c.p.), squared effect of compression pressure, precompression pressure (p.p.) and the interaction term between precompression pressure and tableting speed (Figure 6). The R^2 value was 0.98 and the Q^2 value was 0.77; model validity was 0.70 and the reproducibility was 0.97.

The compression pressure has shown a negative effect on the response RMSEP, whereas the squared effect of the compression pressure was positive and the most significant term in the model. This can be attributed to the fact that tablets manufactured with low compression pressure have high porosity which facilitates the NIR light scattering, contributing to the increase of the prediction error, i.e. RMSEP. The precompression pressure has shown a positive effect on the response RMSEP: an increase in precompression pressure from 13 to 38 MPa resulted in an increase of the response RMSEP. The interaction term between precompression pressure and tableting speed showed a positive effect on the response RMSEP although tableting speed alone did not show a significant effect. The combined effect could be attributed to the fact that an increase of tableting speed (i.e. a decrease in the contact time between the punch tip of the tablet press simulator and the powder bed) resulted in a density inhomogeneity throughout the tablet, and together with the effect of precompression pressure and its interaction with the compact formation stage, increased the RMSEP value.

Figure 7 summarizes the behavior of the response RMSEP when the three studied factors vary from its low to its high level. The plot shows the trend of the response RMSEP when one factor varies and the others are kept at their average value.

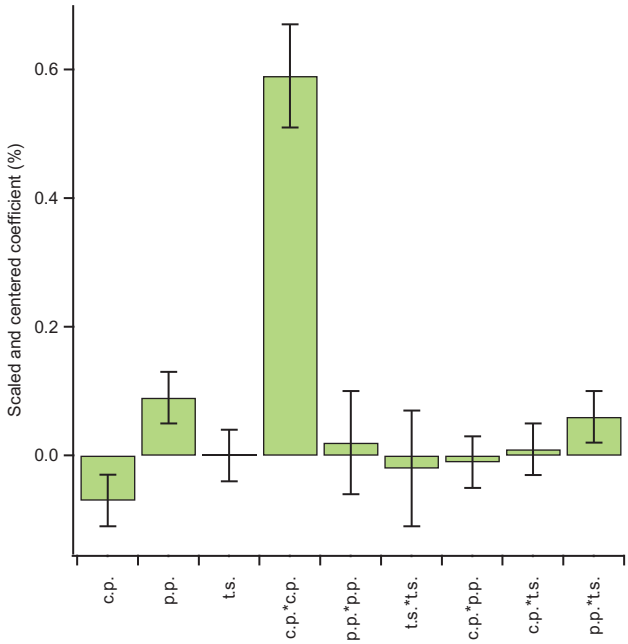

Figure 6. Scaled and centered coefficients of the model for the response RMSEP – diffuse reflectance.

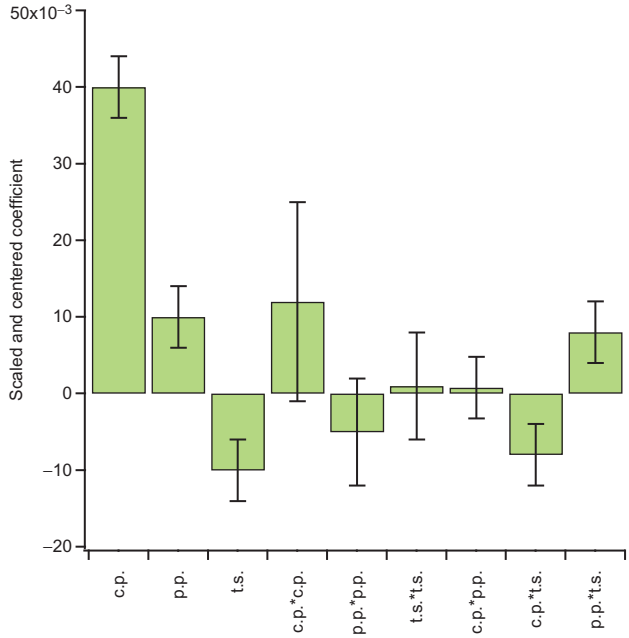

Figure 8. Scaled and centered coefficients of the model for the response AED – diffuse reflectance.

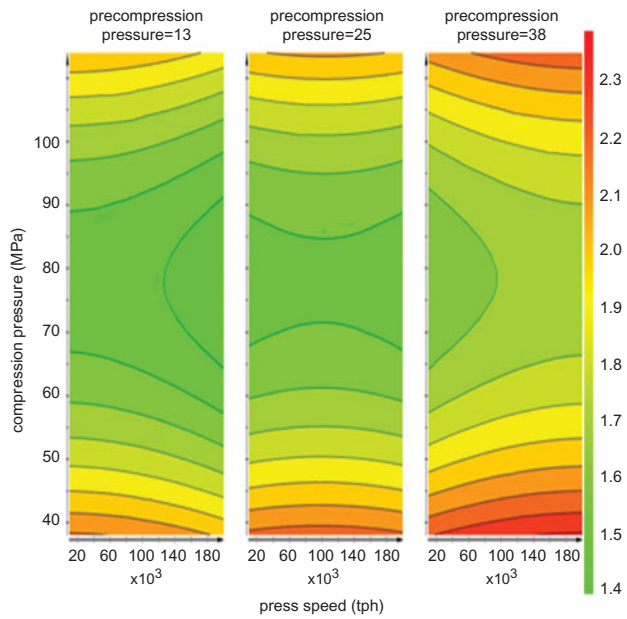

Figure 7. Contour plots for response RMSEP – diffuse reflectance.

Compression pressure affected RMSEP with a squared dependency. On all three plots shown in Figure 7, the lower and the upper parts of the graph indicate that where the compression pressure is low or high relative to the target value of 76 MPa, RMSEP is high (colored in red). It can be seen that with an increase of precompression pressure from 13 MPa (low) to 38 MPa (high), this effect is more pronounced, confirming the positive effect of the precompression pressure on RMSEP. On the first and the second plot in Figure 7, it can be seen that tableting speed had no effect on RMSEP. The third plot shows an increase of RMSEP with an increase of tableting speed when the precompression pressure is high (38 MPa). This demonstrates the positive effect of the interaction in the DoE model between precompression pressure and tableting speed on RMSEP.

Diffuse reflectance DoE study – response AED

The model for the response AED consisted of nine terms. Five out of the nine terms have shown significant effect on the response (with a confidence level 0.95). The significant terms were compression pressure (c.p.), precompression pressure (p.p.), tableting speed (t.s.), the interaction term between precompression pressure and tableting speed, and the interaction term between compression pressure and tableting speed (Figure 8). The R^2 value was 0.99 and the Q^2 value 0.97. Model validity was 0.98 and reproducibility 0.97.

Figure 9 shows the effects of three factors on the response AED. The compression pressure has shown positive effect on the response AED. An increase in compression pressure could result in a decrease of smoothness of a tablet surface, which could increase surface scattering effects and consequently decrease the intensity of the NIR reflectance signal, which was observed.

A positive correlation was shown between precompression pressure and AED. The effect of precompression pressure is formulation dependent and depends mostly on the deformation behavior of the filler (plastic, elastic, visco-elastic or brittle). The tableting speed has shown a negative effect on the AED. With an increase in precompression pressure, the effect of tableting speed on AED was more pronounced (a positive effect of the interaction term between precompression pressure and tableting speed). An increase in compression pressure increased the negative effect of tableting speed on the AED; tableting speed affects the tablet smoothness and the looseness of the tablet surface layers, and therefore contributes to surface light scattering effects.

The conclusions from the DoE study were subjected to further evaluation. The initial local calibration models in DT and DR measurement mode that were used for obtaining the predictions and RMSEP response values for the DoE study were tested against five test sets. The calibration models were then extended to include the variability factors shown by the DoE study to have a significant effect on the responses, and tested again against the same test sets. The prediction errors (RMSEP) of the test sets were evaluated and compared in order to confirm the conclusions of the DoE study.

Global NIR calibration models

The local calibration models were extended with the spectra of the 79 tablet samples. Raw DT and DR spectra were pretreated using log function and multiplicative scatter correction (MSC) pretreatment. The wavenumber range was the same as that used in the local NIR calibration models. Two principal components (PCs) were used to calculate the DT global calibration model, and three PCs were used for the calculation of the DR global model. The global DT model exhibited an RSQ of 0.99 and an SEC of 1.35%. The DR model was characterized with an RSQ of 0.98 and an SEC of 1.72%. Both global calibration models were validated, and a summary of the validation figures of merit is shown in Table 4.

Confirming the conclusions of the DoE study – DT measurement mode

The developed local calibration model in DT mode was tested against five independent test sets (Table 5). The RMSEP for test set 1 was found to be 0.92%, and the prediction error was lower than the RMSEP of the validation set (1%). The RMSEP for the test sets 2 and 3 was 2.33% and 2.57%, respectively; high prediction errors for test sets 2 and 3 have indicated that the DT measurement mode is sensitive to variations in the physical properties of the samples (such as thickness, porosity, optical path length and so on). The prediction errors of test sets 4 and 5 were not different when compared with the RMSEP of the validation set. This observation corresponded with the conclusions of the DoE study. Further tests were done on the global calibration model to confirm these conclusions.

Improvements in performances were apparent in case of global DT model. The RMSEP of test set 1 was higher when compared with the validation set RMSEP, possibly due to an increase in a variability included in the model after the calibration extension. The RMSEP of test sets 2, 3 and 5 was significantly decreased, while the RMSEP of the test set 4 was increased confirming that precompression pressure has not shown any significant effect on NIR predictions, whilst the compression pressure and tableting speed have shown a significant effect. The overall RMSEP value calculated for the 150 tablets of the five test sets was 1.21%. The calculated RMSEP values are summarized in Table 5.

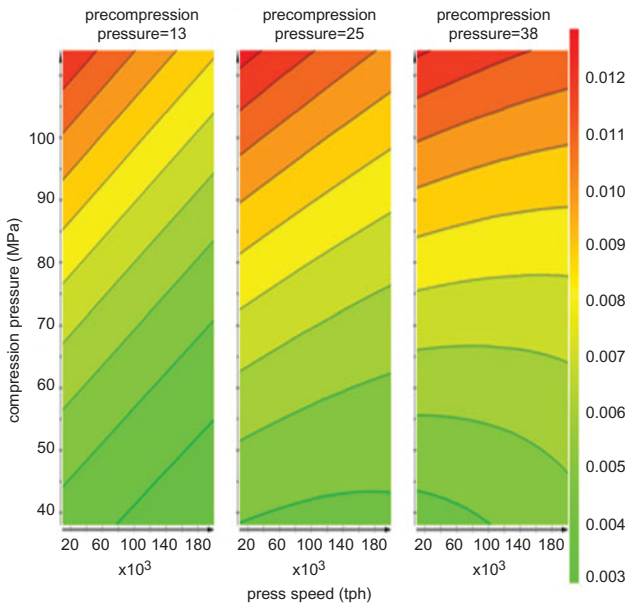

Figure 9. Contour plots for the response AED – diffuse reflectance.

Confirming the conclusions of DoE study – DR measurement mode

The developed local and global calibration models in DR mode were tested against the same five test sets. The local calibration model exhibited an RMSEP of 1.43% for test set 1, compared with the validation set RMSEP of 1.35%. The RMSEP of test set 2 was 1.81% and the RMSEP for test set 3 was 2.07%. Predictions of test sets 4 and 5 resulted in RMSEPs of 1.59% and 1.54%, respectively. It was evident that prediction errors increased significantly when the model was tested on tablets manufactured with a compression pressure different from that used for the manufacturing of the calibration samples. The prediction error was particularly high for the low compression pressure test set (test set 3). This can be attributed to the strong influence of light

Table 5. RMSEP of the test sets for local and global DT and DR models.

Test set no.	DT local RMSEP (%)	DR local RMSEP (%)	DT global RMSEP (%)	DR global RMSEP (%)
1	0.92	1.43	1.03	1.39
2	2.33	1.81	1.19	1.63
3	2.57	2.07	1.42	1.71
4	1.06	1.59	1.13	1.46
5	1.21	1.54	1.11	1.48

Table 4. Validation statistics – global diffuse transmittance (DT) and reflectance (DR) models.

NIR % nominal = *f* (Reference % nominal)

NIR % nominal			Reference % nominal			DT	DR			
N	**DT** (84)	**DR** (91)	**DT** (84)	**DR** (91)	Alpha	0.05	0.05			
Average	101.17	101.10	101.09	101.28	*T* value	1.99	1.99			
Min	82.56	81.53	81.94	82.56	*F* value	1.35	1.34		**Probability**	
Max	121.88	123.86	121.31	121.88					**DT**	**DR**
SD	12.80	12.92	12.71	12.89	Tobs_Bias	0.65	1.06	ns	0.515	0.293
		DT	**DR**							
RMSEP		0.996	1.541		F_sep	1.35	2.01	ns		
BIAS		0.071	0.172							
SEP		0.999	1.540		Tobs_slope	1.22	0.39	ns	0.225	0.702
RSDyx		0.996	1.547							
Slope		0.990	0.995		MAE	0.55	1.17			
Intercept		0.984	0.321							
RSQ		0.994	0.994		Quartile75	1.19	1.87			
RPD		12.832	8.399							

scattering in the high porosity tablet samples, because low compression pressure results in tablets that are highly porous, liable to light scattering and photon attenuation phenomena which cause the deviation from Beer–Lambert law. Test sets 4 and 5, with variable precompression pressure and tableting speed, exhibited higher RMSEPs than test set 1; the observed difference was assumed to be either due to random error effects or the effect of precompression pressure and tableting speed. This was left to be confirmed with the predictions made by the global model. The hypothesis was that the difference could originate from the systematic effect of the tableting factors and not from random effects only if the RMSEP of test sets 4 and 5 decrease when the test sets are predicted by the global model which has the incorporated variability present in the respective test sets.

The global calibration model developed in DR mode was tested with the same five test sets. The RMSEP of test set 1 was lower than the local model test results. The RMSEP of test sets 2 and 3 were 1.63% and 1.71%, respectively, showing the decrease of 11% and 17% relative to the local model. The RMSEP for the test sets 4 and 5 decreased significantly, confirming that the three studied tableting parameters had a significant effect on NIR predictions in DR mode. The overall RMSEP value calculated for the 150 tablets of the 5 test sets was 1.54%. Table 5 summarizes the calculated RMSEP values.

Conclusion

A systematic and science-based approach to studying the critical factors in the tableting process that affect NIR spectra and calibration model performance was proposed in this work. The DoE study was carefully designed with particular attention to the studied responses. The authors suggest the use of AED as a response reflecting the influence of tableting process parameters on NIR spectral features. The effects of the studied factors on AED are independent of the spectral pretreatments or other parameters used during the calibration development. The disadvantage of evaluating the factor effects based on AED is that it does not directly reflect the performance of the developed NIRS model. The second studied response was the RMSEP. RMSEP values reflect the performance of NIRS calibration model but are dependent on the spectral pretreatments and parameters chosen during the modeling phase (number of principal components, wavenumber range and so on). The authors suggest the use of both responses in the interpretation of the effects of the tableting factors on the NIR spectral information of tablets.

Response surface modeling showed that compression pressure and tableting speed have a significant effect on the RMSEP and AED responses when DT measurement mode was used. The effect of precompression pressure was insignificant.

Compression pressure, precompression pressure and tableting speed have all shown a significant effect on the responses RMSEP and AED in DR measurement mode. RMSEP and AED were not always affected in the same way by the three studied factors. For that reason, the authors suggest studying the two responses and drawing the conclusions on the significance of factor effects based on interpretation of the both proposed response models. The effects of the studied factors on the RMSEP of the five independent test sets of caffeine tablets, which were predicted by the developed local and global calibration models, confirmed the conclusions of the DoE study.

The developed global calibration model for the prediction of the caffeine content of tablets in DT measurement mode exhibited an RMSEP of 1.21% calculated on the five test sets composed of 150 tablets. The global calibration model in DR mode performed with an RMSEP of 1.54% when tested on the same five test sets. Direct comparison clearly confirms the superior performance and better suitability of DT measurement mode in tablet analysis. The reason for this could be the larger sampling area in case of DT mode. However, both global models exhibited comparable performances to the UV-spectrophotometric reference method which performed with the standard error of 1%. For increased reliability of the results a larger data set would be needed: the sets used for the DoE study were based on 20 samples per experimental run which is considered to be the minimum statistically relevant number of observations. However, it should be pointed out that such a data set size might still not be sufficient for a validated method accepted by the regulatory authorities.

D-optimal design was chosen for this study for its great flexibility and customisability. However, the authors suggest that the study should be repeated using classical designs in order to compare the results.

Declaration of interest

The authors report no conflicts of interest. The authors alone are responsible for the content and writing of the article.

References

1. International Conference on Harmonization of Technical Requirements for Registration of Pharmaceuticals for Human Use. ICH Harmonized Tripartite Guideline, Pharmaceutical Development Q8 (R2). ICH [Online] 2009;4:1–28. Available from: http://www.ich.org/fileadmin/Public_Web_Site/ICH_Products/Guidelines/Quality/Q8_R1/Step4/Q8_R2_Guideline.pdf [last accessed 8 Nov 2013].
2. International Conference on Harmonization of Technical Requirements for Registration of Pharmaceuticals for Human Use. ICH Harmonized Tripartite Guideline, Quality Risk Management Q9. ICH [Online] 2005;4:1–23. Available from: http://www.ich.org/fileadmin/Public_Web_Site/ICH_Products/Guidelines/Quality/Q9/Step4/Q9_Guideline.pdf2 [last accessed 8 Nov 2013].
3. Gower JC. Euclidean distance geometry. Math Sci 1982;7:1–14.
4. Gower JC. Properties of Euclidean and non-Euclidean distance matrices. Lin Alg Appl 1985;67:81–97.
5. Dattorro J. Convex optimization and Euclidean distance geometry. USA: Meboo Publishing; 2005:19–32.
6. The United States Pharmacopoeial Convention. Rockville: United States Pharmacopoeia USP 29 NF 24; 2006.
7. Council of Europe. European Directorate for the Quality of Medicines. 5th ed. Strasbourg, France: European Pharmacopoeia; 2005.

2.2 Research Project II: Preliminary Study of an Offline Simultaneous Determination of Metoprolol Tartrate and Hydrochlorothiazide in Powders and Tablets by Reflectance Near-infrared Spectroscopy

2.2.1 Introduction

Near infrared spectroscopy (NIRS) belongs to vibrational spectroscopy. It covers the wavelength region of 750 – 2500 nm. The NIR signal is a consequence of the absorbance of light due to molecular vibrations (overtones and combinations of fundamental mid – IR vibrations) of hydrogen bonds like C-H, N-H, O-H, S-H. The benefits of NIRS are well recognized. It is fast, nondestructive, noninvasive analytical technique requiring minimal or no sample preparation. It is able to analyze various pharmaceutical dosage forms. Apart from the number of applications in drug development and quality control, NIRS has proved its efficiency as Process Analytical Technology (PAT) tool in monitoring the critical-to-quality attributes (CQAs) during the manufacturing process.

Existing guidelines on the development and validation of analytical methods (European Medicines Agency, 2012; PASG NIR Subgroup, 2001) suggest that the feasibility study should be done at the onset of analytical method development process. Feasibility study should reveal if the quantitative analysis is possible by initial assessment of the analyte concentration and the NIR spectral response. Linearity of the NIR response should be evaluated by correlating the spectral data with the reference values obtained from the primary analytical method, by using multivariate data analysis methods such as partial least squares regression (PLSR). Sample handling and presentation is investigated at this stage of method development. Repeated measurements of the same sample or representative subsamples should provide a first estimation of the random error and sampling error component of the NIR measurements. In the feasibility study, sample collection should be done to cover the necessary range of the analyte of interest and the variability expected during the routine use of the method. Factors that influence NIR spectral response should be studied, preferably using DoE methodology. Sample size should be suitable to provide the adequate performances of the method. Acquisition parameters should be optimized to give the NIR spectra with suitable signal-to-noise ratio and adequate repeatability on the same sample or the representative subsamples.

2.2.2 Reports – Simultaneous NIRS Quantification of Two APIs

Dou Y. et al. developed a method for simultaneous determination of paracetamol and diphenhydramine hydrochloride in powders using NIR spectroscopy and artificial neural networks (NN) (Dou Y. et al., 2005). The developed NN models based on the pretreated spectra, were compared with the PLS models. The NN models based on first derivative NIR spectra have shown superior performances. Dou Y. et al. have combined NN and principal component analysis (PCA) to simultaneously quantify aminopyrin and phenacetin in tablets (Dou Y. et al., 2006). The authors applied PCA to the pretreated NIR spectra and subsequently, the scores of the principal components were used as inputs nodes for the input layer instead of spectral data. The adopted approach was compared with the NN model based on the spectral data. The PC-NN model provided the best results. Blanco M. et al. developed a NIRS calibration models for simultaneous determination of five active principles in a pharmaceutical preparations (Blanco M. et al., 2006). The authors applied PLS1 algotithm for model development. It was reported that the selection of the calibration samples was crucial for the successful NIRS model development in complex matrices. Sample homogeneity was defined as one of the major difficulties to overcome. The methods have been validated according to ICH and EMA guidelines and have shown to be a good alternative to existing HPLC and redox titrimetric methods.

2.2.3 Reports – Simultaneous Quantification of HTZ and MTP

Garg G. et al. have developed UV-spectrophotometric and HPLC method for simultaneous determination of MTP and HTZ in tablets (Garg G. et al., 2008). The first method was created with seven mixed standards and the absorption maxima at 223 and 271 nm, respectively. Methanol was used as a medium. The developed HPLC method used reverse-phase C18 column with UV detection and methanol-water (95:5) as a mobile phase. Rawool N. D. et al. developed a method for simultaneous determination of HTZ and MTP using reverse-phase HPLC (Rawool N. D. et al., 2011). The authors have used C18 mobile phase with slightly different detection wavelength compared to Garg G. et al., and phosphate buffer – methanol mixture (60:40) as a mobile phase. Gupta K. R. et al. developed UV-spectrophotometric method for HTZ and MTP quantification (Gupta K. R. et al.,2008). The authors have used the absorption peaks at 257.8, 282.9 and 315 nm whereas, first two peaks were specific for MTP and the last one for HTZ. Gao F. et al. have reported the method for simultaneous determination of HTZ and MTP in human plasma by combined liquid chromatography – mass spectrometry (Gao F. et al., 2010). Stolarczyk M. et al. applied derivative spectrophotometry for simultaneous determination of HTZ and MTP in pharmaceutical preparations (Stolarczyk M. et al., 2006). Ramadan N. K. et al. reported a miniaturized membrane sensors for potentiometric

determination of HTZ and MTP (Ramadan N. K. et al., 2012). Alnajjar A. O. et al. developed capillary electrophoresis assay method for HTZ and MTP combined dosage form with the aid of multivariate data analysis tools (Alnajjar A. O. et al., 2013).

2.2.4 Study Aims

Simple and fast method was proposed in this work for the simultaneous determination of metoprolol tartrate and hydrochlorthiazide in powders and tablets by NIR reflectance spectroscopy. The proposed method was shown to be suitable for the feasibility study that should be undertaken and the onset of NIRS method development, indicating the suitability of NIRS method for the intended purpose. The use of the compaction simulator Presster® enabled the fast and cost-effective sample collection by mimicking the industrial rotary tablet press and enabled the robust design of the calibration data set for the NIR method development. Gravimetrical reference method – *Balance Reference Method* (BRM) was introduced as a quick and cost-effective alternative to compendial methods such as UV spectrophotometry or HPLC which are traditionally used for API content determination. BRM has shown adequate performances which enables it to be used at the stage of a feasibility study. Pharmaceutical Analytical Science Group (PASG) suggests that the gravimetrical data from the input ingredients could be used as reference values for NIRS method development (PASG NIR Subgroup, 2001).
With the proposed approach, the crucial information for the analytical method development could be gathered in a fast, simple and cost-effective way.

Research Project II is summarized in a manuscript titled "Preliminary study of an offline simultaneous determination of metoprolol tartrate and hydrochlorothiazide in powders and tablets by reflectance near-infrared spectroscopy" published in the Journal of Pharmaceutical Development and Technology (DOI: 10.3109/10837450.2014.949268).

Pharmaceutical Development and Technology

http://informahealthcare.com/phd
ISSN: 1083-7450 (print), 1097-9867 (electronic)

Pharm Dev Technol, Early Online: 1–6
 DOI: 10.3109/10837450.2014.949268

informa healthcare

RESEARCH ARTICLE

Preliminary study of an offline simultaneous determination of metoprolol tartrate and hydrochlorothiazide in powders and tablets by reflectance near-infrared spectroscopy

Branko Z. Vranic[1,2] and Thierry F. Vandamme[3]

[1]Department of Pharmaceutical Sciences, University of Basel, Basel, Switzerland, [2]BÜCHI Labortechnik AG, Flawil, Switzerland, and [3]CNRS 7199 Laboratoire de Conception et Application de Molécules Bioactives, Équipe de Pharmacie Biogalénique, Faculté de Pharmacie, Université de Strasbourg, Illkirch Cedex, France

Abstract

A preliminary study of the feasibility of using near-infrared spectroscopy (NIRS) for the offline simultaneous determination of metoprolol tartrate (MTP) and hydrochlorothiazide (HTZ) in powders and tablets has been carried out. An industrial tableting process was simulated using an instrumented tablet press replicator – Presster™. Conventional reference analytics were replaced with gravimetric analysis. The NIRS models for powder and tablet analysis were developed using 55 samples, and tested on 80 independent samples. Powder mixture components were weighed in glass vials to collect reference values, mixed and manually transferred to a tablet press replicator and compacted to form tablets. NIRS calibration models were developed using spectral and gravimetric reference data. The two model drugs were simultaneously quantified exhibiting root mean-squared error of prediction (RMSEP) of 1.69 and 1.31 mg for HTZ powder and tablet samples, respectively, and RMSEP of 3.15 and 3.00 mg for MTP powder and tablet samples, respectively. NIRS analysis of MTP and HTZ in powder and tablet form has not been reported elsewhere.

Keywords

Diffuse reflectance, hydrochlorothiazide, metoprolol tartrate, simulation, tablet press replicator

History

Received 25 November 2013
Revised 6 July 2014
Accepted 23 July 2014
Published online 14 August 2014

Introduction

Near-infrared spectroscopy (NIRS) has been investigated as a method for the simultaneous offline determination of metoprolol tartrate (MTP) and hydrochlorothiazide (HTZ) in both powder and tablet forms in this feasibility study. Existing guidelines on the development and validation of analytical methods[1,2] suggest that a feasibility study should be done at the onset of any analytical method development process; in this case, the feasibility study should reveal if a quantitative analysis is possible by initial assessment of an analyte concentration and NIRS response. The linearity of the NIR response was evaluated by correlating the spectral data with reference values obtained from the primary analytical method. A compaction simulator was used for calibration sample design and collection by mimicking an industrial rotary tablet press. The active pharmaceutical ingredient (API) content is traditionally determined using compendial methods such as UV spectrophotometry or HPLC; as an alternative to these methods, gravimetric analysis (balance reference method, BRM) was introduced in this study. The Pharmaceutical Analytical Science Group (PASG) states that gravimetric data from the input ingredients could be used as reference values for NIRS method development[2]. BRM has shown in this study suitable performance to be used at the feasibility stage of a method development. With the proposed alternative approach, useful information could be gathered for NIRS method development.

Address for correspondence: Branko Z. Vranic, Department of Pharmaceutical Sciences, University of Basel, Klingelbergstrasse 50, CH-4056 Basel, Switzerland. Tel: + 41 762739727. E-mail: branko.vranic@unibas.ch

Materials and methods

Materials

The two model drugs, HTZ and MTP were supplied by Sigma–Aldrich (Switzerland). Mean particle size of the HTZ was 124 ± 1.5 µm, with a moisture content of $0.51 \pm 0.2\%$. Mean particle size of the MTP powder was 64 ± 2.2 µm and moisture content $0.32 \pm 0.1\%$. Microcrystalline cellulose was supplied by the company FMC BioPolymer (Philadelphia, PA). The mean particle size was 106 ± 0.5 µm, and moisture content $4.3 \pm 0.1\%$.

Equipment

The Mettler Toledo AG (Greifensee, Switzerland) XS204 analytical balance XS 204 was used for weighing the powder components. Powders were mixed using a tumbling mixer, a Turbula T2A (Willy A. Bachofen AG Maschinenfabrik, Basel, Switzerland). A Malvern Mastersizer X (Malvern Instruments, Worcestershire, UK) was used to determine average particle size. An LP 16 M infrared balance (Mettler Toledo AG, Greifensee, Switzerland) was used for moisture content determination. Direct compression tableting was done on a Presster™ tablet press simulator (Metropolitan Computing Corporation, East Hanover, NJ). A NIRFlex N-500 FT-NIR spectrometer (BÜCHI Labortechnik AG, Flawil, Switzerland) with a diffuse reflectance

measurement cell was used for spectra acquisition. NIRCal 5.4 chemometric software (BÜCHI Labortechnik AG, Flawil, Switzerland) was used for generating the calibration models.

Methods

Preparation of powder and tablet samples

Metoprolol tartrate and HTZ were the drugs chosen for this study. Microcrystalline cellulose was used as the filler and dry binder for direct compression tableting using the tablet press simulator. Microcrystalline cellulose, MTP and HTZ were weighed on an analytical balance in 4 mL glass vials (15 mm $\times$ 45 mm, flat bottom) for each sample separately. About 55 samples covering the nominal drug content range of 60–140% (i.e. 18–42 mg of HTZ and 96–144 mg of MTP) were prepared for the NIRS calibration model development, and 80 samples were prepared separately as an independent test set. Microcrystalline cellulose was added to the drugs to make the constant weight of 250 mg. Nominal values of the HTZ and MTP powder weight were used as reference values for developing the NIRS calibration models. The powder samples in glass vials were bound together with a rubber band and placed in a 200 mL glass jar. This jar was then placed in the tumbling mixer for 300 s. The moving block of standard deviation (MBSD) method was applied for the determination of a mixing end-point[3,4]. After the mixing process, spectra of the powder samples were acquired on the NIR spectrometer in diffuse reflectance measurement mode; the powders were then manually transferred from the glass vials to the die of the tablet press simulator and compressed into tablets. Tableting speed was simulated by replicating tablet punch speeds at a given rates expressed as tablets per hour. The tableting speed replicated was 10 800 tablets per hour (tph), with a compression force of 6 ± 0.2 kN adjusted indirectly through setting the gap between upper and lower punch of Presster™ tableting station, and a set of flat face punches with 10 mm diameter was used. The weight of the tablets was kept constant at 250 mg. After the tableting process, tablets were weighed on the analytical balance to measure any weight loss and calculate the error component of the balance reference method (BRM); any weight loss may occur during the manual powder transfer from the glass vial to the tableting machine die and due to the tableting process itself. After weight determination, tablets were stored in a desiccator for 24 h to allow the post-compaction relaxation to finish. NIR spectra of the tablets were acquired in diffuse reflectance measurement mode.

NIR measurements

A NIRFlex N-500 FT-NIR spectrometer with a diffuse reflectance measurement cell and vial and tablet sample holder was used for the acquisition of the powder and tablet spectra. Each sample was measured 3 times. Diffuse reflection measurements were carried out with 8 cm^{-1} optical resolution, and the digital resolution was 4 cm^{-1}. The wavenumber range was 10 000–4000 cm^{-1}. Each spectrum was the average of 32 scans. Spectralon®[5] was used as an external reference. NIRCal 5.4 chemometric software was used for generating the calibration models. Figure 1 shows the pretreated spectra of the formulation components.

Balance reference method

Each component of the powder mixture for each sample was weighed in a glass vial on the analytical balance. The value of the powder component weight was used as a reference value for the NIRS calibration model development. The error of the balance reference method[6] was estimated using equation (1):

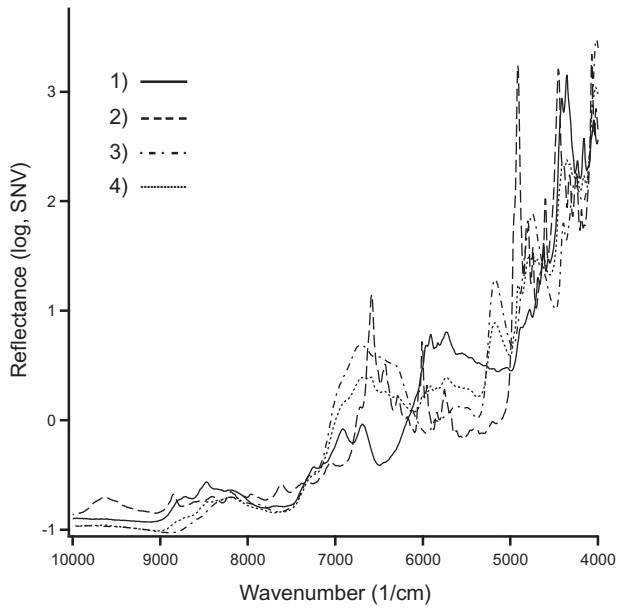

Figure 1. Pretreated spectra of microcrystalline cellulose (4), metoprolol tartrate (3), hydrochlorothiazide (2) and the powder mixture (1).

$$\text{Total error} = \sqrt{e_R^2 + e_1^2 + e_2^2 + Bias_2^2} \quad (1)$$

where e_R is the repeatability standard deviation of the analytical balance, e_1 the error of powder weighing, e_2 the error due to powder loss during tableting process and the manual transfer from a vial to a tableting machine die, and bias is the average difference between the powder mixture weight and tablet weight (average powder loss). The weighing error for 250 mg powder mixture was found to be 4.6 mg. The average percentage of HTZ in the powder mixture was 12%, i.e. the error on weighing HTZ was 0.55 mg. The average percentage of MTP in powder mixture was 48%, i.e. the error on MTP weighing was 2.21 mg.

NIR calibration model development and evaluation

Raw spectra were collected by scanning the powders and tablets on the NIR spectrometer in diffuse reflectance measurement mode. After selecting the spectral pretreatment, partial least squares regression (PLSR) was applied for correlating the spectral data with the drug content reference values for each individual substance. The NIRS calibration models developed were validated using a cross-validation method. The calibration set was divided into five property segments, and each segment was then iteratively left out of the data set and predicted by the model as calculated using the rest of the data set. The optimal number of principal components was chosen by observing the plot of principal components (PCs) against the standard error of cross-validation (SECV). The PCs giving the lowest SECV values were chosen. The models were tested using the independent test set which was made up of 80 samples. The developed NIRS models were judged based on the coefficient of determination (RSQ), standard error of calibration (SEC) and SECV. The Durbin–Watson test was applied to the prediction residuals to look for evidence of serial correlation between them. The first loading plot and the regression coefficient plot of the calibration model under evaluation were compared with the pretreated spectra of the pure analyte (MTP or HTZ) to evaluate the specificity of the model.

The calibration performance was evaluated by calculating the root mean-squared error of prediction (RMSEP) as a main performance indicator and the ratio of performance to deviation (RPD). According to Williams and Sobering, the RPD value can be used for descriptive calibration performance assessment[7]. RSQ of the test set predictions against reference analysis values was used to assess the linearity. Standard error of prediction (as a measure of a random prediction error) was calculated with associated confidence interval. The slope of the regression line and bias were tested for significance based on the Student's *t*-test. Population of the absolute prediction errors of the test set were evaluated, and the mean absolute error (MAE) and the third quartile of the respective population were calculated. Median absolute error is a measure of prediction residual dispersion, and is a robust statistic, being more resilient to outliers in a data set than a standard deviation. Quartiles are used to divide the populations into groups; the third quartile (Quartile75) of the absolute errors is the middle value between the population median and the maximum value of the population of the absolute errors. This was used to provide more information on the distribution of the absolute errors in the studied population.

Results and discussion

NIRS model for HTZ analysis in powders

The raw spectra of the 55 powder samples were log transformed and then Standard Normal Variate (SNV) spectral pretreatment was applied to reduce the optical pathlength differences. The full wavenumber range was used for the model calculation. The property range covered was 18.0–42.0 mg of the HTZ content. Calibration model was calculated on 163 spectra of powder samples exhibiting an RSQ of 0.95, SEC of 1.89 mg and SECV of 2.1 mg. The Durbin–Watson test result of 1.73 indicated that there was no significant correlation between the prediction residuals. The cross-validation property residuals were plotted against the HTZ reference values and the RSQ was 0.06, confirming good linearity of the developed calibration model. The developed calibration model was tested on the independent test set, consisting of 80 powder samples measured 3 times; the triplicates were then averaged; the property range was 18–42 mg of HTZ. An RSQ of 0.957 was achieved, and the RMSEP was calculated as a measure of the total error of the model and was found to be 1.70 mg. Bias was −0.04 mg and was tested for significance based on Student's *t*-test as described by ISO 12099[8]. The observed *t*-value for the bias was smaller than the critical *t*-value, which indicated that the bias was not significant with a probability of 0.84 (significance level 0.05), i.e. there was no significant systematic error observed in the predictions of the test set. The SEP value as a measure of a random model error was 1.71 mg; the confidence limit for the SEP was ±2.87 mg (significance level 0.05). RSD_{yx} as the standard error of the predicted y value for each x in regression was 1.7 mg. Compared to the estimated total error for HTZ balance reference method – 0.55 mg – prediction error of the test set for the HTZ calibration model of 1.7 mg was significantly higher. This could be attributed to inhomogeneity of the powder mixture, or imperfections in the glass vials which were used as powder sample holders for the NIR measurements. The slope of the regression line was 0.972; it was tested for the significance in accordance with ISO 12099, based on Student's *t*-test. The observed *t*-value was smaller than the *t*-critical, indicating that the slope was not significant with the probability of 0.24 (significance level 0.05). The ratio of performance to deviation (RPD) was found to be 4.8, which shows that the calibration performance was fair. The MAE was found to be 1.26 mg. The upper quartile in the studied population was found to be 2.11 mg.

The prediction residuals of the 80 test set powder samples were plotted and compared with the $\pm 2 \times$ SECV limits (2×1.71 mg) together with the bias in order to show the prediction performance and the magnitude of the bias. It was observed that no prediction residual was higher than the $\pm 2 \times$ SECV limit (Figure 2). The specificity of the model was confirmed by the fact that the samples with HTZ content of 18 mg (60%) that contained 142 mg of MTP (140%) were predicted just as well as the rest of the test set (the RMSEP for the 15 independent test samples was 1.71 mg), indicating that there was no significant spectral interaction between the two active pharmaceutical ingredients. Table 1 summarizes the calibration model test set statistics.

NIRS model for HTZ analysis in tablets

The raw spectra of the tablets used for the development of the NIRS calibration model were log transformed; SNV spectral pretreatment and first derivative were then applied to correct for baseline offsets and optical pathlength differences. The full wavenumber range was used for the model calculation. Six principal components were selected for model calculation. The property range covered was 18.0–42 mg of HTZ. Calibration was calculated on 151 spectra of the tablet samples exhibiting an RSQ of 0.988 and SEC of 0.9 mg; the SECV was 1.6 mg. The Durbin–Watson test result of 1.89 indicated that there was no significant correlation between the prediction residuals. The cross-validation property residuals were plotted against HTZ reference values; the RSQ was 0.03, confirming the good linearity of the developed calibration model. The developed calibration model was tested with an independent test set composed of 80 tablet samples measured 3 times on the NIR spectrometer and subsequently averaged. The test set tablets were prepared from the powder samples also used for the HTZ powder calibration model. The property range was 18–42 mg of HTZ. An RSQ of 0.976 was achieved, and the RMSEP was found to be 1.31 mg. Bias was −0.29 mg, and was tested for the significance based on the Student's *t*-test. The observed *t*-value for the bias was lower than the critical *t*-value, which indicated that the bias was not significant, with a probability of 0.051 (0.05 significance level), i.e. there was no significant systematic error observed in the

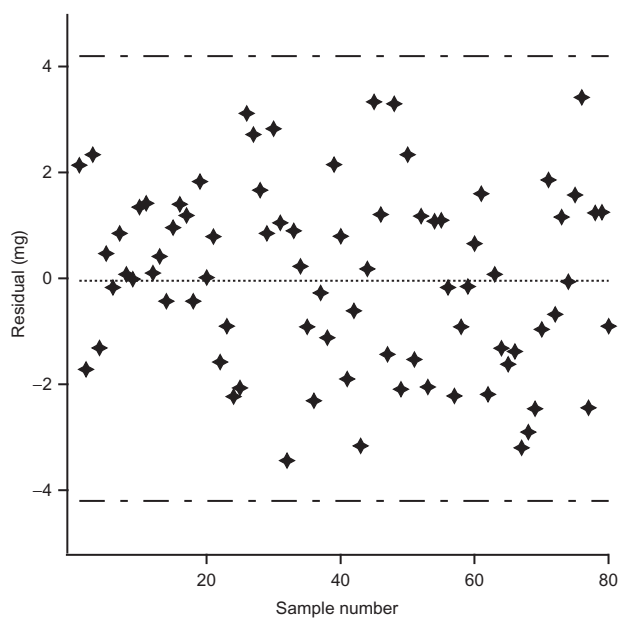

Figure 2. Hydrochlorothiazide test set predictions in powders – prediction residuals and bias versus $2 \times$ SECV limits.

Table 1. Hydrochlorothiazide powder and tablet calibration models – test statistics.

NIR % nominal = *f* (Reference % nominal)										
	NIR [% nominal]				Reference [% nominal]					
N = 80	Powder	Tablet					Powder	Tablet		
Average	29.66	29.92			29.63	Alpha	0.05	0.05		
Min	15.56	16.26			18.00	*T* value	1.99	1.99		**Probability**
Max	44.34	44.64			42.00	*F* value	1.37	1.37		**Powder** **Tablet**
SD	8.18	8.22			8.23				ns	0.842 0.051
			Powder	**Tablet**		Tobs_bias	0.20	1.98		
RMSEP			1.698	1.309					ns	
BIAS			−0.038	−0.292		F_sep	2.87	2.17		
SEP			1.708	1.284					ns	0.235 0.459
RSD*yx*			1.703	1.288		Tobs_slope	1.20	0.75		
Slope			0.972	0.987						
Intercept			0.863	0.680		MAE	1.26	0.79		
RSQ			0.957	0.976						
RPD			4.833	6.425		Quartile75	2.11	1.11		

N, number of samples; powder: figures of merit for HTZ predictions in powders; tablet: figures of merit for HTZ predictions in tablets; SD, standard deviation; RMSEP, root mean-squared error of prediction; SEP, standard deviation of the prediction residuals; RSD*yx*, standard error of the predicted *y* value for each *x* in regression model; RSQ, coefficient of determination; RPD, ratio of performance to deviation; Alpha, significance level; *T* value, *T* critical value of the Student's *T* test; *F* value, *F* critical value of the *F* test; Tobs_bias, *T* observed value returned from the BIAS significance testing according to ISO 12099; F_sep, SEP (SECV) of the validation set multiplied with *F* critical value for SEP (SECV) confidence limits estimation according to ISO 12099; Tobs_slope, *T* observed values returned from slope significance testing according to ISO 12099; probability, probability for the Student's *T* distribution calculated for the *T* observed values; MAE, mean of absolute errors; Quartile75, third quartile value for the absolute errors; ns, non-significant.

predictions of the test set. The SEP value was 1.28 mg; the confidence limit for the SEP was ±2.17 mg (level of significance 0.05). RSD_{yx} as the standard error of the predicted y value for each x in regression was 1.29 mg. The slope of the regression line was 0.987; it was tested for the significance as described by ISO 12099, based on the Student's *t*-test. The observed *t*-value was lower than *t*-critical, indicating that the slope was not significant with the probability of 0.46 (significance level 0.05). The median absolute error was found to be 0.79 mg. Upper quartile in the studied population of the test set prediction residuals was 1.11 mg.

The prediction residuals of the 80 test set tablet samples were plotted and compared with the ±2 × SECV limits (2 × 1.58 mg) together with the bias in order to show the prediction performance and the magnitude of the bias. It was observed that the two prediction residuals were higher than ±2 × SECV limit (Figure 3). Specificity of the model was confirmed by the fact that the samples with HTZ content of 18 mg (60%) that contain 142 mg of MTP (140%) were predicted just as accurately as the rest of the test set (the RMSEP for the 15 independent test samples was 0.88 mg), indicating that there was no significant spectral interaction between the two active pharmaceutical ingredients. Table 1 summarizes the test set statistics.

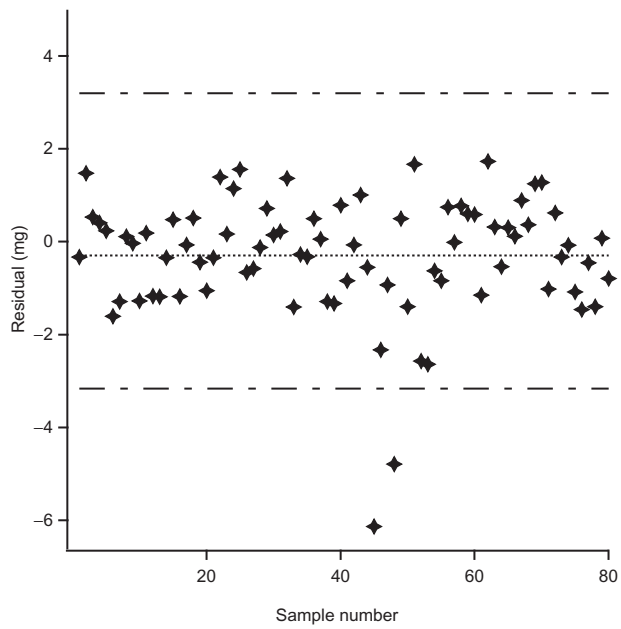

Figure 3. Hydrochlorothiazide test set predictions in tablets – prediction residuals and bias versus 2 × SECV limits.

NIRS model for MTP analysis in powders

The calibration model was developed with 55 powder samples. The raw spectra were pretreated using SNV spectral pretreatment and first derivative Savitzky-Golay 9 points, gap 0. The wavenumber ranges of 4000–5080 cm^{-1} and 5440–9000 cm^{-1} were used to calculate the model. The first loading vector of the initially calculated model indicated that there is a high correlation between MTP content and the OH group absorption band of the microcrystalline cellulose and water (5080–5440 cm^{-1}), so the respective wavenumber region was excluded from the model calculation. Seven principal components were selected to calculate the model. The property range covered was 96–144 mg of MTP. The calibration was calculated using 143 spectra of powder samples exhibiting an RSQ of 0.99 and an SEC of 1.46 mg; SECV was 3.1 mg. The Durbin–Watson test statistics of 1.88 indicated that there was no significant correlation between the cross-validation residuals. The residuals were plotted against HTZ reference values, and the RSQ was 0.03, confirming good linearity of the developed calibration model. The developed calibration model was tested on the independent test set which consisted of 80 powder samples measured in triplicate; the triplicates were then averaged to give a single spectrum. The property range was 96–144 mg of MTP, and an RSQ of 0.964 was achieved. Linearity was further assessed by plotting the prediction residuals against reference values and the NIR predicted values. Neither linear correlation nor specific pattern among residuals was observed. The RMSEP was calculated as a measure of the total error of the model and was found to be 3.24 mg. Bias was −0.62 mg and was tested for the significance based on the

Student's *t*-test. The observed *t*-value for the bias was lower than the critical *t*-value which indicated that the bias was not significant with probability of 0.09 (significance level 0.05), i.e. there was no significant systematic error observed in the predictions of the test set. The SEP value as a measure of a random model error was 3.2 mg. The confidence limit for SEP was ±4.34 mg (significance level 0.05). RSD_{yx} as the standard error of the predicted *y* value for each *x* in regression was 3.22 mg. The slope of the regression line was 0.987. It was tested for the significance according to Student's *t*-test. The observed *t*-value was lower than the *t*-critical, indicating that the slope was not significant with the probability of 0.56 (significance level 0.05). The median absolute error was found to be 1.12 mg. The upper quartile in the studied population was 2.18 mg.

The prediction residuals of the 80 test set tablet samples were plotted and compared with the ±2 × SECV limits (2 × 3.08 mg) together with the bias. It was observed that six prediction residuals were higher than ±2 × SECV limit (Figure 4). Specificity of the model was confirmed by the fact that the samples with MTP content of 96 mg (60%) that contain 42 mg of HTZ (140%) were predicted as accurately as the rest of the test set (the RMSEP for the 14 independent test samples was 2.86 mg), indicating that there was no significant spectral interaction between the two active pharmaceutical ingredients. Table 2 summarizes the calibration model test set statistics.

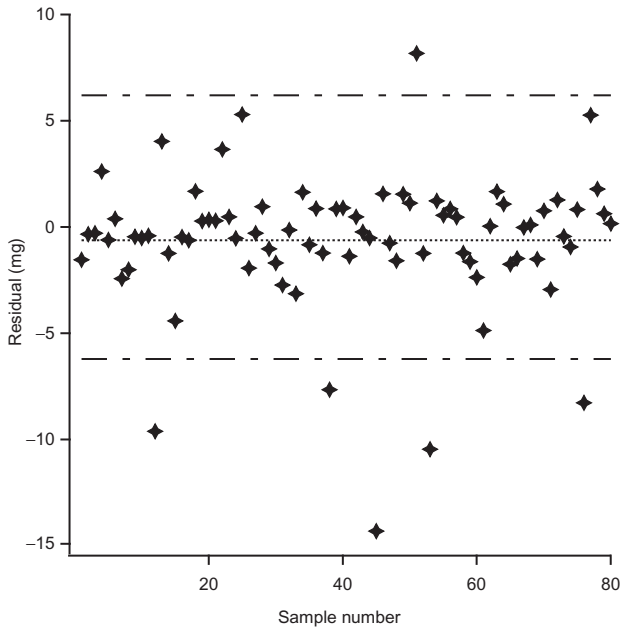

Figure 4. Metoprolol tartrate test set predictions in powders – prediction residuals and bias versus 2 × SECV limits.

NIRS model for MTP analysis in tablets

The calibration model was developed with 55 tablet samples. The raw spectra were pretreated using Multiplicative Scatter Correction (MSC) pretreatment and first derivative Savitzky-Golay 9 points, gap 0. The wavenumber ranges 4000–5080 cm^{-1} and 5440–9000 cm^{-1} were used to calculate the model. Eight principal components were selected to calculate the model. The property range covered was 96.0–144 mg of MTP. The calibration was calculated using 143 spectra of the tablet samples, exhibiting an RSQ of 0.99 and SEC of 1.18 mg; SECV was 3.26 mg. The Durbin–Watson test statistics of 2.1 indicated that there was no significant correlation between the cross-validation residuals. The residuals were plotted against HTZ reference values. The RSQ was 0.03, confirming good linearity of the developed calibration model. The developed calibration model was tested on the independent test, 80 tablet samples measured in triplicate with triplicates then averaged to give a single spectrum. The property range was 96–144 mg of MTP. An RSQ of 0.968 was achieved. Linearity was assessed further by plotting prediction residuals against reference values and the NIR predicted values. Neither linear correlation nor specific pattern among residuals were observed. The RMSEP was found to be 3.05 mg. Bias was −0.47 mg and was tested for the significance based on Student's *t*-test. The observed *t*-value for the bias was lower than critical *t*-value, which indicated that the bias was not significant with a probability of 0.17 (significance level 0.05), i.e. there was no significant systematic error observed in the predictions of the test set. The SEP value as a measure of the random model error was 3 mg; the SEP confidence limit was ±4.5 mg (significance level 0.05). RSD_{yx} as the standard error of the predicted y value for each x in regression was 3 mg. The slope of the regression line was 0.99. It was tested for the significance based on Student's *t*-test, and the Observed *t* value was smaller than the *t*-critical indicating that the slope was not significant, with the probability of 0.62 (significance level 0.05). The median absolute error was found to be 0.94 mg. The upper quartile in the studied population of the test set absolute prediction errors was 1.65 mg.

The prediction residuals of the 80 test set tablet samples were plotted and compared with the ±2 × SECV limits (2 × 3.26 mg)

Table 2. Metoprolol tartrate powder and tablet calibration models – test statistics.

NIR % nominal = *f* (Reference % nominal)											
	NIR [% nominal]				Reference [% nominal]						
N = 80	Powder	Tablet			120.45		Powder	Tablet			
Average	121.07	120.92			96.00	Alpha	0.05	0.05			
Min	90.72	89.99			144.00	*T* value	1.99	1.99		**Probability**	
Max	154.45	156.23			16.80	*F* value	1.47	1.38		**Powder**	**Tablet**
SD	16.89	16.91			120.45				ns	0.091	0.171
			Powder	**Tablet**		Tobs_bias	1.71	1.38			
RMSEP			3.147	3.046					ns		
BIAS			−0.624	−0.474		F_sep	4.61	4.51			
SEP			3.110	3.028					ns	0.556	0.623
RSD*yx*			3.216	3.043		Tobs_slope	0.59	0.49			
Slope			0.987	0.990							
Intercept			2.157	1.685		MAE	1.09	0.94			
RSQ			0.964	0.968							
RPD			5.286	5.592		Quartile75	2.10	1.65			

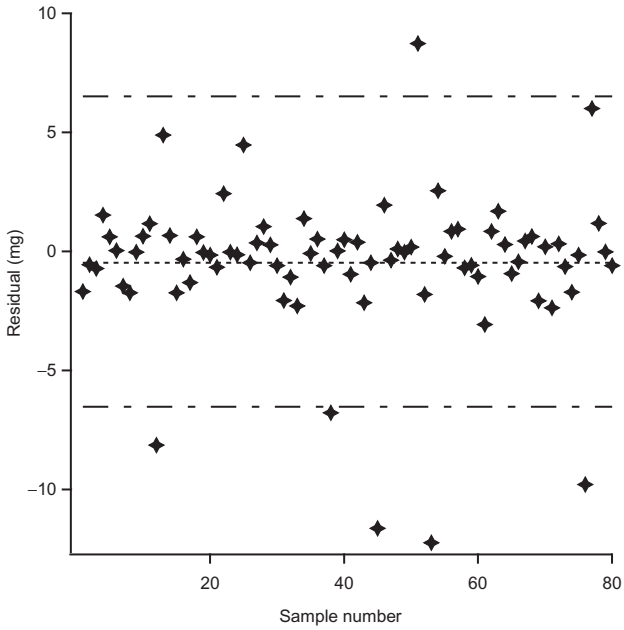

Figure 5. Metoprolol tartrate test set predictions in tablets – prediction residuals and bias versus 2 × SECV limits.

together with the bias. It was observed that six prediction residuals were higher than ±2 × SECV limit (Figure 5). Specificity of the model was confirmed by the fact that the samples with MTP content of 96 mg (60%) that contain 42 mg of HTZ (140%) were predicted as accurately as the rest of the test set (the RMSEP for the 14 independent test samples was 3.25 mg), indicating that there was no significant spectral interaction between the two active pharmaceutical ingredients. Summary of the calibration model test set statistics is shown in Table 2.

Conclusion

EMA, ICH and PASG guidelines on NIRS method development and validation suggest that a feasibility study should be carried out at the start of any method development to evaluate the suitability of NIRS for the intended analytical purpose.

The authors suggest that the experimental setup for the development of an offline NIRS method for quantification of HTZ and MTP in both powder and tablet forms as proposed in this work shows the feasibility of this method and could be a useful alternative for the initial stages of NIRS method development.

The proposed approach could be applied for the optimization of sample presentation and scanning, study of the variables affecting spectral response, the evaluation of the quality of NIR scans, the effect of powder inhomogeneity and so on.

However, the studied approach is an offline, preliminary study of the suitability of NIRS to quantify the two model drugs in one formulation under controlled circumstances. The processes, formulation and other variability factors actually seen in commercial scale manufacturing should also be studied.

Declaration of interest

The authors report no conflicts of interest. The authors alone are responsible for the content and writing of the article.

References

1. European Medicines Agency, Committee for Human Medicinal Products (CHMP), Comity for Veterinary Medicinal Products (CVMP). Guideline on the use of Near Infrared Spectroscopy (NIRS) by the pharmaceutical industry and the data requirements for new submissions and variations. London: European Medicines Agency; 2012:1–28.
2. PASG Guidelines for the development and Validation of Near-Infrared (NIR) Spectroscopy methods. PASG NIR Subgroup [Online]; 2001:1–40. Available from: http://www.pasg.org.uk/NIRmay01.pdf [last accessed 15 Nov 2013].
3. Hailey PA, Doherty P, Tapsell P, et al. Automated system for the on-line monitoring of powder blending processes using near-infrared spectroscopy part I. System development and control. J Pharm Biomed Anal 1996;14:551–559.
4. Momose W, Imai K, Yokota S, et al. Process analytical technology applied for end-point detection of pharmaceutical blending by combining two calibration-free methods: simultaneously monitoring specific near-infrared peak intensity and moving block standard deviation. Powder Technol 2011;210:122–131.
5. Bruegge CJ, Stiegman AE, Rainen RA, Springsteen AW. Use of Spectralon as a diffuse reflectance standard for in-flight calibration of earth-orbiting sensors. Opt Eng 1993;32:805–814.
6. Bevington PR, Robinson DK. Data reduction and error analysis for the physical sciences. New York: McGraw-Hill Inc.; 1992:36–51.
7. Williams PC. Implementation of near-infrared technology. In: Williams P, Norris K, eds. Near-infrared technology in the agriculture and food sciences. St. Paul (MN): American Association of Cereal Chemists; 2001:145–169.
8. International Conference for Standardization. ISO 12099: 2010 – Animal feeding stuffs, cereals and milled cereal products Guidelines for the application of near infrared spectrometry. ISO [Online]; 2010:1–30. Available from: http://www.iso.org/iso/catalogue_detail.htm?csnumber=51197 [last accessed 15 Nov 2013].

2.3 Research Project III: Assessing Compressibility and Compactibility of Powder Formulations Using Near-Infrared Spectroscopy

2.3.1 Study Aims

In the research project III the authors have proposed an NIRS method as an alternative to the conventional determination of tablet relative density and tensile strength. Multivariate prediction models for the respective tablet parameters were developed. Powder formulations chosen for the study were compressed into tablets with different relative densities and tensile strengths. NIR spectra of the produced tablets were collected and subsequently relative density and tensile strength of the produced tablets were determined conventionally. Multivariate prediction model for the estimation of relative density and tensile strength of the tablets has been developed based on the NIR spectra and traditionally determined tablet parameters. The predicted tablets parameters and the traditionally determined ones were fitted into mathematical equations used for the evaluation of powder compressibility and compactibilit. The outcomes of the two approached were compared.With the proposed NIR spectroscopic approach, an alternative method for the assessment of compaction properties of powder formulations was established and evaluated.

Research Project III is summarized in a manuscript titled "Assessing compressibility and compactibility of powder formulations with Near-Infrared Spectroscopy" published in the Journal of Pharmaceutical Development and Technology (DOI: 10.3109/10837450.2012.663388).

Pharmaceutical Development and Technology, 2013; 18(1): 156–171

ISSN 1083-7450 print/ISSN 1097-9867 online
DOI: 10.3109/10837450.2012.663388

informa
healthcare

RESEARCH ARTICLE

Assessing compressibility and compactibility of powder formulations with Near-Infrared Spectroscopy

Nicolaos D. Gentis, Branko Z. Vranic, and Gabriele Betz

Department of Pharmaceutical Sciences, Industrial Pharmacy Research Group, University of Basel, Basel, Switzerland

Abstract

Context: The compressibility and compatibility of a powder formulation is usually determined by compaction and following destructive tensile strength and relative density measurement of the final compact.

Objective: In this study, a non-destructive method with Near-Infrared Spectroscopy (NIRS) was designed and evaluated for the measurement of powder compressibility and compactibility.

Materials and Methods: 12 different formulations with a wide range of difference in properties were investigated by compaction and analysis of the resulting tablets. Two similar tablet batches were produced with every formulation. Relative density and tensile strength were measured with the traditional, destructive method on one tablet batch while a newly developed non-destructive chemometric NIRS method was applied for the second batch. The outcomes of the two approaches were compared to validate the developed method. All data sets were applied to three established mathematical equations to calculate equation factors, which are claimed to represent the formulation compressibility and compactibility. The study focus was set on the equation factor value comparison between the traditional and the newly designed method.

Results & Discussion: The results showed a high similarity between the outcomes of the two methods. An essential difference was noticed for the outcomes of the equation factors after application to the Leuenberger equation.

Conclusion: The approach with the NIRS is suggested as a promising tool for a reliable inline quality monitoring in the tablet manufacturing process.

Keywords: Solid dosage form, powder compaction, tablet, quality, development, drug design

Introduction

The most common dosage form on the pharmaceutical market is the tablet. The production of tablets should be as economical as possible and the production should only comprise a few working steps.[1] Studies of tablet formation by direct compression are focused on single powders, powders with small percentage of binder and granulated powders. Since it is a big challenge to predict the compaction properties of powder mixtures from the properties of the individual components, a main focus has been set to the development of prediction techniques for a successful design of reliable powder formulations.[2] The main prerequisite for a reliable formulation is a satisfactory compressibility of the powder and tensile strength of the final compact in an acceptable range.

All the mechanisms and phenomena of powder compaction have been the subject of numerous research investigations and already a wide variation of compaction parameters and used equipment have been investigated.[3] Nevertheless, the compaction process is still far from being completely understood. Multitudinous powder properties and external factors have an impact on the quality of the final tablet.[1,4–6]

This leads in the last decades to the choice of many different approaches for characterization of powder compaction along with the development of numerous mathematical equations. The choice of the most

Correspondence: Nicolaos D. Gentis, Department of Pharmaceutical Sciences, Industrial Pharmacy Research Group, University of Basel, Klingelbergstr 50, Basel, 4056, Switzerland. E-mail: n.gentis@unibas.ch

(Received 22 July 2011; revised 28 November 2011; accepted 26 January 2012)

preferable equation out of this wide collection is challenging because every equation can be applied only to a constricted range of compaction force and to a limited number of materials.[7,8]

The relative density of a compact and its tensile strength can be seen as a basic and crucial tablet quality characteristic. The relative density is assumed as the true area of contacts between particles as a result of interparticulate bonds. It is usually calculated with the true density value of the powder[9] and represents in an inverse way the porosity of the compact.

The mechanical strength is a very important tablet property since it has crucial impacts on itspharmacokinetical and pharmacodynamical behaviour. The strength depends on several processing and formulation parameters. An essential focus is set on this parameter for characterising the mechanical behaviour of a compact, as the tablet must possess a minimum mechanical strength to sustain potential loading during processing and handling.[2,10]

A compaction equation relates compaction elements with the applied compaction pressure. The initial step for fitting the data to an equation is to linearize the data and the corresponding plots. With this approach, comparisons between data sets are simplified and also the fitting parameters of the applied equations can be used for data comparison.

Till today, numerous equations have been proposed for the analysis of the compaction process. While some seem to have a theoretical basis, for example, the Kawakita[11] equation, many of them are purely empirical fits of specific limited data and cannot claim any general validity.[12]

For a reliable and satisfying application of compaction equation to investigate and compare compression of powder formulations, an equation should not only linearize the data.[12] The parameters should relate to basic physical and mechanical properties of the compacted material. Ideally the equation should be allowed to be applied to all materials which are compacted in the same way.

The compressibility measurement of powder formulations with support of mathematical equations has been since a longer time ago a main target for scientific research. The main principle is the analysis of quantitative data like a relation of pressure to volume reduction or the relation of the applied pressure to the corresponding porosity.[11] The aim of this calculation step is the determination of a linear relation and in a second step the comparison between powder formulations.

One of the most known mathematical approaches for the evaluation of tablet compressibility is the Heckel-equation. The detailed evaluation of the Heckel-equation was performed and published by J.M. Sonnergaard[11] and P.J. Denny.[12]

Celik and Marshall[3] investigated numerous excipients by developing the corresponding Heckel-Plots. Nonlinearity was observed in many of these profiles, which were obtained under dynamic conditions.

A modified Heckel equation was designed by Kuentz and Leuenberger,[13] which takes into consideration the pressure susceptibility, defined as decrease of porosity under pressure. The classical Heckel-equation assumes a constant pressure susceptibility while in the designed modified Heckel-equation the susceptibility corresponds to the relative density. In addition, a term for the critical density has been introduced, which represents the specific relative density where a rigidity between the punches starts to occur.

The ability of a powder formulation to be compressed into tablets with specified strength can be expressed as the formulations' compactibility. Leuenberger developed an equation,[14] which includes one factor for the compressibility and one for the compactibility. This inclusion of the compactibility term makes this equation, the so-called Leuenberger equation, an attractive tool for investigating powder formulations.

Near-infrared spectroscopy (NIRS) is an analytical technique with various applications in the pharmaceutical field. Major advantages of NIR spectroscopy are its non-destructive nature, no need for sample preparation and immediate delivery of results. NIRS has proven its ability to analyze intact pharmaceutical dosage forms such as tablets.

Quantification and qualification of active pharmaceutical ingredients and other tablet constituents is well established.[15–20] Tablet physical properties, for example, relative density and tensile strength, contribute to high extent to NIR signal[21] and are usually considered as interferences. Various spectral preprocessing methods were applied to NIR spectra in order to minimize these effects.[22] Variations in compression force during tableting process have been reflected in variable relative densities and tensile strengths of the tablets. This effect is observed in NIR spectra as baseline shift.[23,24] The spectral effect caused by varying relative density/tensile strength could be used to quantify these tablet parameters.[25,26]

Theoretical section

For this study, the compaction outcomes have been plotted with the Heckel-Plot,[27,28] the modified Heckel-Plot[29] and the Leuenberger equation.[14,30]

Heckel-Plot

The Heckel-Plot is still one of the most commonly used equation in the pharmaceutical compaction studies. It was published by R.W. Heckel in 1961.[27,28] In this equation, the first-order kinetics type of reaction behaviour of the voidage reduction with applied pressure has been approached.

$$\ln\frac{1}{1-D} = k \cdot P + A \tag{1}$$

where D is the relative density of a powder compact at pressure P. Constant k is a measure of the plasticity of a compressed material.

The Constant *A* is related to the die filling and particle rearrangement before deformation and to the bonding of the discrete particles.

Modified Heckel-Plot

The pressure susceptibility (χ_p) is defined as the decrease of porosity under pressure. This term is assumed to be constant in the Heckel-Plot.

Kuentz and Leuenberger[29] incorporated the pressure susceptibility (χ_p) in their calculation and developed a modified Heckel-Plot:

$$\sigma = \frac{1}{c}\left[\rho_c - \rho - (1-\rho_c)\cdot \ln\left(\frac{1-\rho}{1-\rho_c}\right)\right] \quad (2)$$

ρ is the relative density, σ is the pressure, ρ_c is the critical density and *C* is a constant, which is claimed to represent the compressibility of a powder.

For the compressibility calculation of powder formulations, the constant *K* from the Heckel equation and the constant C from the modified Heckel equation can be determined.

Well compressible, ductile and soft powders have higher values for *C* and *K* than poor compressible, brittle and hard powders.

The parameter ρ_c is defined as rigidity threshold. It represents the critical relative density, producing a negligible mechanical resistance between the punches. With a geometrical focus, this threshold represents the transition point between dispersed solid in air and voids in a solid matrix.

Leuenberger equation

This equation was developed and published in the early 1980s by H. Leuenberger.[14,30]

$$\sigma_t = \sigma_{t\max}\cdot(1-e^{-\gamma\sigma p_r}) \quad (3)$$

σ_{tmax} is the tensile strength (kg/cm²) when *P* (compression pressure) → ∞, ρ_r → 1, and γ is compression susceptibility, expressing the compressibility of the powder formulation.

This equation allows the compressibility to be further determined and in a second step the compactibility, defined as the ability of the powder to be compressed to a tablet of specific strength, can be evaluated by focusing on the maximum tensile strength σ_{tmax}.

Each of these three described equations contains a specific factor which is claimed to represent the compressibility of the formulation.

By fitting the measured and recorded compaction data to these three mathematical equations, those technical factors (k, C, γ) can be calculated and evaluated.

Since these factors represent the similar tablet quality parameter, the outcome values were expected to show a certain proportionality between each other for the whole collection of formulations.

PLS regression for evaluation of NIRS signals

Partial least squares regression (PLS regression) is a statistical method to create a linear regression model by projecting the predicted variables (y) and the observable variables (x) to a new space.[31] PLS finds the fundamental relations between the matrix of predictors (X matrix) and the matrix of responses (Y matrix), that is, it can be seen as a latent variable approach to model the covariance structures in these two matrices. The goal of PLS regression is to predict Y from X and to describe their common structure. A PLS model to determine the multidimensional direction in the X space explains the maximum multidimensional variance direction in the Y space. PLS regression is particularly useful when the matrix of predictors has more variables than observations, and when there is multicollinearity among x values. It can analyze data with strongly collinear, correlated, noisy, and numerous x variables, and also simultaneously model several response variables.

Aim of the study

In this article, the authors propose a NIRS method as an alternative to the conventional determination of tablet relative density and tensile strength. Multivariate prediction models for the respective tablet parameters were created. Every chosen formulation was compressed into tablets with different relative densities.

As next step, the tablet parameters of tensile strength and relative density were measured with NIR and also in the traditional way. The data set with the values received from the NIR spectras and also the data of the traditional method were fitted into mathematical equations used for the evaluation of powder compressibility and compactibility properties. The outcomes of the two data set evaluations were compared and tested for potential similarity.

With this approach, an alternative method for the assessment of compaction properties of powder formulations was established and evaluated.

Materials and methods

Materials

For a reliable study of the compressibility measurement with the support of NIRS, favoured excipients differing in mechanical properties (compressibility, ductile or brittle behaviour under pressure, disposition of sticking, etc.) were chosen to be investigated.

Also binary mixtures of a poorly compressible API and a well-compressible filler were investigated and evaluated in this study.

An overview list of all investigated formulations is given in the following Table 1.

Mefenamic acid (Sigma-Aldrich Inc., Batch 093K1608) and Paracetamol (Mallinckrodt, Batch 0048992565) were chosen as brittle, poorly compressible API. They have both a similar particle size distribution. Mefenamic acid[32,33] differs basically from Paracetamol because of

Table 1. List of investigated powder formulations.

Formulation	Drug load (%)
Single powder	
MCC 101 L	
MCC 102 G	
Emcompress anhydrous	
Starch 1500	
Binary mixture	
Paracetamol/MCC 101 L	20
Paracetamol/MCC 101 L	40
Paracetamol/MCC 102 G	30
Mefenamic acid/MCC 101 L	20
Mefenamic acid/MCC 102 G	20
Mefenamic acid/MCC 102 G	40
Paracetamol/Parteck M 200	20
Paracetamol/Parteck M 300	20

its very high tendency to stick on the die wall and the punches.

The microcrystalline celluloses MCC 101 L (Pharmatrans Sanaq AG, Basel, Switzerland) and MCC 102G (Pharmatrans Sanaq AG, Basel, Switzerland) were chosen as ductile, well compressible excipients. Both are known for their high compressibility, even they differ in particle size.[34–36]

The directly compressible Mannitol products Parteck M200 and Parteck M300 (Merck KGaA, Darmstadt, Germany) show a plastic deformation behaviour during compaction.[36]

Anhydrous calcium hydrogen phosphate (Emcompress anhydrous, JRS Pharma, Rosenberg, Germany) can be used as excipient or as a calcium source in nutritional supplements. The predominant deformation mechanism for this powder is brittle fracture. This simplifies the scale-up to market production since the sensitivity to the strain-rate is reduced. However, at higher pressures, capping and lamination can occur. In this study, Emcompress anhydrous was chosen for investigating the influence of brittle deformation on the compressibility prediction with NIR. For the compaction of Emcompress, an external lubrification of the punch and die wall with Magnesium Stearate (Mg-stearate, Sandoz AG, Basel, Switzerland) was performed to keep the sticking tendency of the powder and the tablet ejection force on acceptable levels.

Pregelatinized starch (Sta-Rx 1500, Colorcon, Idstein, Germany) is a modified starch which is chosen in tablet production as binder, disintegrant and diluent[37]. Its compressibility is not very satisfying, but a plastic behaviour under pressure is mentioned in the literature.[38]

A detailed overview of the individual deformation behaviour of the investigated compounds can be seen in the Table 2 (information taken from (ref. 38)).

True density measurement

The true density of the investigated powders was measured with an AccuPyc 1330 helium pycnometer (Micrometrics, Norcross, GA, USA). Values were determined as the mean of three or five parallel measurements.

Table 2. Deformation mechanisms of investigated powders.

Material	Deformation mechanism
Paracetamol	Elastic, Brittle
Mefenamic acid	Brittle, sticky
Microcrystalline Cellulose powder MCC 101,102	Viscoelastic
Emcompress anhydrous powder	Brittle
Parteck M200, M300	Plastic
Sta-Rx 1500	Plastic

Design of binary powder mixtures

All powders were sieved (mesh size 355 μm) before weighting and mixing (Turbula mixer, Type T2A, Willy A. Bachofen AG Maschinenfabrik, Basel, CH) for 5 min. After the second sieving (mesh size 355 μm), the formulation was mixed for further 5 min.

Methods: Calculation of the true density for binary mixtures

The true density of the binary mixtures was calculated using the obtained results of the true density measurements for all starting materials (see Equation 4):

$$\rho_{true[mixture]} = \frac{C_{API[\%]} \times \rho_{true[API]} + C_{Excipient[\%]} \times \rho_{true[Excipient]}}{100} \quad (4)$$

where $C_{API[\%]}$ is the concentration of active ingredient, $C_{Excipient\ [\%]}$ is the concentration of the excipient, $\rho_{true[API]}$ and $\rho_{true[Excipient]}$ are the corresponding true densities.

Particle size distribution

A Malvern Mastersizer X (Malvern Instruments, Worcestershire, UK) was applied to determine the average particle size by laser diffraction. Three measurements were performed for each sample. The values of mean and median particle size, the span and the specific surface area were detected.

Powder compaction

The powder compaction was operated using a mechanical compaction simulator (Presster, Metropolitan Computing Corporation, New Jersey, USA). The tablet press Korsch PH336 with 36 stations was simulated. A flat-faced B-Tooling with 10 mm of diameter was chosen for compacting tablets of 300 mg weight. The powder feeding was performed manually and an external lubrification was applied to prevent sticking of punches and tools during compaction.

In a first step, some preliminary experiments were performed to determine the maximal gap, where a robust tablet could be produced. Then, the gap was decreased continuously in small steps to receive resulting compaction forces from 0.5 kN to 20.0 kN.

For every formulation, two different compaction speeds were applied. One was corresponding to 100,000

tablets/h (dwell time: 9.6 ms) and the second was corresponding to 216,000 tablets/h (dwell time: 4.4 ms). A batch of around 40–80 tablets was produced with lower speed and one batch of around 40–80 tablets was produced with application of the higher speed. Every batch contained tablets with a uniformly distributed range of applied compaction force, from 0.5 kN to 20.0 kN. This compaction design led to a wide distribution of the final compacts relative density.

Measurement of tablet tensile strength

The breaking force of the produced tablets was measured with the Tablet Tester 8 M (Dr. Schleuniger, Pharmaton, Switzerland). The tensile strength was calculated according to Equation 5.

$$TS = \frac{2 \cdot CS}{\pi \cdot D \cdot T} \quad (5)$$

where TS is the tensile strength [N/cm^2], CS is the crushing force [N], D is the diameter [cm], and T is the thickness [cm] of the tablet. The diameter and thickness of tablets were measured with a 3-button digital calliper.

NIR measurements

Spectra were recorded in diffuse transmission measurement mode on a Fourier transform near infrared spectrometer NIRFlex N-500 (Büchi Labortechnik AG). A Diffuse Transmittance measurement module, mounted on a polarization interferometer, was equipped with tablet sample plate with ten iris apertures. Source of radiation was a Tungsten halogen lamp. Temperature controlled Indium-Galium-Arsenide (InGaAs) detector was positioned externally, above the sample holder. Each spectrum was an average of 64 scans at a resolution of 16 cm^{-1}. Spectra were scanned over the spectral range of 11520–6000 cm^{-1} (870–1660 nm). In total, 1381 data points were collected (Data point interval: 4, Apodisation for phase correction: Blackman, Photometric dynamic range: 2 AU, Wavelength accuracy: ±0.2 cm^{-1}, Signal to noise ratio: 10000, Number of scans per second: 2–4, Analog-Digital- Changer: 24 Bit). 1203 tablet spectra from 22 batches were collected by NIRWare software (Büchi Labortechnik AG) and further analyzed by NIRCal 5.2 chemometrics software (Büchi labortechnik AG). The NIR spectras were measured 48 h after compression and storage of the compacts in a glass dessicator over white silica gel beads (1–3 millimeters layer).

Model development

In the conducted study all tablet samples were prepared from the materials that originate from the same lot. For preparing the samples, the components were weighed in a glass bottle. The tableting mixture was prepared in a mix-sieve-mix manner and subsequently compressed. The tablet samples for calibration, internal and external validation were prepared in a same manner (in a separate glass bottles from the components that are from the same lot). The total ratio of the samples in a calibration/internal validation/external validation set was 25%/25%/50%. Samples in all the sets were spanning the relative density range from 0.5 to 1.0 and tensile strength range from 0.1 to 9.4 MPa. Spectral preprocessing methods were applied to the raw spectra in order to reduce the excessive baseline variations and ordinate offsets caused by different physical properties of the samples and to group the spectra with similar values of analyzed tablet parameters. The light scattering information is correlated to the relative density and tensile strength of the compacts and enables the quantification of these parameters. Standard Normal Variate (SNV) and Normalization by Closure (ncl) were applied to reduce the scaling of the spectra due to very wide range of the compact porosity. Normalisation by Closure (ncl) spectral pretreatment is used to reduce the baseline variations due to different particle size or packing density differences.[39] It is a wavelength dependent pre-processing method. Savitsky-Golay first derivative (9 points) was used to correct for the baseline offsets and to minimize the noise by imposing the signal smoothing effect.

Calibration models for the prediction of relative density and tensile strength of the tablets were constructed using PLS algorithm. The number of significant latent variables (LVs) was chosen based on the value of sum of squares of the spectral residuals (X-PRESS) assuring adequate reconstruction of the spectra by the models and secondly, based on the calibration and validation predicted residual error sum of squares (C-set and V-set PRESS), as well as on the values of the root mean square error of prediction of an external validation set (RMSEP), validation set BIAS and coefficient of determination (r^2). The quality of the models was evaluated by calculating the root mean square error of calibration (RMSEC) and also the root mean square error of internal validation (RMSEV). The most important figures of merit were RMSEP of the external validation set and the r^2. Apart from the r^2, linearity was assessed by evaluating the slope and the intercept of the calibration line. The prediction residuals were tested for the normality. Durbin-Watson test was applied to the prediction residuals to check if there are some evidences of serial correlations. Every model was tested for the outliers in both calibration and validation set by visual inspection of the scatter plots of the scores, Mahalanobis distances, spectral residuals and original vs. predicted property scatter plots. Obtained calibration models were fine-tuned by outlier exclusion and wavelength selection. Calibration wavelength regions were selected by observing the pretreated spectra, loadings and PLS regression coefficients.

Equations and concepts of physics for the calculation of the outcomes

The obtained data sets of relative density, compaction pressure and tensile strength were analyzed and evaluated with the equations of the Heckel-Plot, the modified

Heckel-Plot and the Leuenberger equation by using Mathematica 7.0 (Wolfram Research Inc., USA), Excel (Microsoft, USA), GraphPad Prism (GraphPad Software Inc, USA) and OriginPro (OriginLab Corporation, USA). For every formulation, there were two data sets evaluated, one of the traditional method application and a second data set obtained with the predicted method.

Mathematical comparison of the technical factors

An essential part in this study was the scientific evaluation of the technical factor outcomes obtained with the two data sets (traditional measurement vs. NIR) for every formulation.

In a first step the obtained values of an equation factor were plotted on a two-dimensional diagram, where the x-axis represents the values calculated with the traditional method and the y-axis represents the predicted values for the different formulations.

The similarity between the outcomes of the two methods can be declared, if the data points on the diagram can be fitted with a high coefficient of determination (r^2) on a trendline on the form of the following equation 6, with values for λ preferably close to 1 and a value for ϕ close to 0.

$$y = \lambda \cdot x + \phi \quad (6)$$

Results

True density of components

The following table shows the true density values of all pharmaceutical powders used in the investigated formulations. Since a main criterion of the component choice was the similar range of true density, no big deviation can be noticed between the true density values of the chosen components. The only exception here is Emcompress anhydrous, whose true density was almost double (Table 3).

Particle size measurement

Since the influence of the particle size was a main investigation target in this study, a focus was set on the particle size distribution of the investigated material.

In the following table, the mean value and the median value (incl. standard deviation) of the handled compounds is shown.

The mean particle size between the investigated compounds showed a wide range from 74.13 µm for Mefenamic acid up to 248.70 µm for Parteck M 300 (Table 4).

Powder compaction: technical factor outcomes

The relative density, compaction pressure and tensile strength were recorded for every single tablet. The relative density was obtained by manual dimension measurement and true density value consideration. The tensile strength was measured by the destructive hardness test and the compaction pressure was measured during compaction with the Presster simulator.

Table 3. True density of components.

Powder	True density (g/cm³)	SD (g/cm³)
Paracetamol	1.22	0.00
Mefenamic acid	1.16	0.00
MCC 101 L	1.48	0.01
MCC 102 G	1.43	0.00
Emcompress anhydrous	2.49	0.00
Parteck M 200	1.52	0.00
Parteck M 300	1.39	0.00
Pregelatinzed starch 1500	1.50	0.00

Table 4. Particle size distribution of investigated compounds.

Powder	Mean (µm)	SD (µm)	Median (µm)	SD (µm)
Paracetamol	82.78	5.79	51.35	1.08
Mefenamic acid	74.13	6.05	38.35	1.83
MCC 101 L	83.35	2.31	73.76	0.88
MCC 102 G	119.74	0.15	114.06	0.53
Emcompress anhydrous	188.02	2.90	181.71	3.02
Parteck M 200	149.22	2.55	131.15	1.99
Parteck M 300	248.70	5.49	179.04	5.38
Pregelatinzed starch 1500	94.90	0.03	86.51	0.16

This data set was applied to the Heckel-Plot, the modified Heckel-Plot and the Leuenberger equation for fitting. With this approach, the technical factors of the plots were calculated.

Table 5 shows the values for the factors *k* (Heckel-Plot) and *C* (modified Heckel) of all investigated powder formulations.

The formulations Paracetamol/Parteck M200 (20% drug load) and Paracetamol Parteck M300 (20% drug load) could not be compacted successfully with the higher compaction speed since the distinctive sticking tendency of the formulations did not allow an application of a high compaction speed. Therefore, these formulations are skipped in the part (b) of the table.

For a more convenient analysis and comparison, the outcome values were plotted on a bar chart (see Figure 1).

At first sight, it could be noticed that the absolute values of k were higher than those of C for all investigated formulations. This was an expected outcome which fits to the literature[13] because the mathematical structure of a plot mainly determines the absolute value of its factors.

Technical factors gain only explanatory power when they are systematically collected and the data sets of different formulations and batches are compared.

The value ratios between investigated formulations showed a parallel proportionality for the values *C* and values *k*.

Some deviations were noticed for the formulations with MCC 101 L, compacted with the higher speed. In these cases, the value *C* was decreasing with higher drug load. In the meantime, the value k showed higher values with increasing drug load.

For the formulations with MCC 102 G and all the other single compound formulations, the ratios showed the

Table 5. Technical factors of the investigated formulations: (a) low speed; (b) high speed.

	Value k (Mpa^{-1})		Value C (Mpa^{-1})	
	tra	SD	tra	SD
Low speed				
MCC 101 (100%)	0.01289	0.0001598	0.00886	0.0009103
Paracetamol/MCC 101 L (20%)	0.009729	0.0002309	0.002869	0.0001015
Paracetamol/MCC 101 L (40%)	0.0101	0.0001972	0.004342	0.0000955
Mefenamic acid/MCC 101 L (20%)	0.01352	0.0003581	0.006664	0.0002033
MCC 102 G (100%)	0.01623	0.0002451	0.01273	0.0004921
Mefenamic acid/MCC 102 G (20%)	0.01439	0.0003148	0.006273	0.000537
Mefenamic acid/MCC 102 G (40%)	0.01048	0.0003815	0.00507	0.0002348
Paracetamol/MCC 102 G (30%)	0.0128	0.0001163	0.007499	0.0002061
Paracetamol/Parteck M200 (20%)	0.005413	0.000332	0.002054	0.0001315
Paracetamol/Parteck M 300 (20%)	0.006301	0.0001224	0.002524	0.0000963
Emcompress (100%)	0.00162	0.0006309	0.000247	0.0000097
Starch 1500 (100%)	0.005043	0.0001389	0.001017	0.0000446
High speed				
MCC 101 (100%)	0.0126	0.0002089	0.0064	0.0001462
Paracetamol/MCC 101 L (20%)	0.009018	0.0002466	0.00526	0.0001813
Paracetamol/MCC 101 L (40%)	0.0107	0.0002046	0.00488	0.0001953
Mefenamic acid/MCC 101 L (20%)	0.01296	0.0004983	0.00466	0.000369
MCC 102 G (100%)	0.016	0.000709	0.01021	0.0009444
Mefenamic acid/MCC 102 G (20%)	0.01025	0.0004969	0.003378	0.0003149
Mefenamic acid/MCC 102 G (40%)	0.007095	0.0005402	0.002355	0.0003452
Paracetamol/MCC 102 G (30%)	0.01556	0.000161	0.009738	0.0004921
Emcompress (100%)	0.001657	0.0000608	0.000245	0.000106
Starch 1500 (100%)	0.003842	0.0001623	0.001073	0.000216

expected parallel value trends for the two compaction speeds.

In a further step, the evaluation focus was set to the factor value comparison between the formulations.

For this study, some single powders, like Emcompress, Starch 1500, and a number of binary mixtures with a poorly compressible active drug (Mefenamic acid and Paracetamol) and Microcrystalline Cellulose (MCC 101 L and MCC 102 G) as filler were investigated. The main scientific focus was the evaluation and comparison of the technical factor values for different drug loads and for different single powders.

For the binary mixtures, a decrease of the compressibility with increasing drug load was expected and also noticed during handling. Since the investigated factors values k (Heckel-Plot) and C (modified Heckel-Plot) have been claimed[28–30,40] to represent the formulation compressibility, lower factor values were expected with increasing drug loads.

The pure MCC 102 G showed the highest factor values of all investigated formulations, followed by binary mixtures (20% drug load) of MCC 102 G with Paracetamol or Mefenamic acid.

Paracetamol (30%)/MCC 102 G showed higher factor values than Mefenamic acid (20%)/MCC 102 G. This outcome allowed us to assume a stronger negative influence of Mefenamic acid to the compressibility of a binary mixture than Paracetamol.

The binary mixtures with MCC 101 L showed a confusing outcome: For the formulation with 40% of Paracetamol some higher factor values were noticed than for the formulation with 20% of Paracetamol.

By assuming the factor values to represent compressibility, this outcome would show a better compressibility of a binary mixture after increasing the poorly compressible compound. Such a behaviour would not be realistic and could not be supported with literature findings. Also physical aspects, like the occurrence of percolation cannot provide an explanation for such a behaviour.

Powder susceptibility γ

The data set of all investigated formulations was fitted to the Leuenberger equation. Leuenberger et al.[30] claimed the parameter γ (powder susceptibility) of this equation to represent the compressibility of a formulation.

Therefore, the outcome values for γ were expected to be somehow proportional to the calculated values for factors k and C.

The powder susceptibility values for the investigated formulations are depicted in the following bar chart.

The factor calculation showed a high susceptibility for low speed compaction of single powder MCC 101 L and the high speed compaction of Mefenamic acid/MCC 101 L (20% drug load). For the other formulations, their values were in a range between 0.0020 and 0.0060,

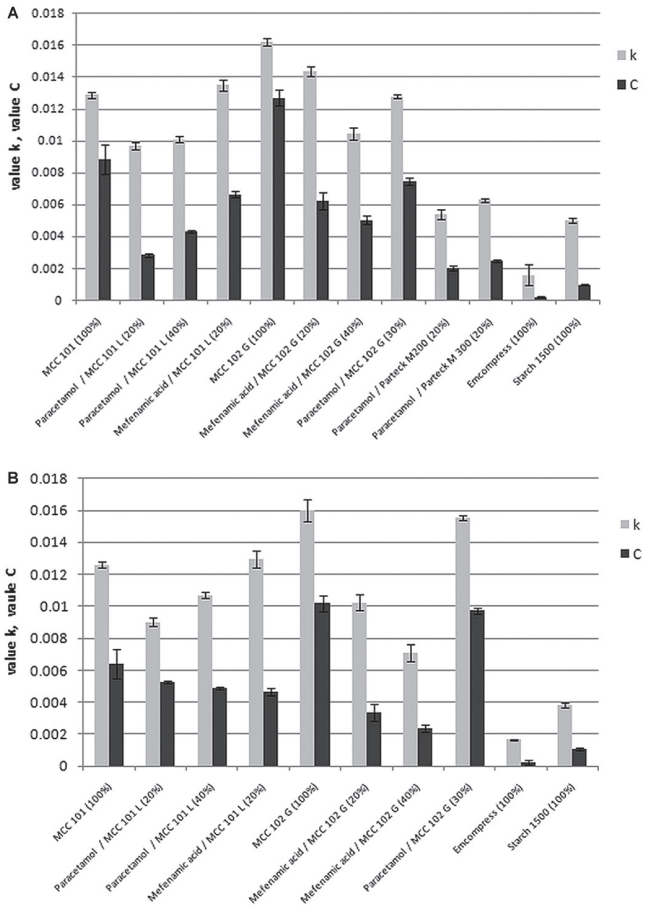

Figure 1. Values k and C of investigated formulations: (a) low speed; (b) high speed.

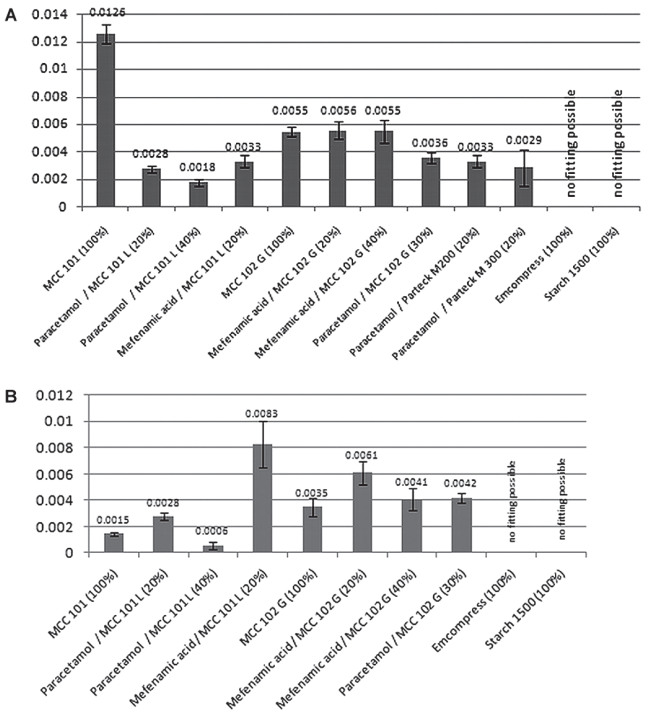

Figure 2. Powder susceptibility γ: (a) low speed; (b) high speed.

whereas a quiet significant standard deviation was noticed for the most formulations.

Even though, the single compounds of Microcrystalline Cellulose are known for their high compressibility the fitting outcome values were in the same order of magnitude as the biggest part of the formulations.

A crucial finding was the fitting limitation for some formulations. The tensile strength values of the

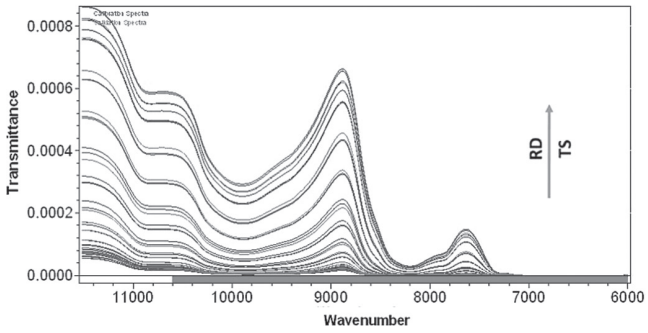

Figure 3. Transmittance spectra of MCC 102G tablets with increasing tensile strength and relative density. (See colour version of this figure online at www.informahealthcare.com/phd)

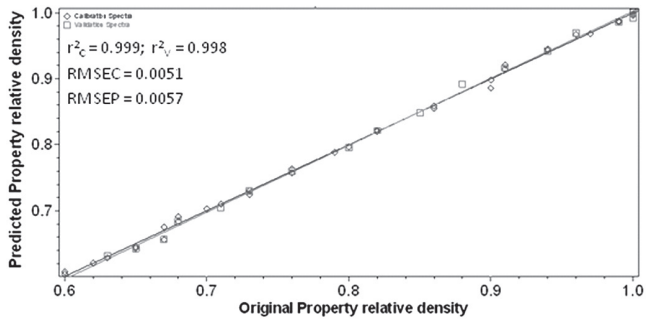

Figure 4. Calibration and internal validation reference vs. predicted property scatter plot of MCC 102G tablet RD prediction model; In the upper left corner are the figures of merit of the model. (See colour version of this figure online at www.informahealthcare.com/phd)

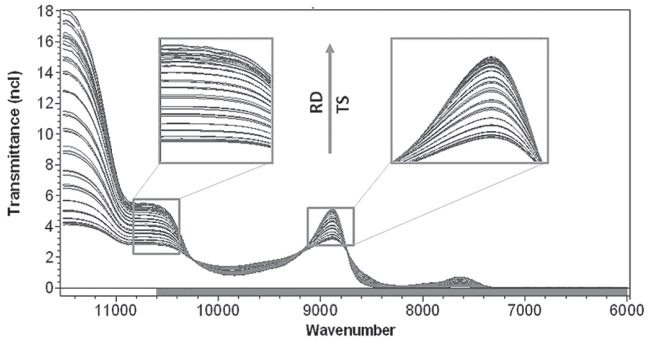

Figure 5. Spectra of MCC 102G tablets pretreated with normalization by closure; The enlarged regions were used for calibration and show the grouping of the spectra according to RD. (See colour version of this figure online at www.informahealthcare.com/phd)

tablets compacted with these formulations showed significantly lower values than the tablets of the other formulations.

The occurence of this plotting limitation is a clear hint for an essentialy low compressibility. A formulation which need to be compressed into tablets with very low porosity for reaching a sufficient hardness is the best example for a formulation with low compressibility.

By comparing Figure 2 with the bar charts of Figure 1, no parallel value distribution for the parameter γ in relation to the factors k and C could be noticed.

A possible explanation for this outcome is the different structure of the Leuenberger equation in comparison to the Heckel and the modified Heckel equation. Whereas the Heckel and modified Heckel equation have a two dimensional structure, the Leuenberger equation is based on a 3-axis format.

The additional axis arised from the tensile strength values, which are a main part of the Leuenberger equation, while the Heckel Plot and the modified Heckel equation are only considering the compression pressure and the relative density of the produced compact.

The fitting of the data set to the Leuenberger equation uncovered a main element of this plot. As mentioned earlier, two compaction speeds were used in this project. For every formulation, one tablet batch was produced at

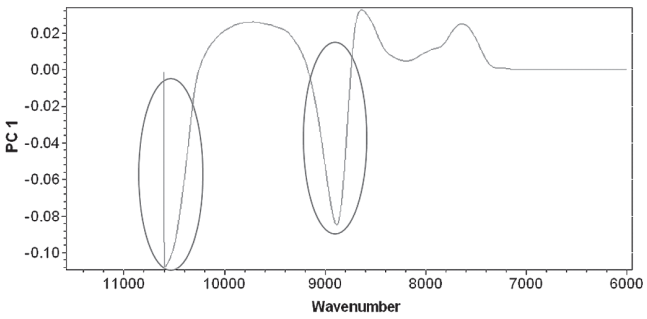

Figure 6. The first loading vector of MCC 102G tablet RD prediction model; The encircled regions carry the most spectral information and correspond to wave number regions used for calibration. (See colour version of this figure online at www.informahealthcare.com/phd)

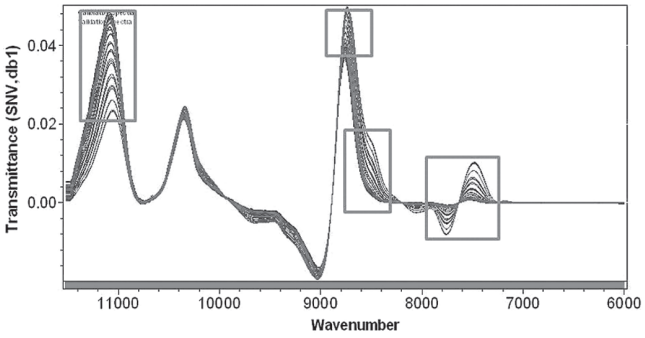

Figure 7. Spectra of MCC 102G tablets pretreated with Standard Normal Variate and Savitsky-Golay first derivative; The enlarged regions were used for calibration and show the grouping of the spectra according to TS. (See colour version of this figure online at www.informahealthcare.com/phd)

Table 6. Summary of the figures of merit obtained for the relative density and tensile strength calibration models.

		Relative density models				Tensile strength models			
Formulation		Data pretreatment	LV	R^2	RMSEP	Data pretreatment	LV	R^2	RMSEP
F1	LS	ncl	2	0.997	0.0072	SNV	3	0.997	0.0908
	HS	ncl	2	0.997	0.0090	ncl	2	0.998	0.1275
F2	LS	ncl	3	0.999	0.0057	SNV, 1 D	2	0.999	0.1242
	HS	ncl	3	0.993	0.0106	1 D	3	0.992	0.3099
F3	LS	SNV	5	0.982	0.0058	SNV	2	0.923	0.0415
	HS	SNV	5	0.992	0.0141	SNV	3	0.963	0.1211
F4	LS	ncl	2	0.984	0.0101	ncl	3	0.983	0.0229
	HS	ncl	5	0.973	0.0170	ncl	3	0.945	0.0336
F5	LS	ncl	2	0.998	0.0066	SNV	2	0.999	0.0970
	HS	ncl	4	0.995	0.0103	SNV	5	0.999	0.1062
F6	LS	ncl	3	0.996	0.0105	ncl	2	0.999	0.0695
	HS	ncl	4	0.997	0.0108	1 D	4	0.998	0.0917
F7	LS	SNV	3	0.989	0.0092	ncl	2	0.992	0.0650
	HS	SNV	3	0.981	0.0110	1 D	3	0.974	0.1461
F8	LS	ncl	2	0.997	0.0062	SNV, 1 D	2	0.983	0.1530
	HS	ncl	2	0.992	0.0104	SNV	4	0.988	0.2522
F9	LS	SNV	2	0.999	0.0030	ncl	2	0.997	0.0350
	HS	ncl	5	0.997	0.0090	ncl	5	0.988	0.0600
F10	LS	ncl	2	0.998	0.0068	SNV	2	0.996	0.0582
	HS	ncl	3	0.994	0.0080	SNV	4	0.985	0.0840
F11	LS	ncl	3	0.992	0.0111	SNV	5	0.983	0.1313
	HS	—	—	—	—	—	—	—	—
F12	LS	ncl	4	0.996	0.0077	SNV	4	0.996	0.1034
	HS	—	—	—	—	—	—	—	—

lower speed and one batch at higher speed. Each batch contained around 40–80 tablets.

With a data set in this size, the value of every single tablet had an essential influence on the curve fitting. A small change in a data set for a single tablet can lead to a big change of the susceptibility value after fitting.

This could be a possible explanation for the deviation of the susceptibility values to the calculated numbers for the factors *k* and *C*.

The necessity of three variables per compacted tablet instead of two in combination with the high sensitivity of the curve fitting on single variable value deviations made the application of the Leuenberger equation to the compressibility measurement being a challenging approach for this project.

NIRS measurement and model development

The construction of the calibration models in this article is given on an example of the tablets composed of microcrystalline cellulose 102 G, manufactured using low tableting speed. After the spectra were recorded, as shown in Figure 3, different spectral preprocessing methods were applied in order to enhance the spectral data relevant to the analysis and to exclude the excessive scattering effect.

Modeling the tablet relative density and tensile strength is based on a different degree of scattering between the samples but too high ordinate offsets and baseline shifts would impair the models. The criteria for the selection of the preprocessing method were the degree to which the preprocessed spectra are grouped according to the similar reference values and finally, the model performance (RMSEP). NIR transmittance values increased regularly with an increase in the compression force applied to the powder bed as for an increase in the tensile strength and relative density of the tablets. Transmittance spectra were transformed to absorbance by Log 1/T function and it was noticed that the baselines are linearly shifted and no evidences of multiplicative effect were seen. The effect of the increasing compression force was seen as an overall spectral effect not related to the specific wavelength since the tablet hardness does not have an analytical wavelength. Certain wavelength domains had higher correlation with the analyzed physical properties ($r > 0.90$) and were selected for the construction of the calibration model.

The baseline shifts as well as the offsets on a y-axis originate not only from different relative densities and tensile strengths but also from the different particle size of the samples which is not relevant information in this study. The spectral offset on a y-axis does not carry information on the relative density/tensile strength only. It is multi-factorial effect and was reduced by applying the derivative or normalisation pre-treatment. The external testing has shown that the calibration model predictability was higher when the spectra were grouped by applying spectral pre-treatment.

Tablet relative density models (Figure 4) gave the best performance when the Normalization by Closure (ncl) was applied, as seen in Figure 5.

The pretreated spectra were clearly grouped according to different relative density values. The calibration wave-number range was selected based on the

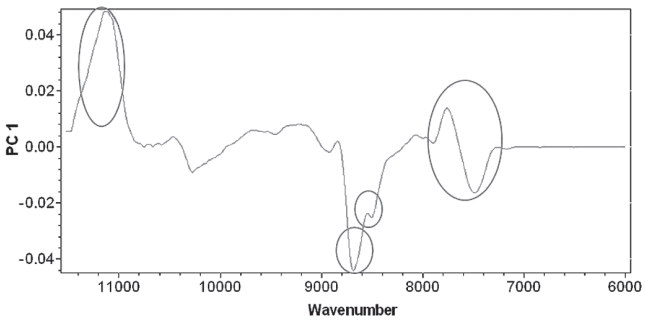

Figure 8. The first loading vector of MCC 102G tablet TS prediction model; The encircled regions carry the most spectral information and correspond to wave number regions used for calibration. (See colour version of this figure online at www.informahealthcare.com/phd)

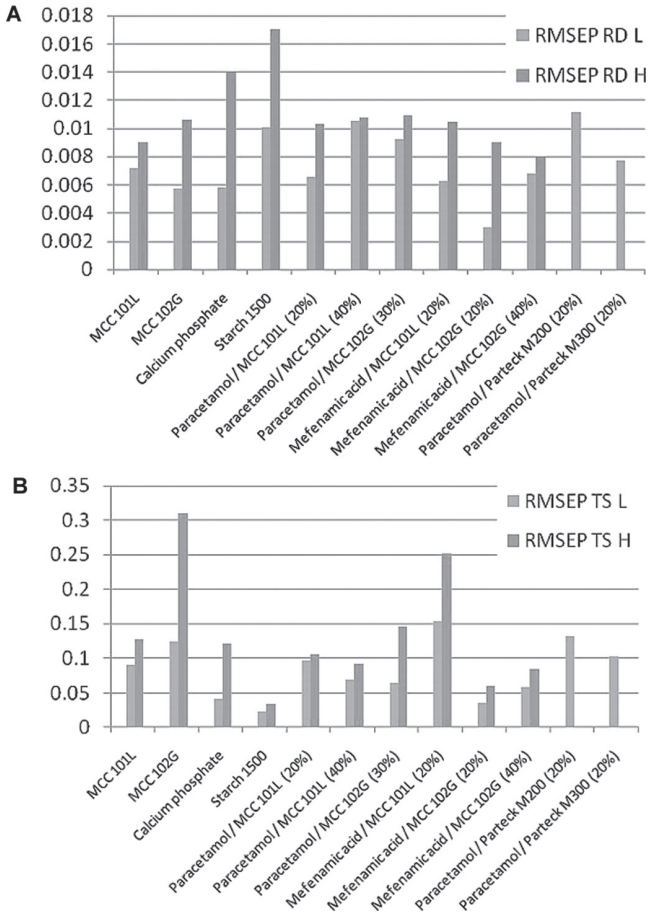

Figure 9. Comparison of the RMSEP values of the external validation set relative density (a) and tensile strength (b) predictions for all the studied formulations; L: low tableting speed, H: high tableting speed. (See colour version of this figure online at www.informahealthcare.com/phd)

Table 7. Outcomes of factor values by using the traditional (tra) approach or the developed method (pre).

	Heckel equation								Modified Heckel equation			
	K				A				C			
	tra	SD	pre	SD	tra	SD	pre	SD	tra	SD	pre	SD
Low speed												
MCC 101 (100%)	0.0129	0.00016	0.0131	0.00018	0.6196	0.00569	0.6141	0.00583	0.00886	0.000910	0.009703	0.0005259
Paracetamol/MCC 101 L (20%)	0.0097	0.00023	0.0095	0.00027	0.9515	0.02797	0.9674	0.03324	0.00287	0.000102	0.004728	0.0002159
Paracetamol/MCC 101 L (40%)	0.0101	0.00020	0.0098	0.00033	0.9142	0.01833	0.935	0.03108	0.00434	0.000096	0.004292	0.0003808
Mefenamic acid/ MCC 101 L (20%)	0.0135	0.00036	0.0141	0.00090	0.7686	0.01219	0.739	0.02551	0.00666	0.000203	0.006576	0.0005465
MCC 102 G (100%)	0.0162	0.00025	0.0172	0.00027	0.7778	0.01942	0.724	0.02128	0.01273	0.000492	0.01288	0.0004217
Mefenamic acid/ MCC 102 G (20%)	0.0144	0.00031	0.0146	0.00031	0.8257	0.02401	0.8103	0.02381	0.00627	0.000537	0.006565	0.0005159
Mefenamic acid/ MCC 102 G (40%)	0.0105	0.00038	0.0114	0.00032	1.205	0.04146	1.147	0.00349	0.00507	0.000235	0.005188	0.000234
Paracetamol/MCC 102 G (30%)	0.0128	0.00012	0.0126	0.00015	0.8302	0.01063	0.8371	0.014	0.00750	0.000206	0.007255	0.0002624
Paracetamol/ Parteck M200 (20%)	0.0054	0.00033	0.0058	0.00026	1.031	0.04882	0.9891	0.03756	0.00205	0.000132	0.002131	0.0001315
Paracetamol/ Parteck M 300 (20%)	0.0063	0.00012	0.0062	0.00019	0.9484	0.01348	0.9553	0.00219	0.00252	0.000097	0.002413	0.0000908
Emcompress (100%)	0.0016	0.00063	0.0016	0.00088	0.5763	0.00620	0.5814	0.00854	0.00025	0.000010	0.000271	0.0000727
Starch 1500 (100%)	0.0050	0.00014	0.0055	0.00025	0.8105	0.00685	0.7839	0.01287	0.00102	0.000045	0.000829	0.0000612
High speed												
MCC 101 (100%)	0.0126	0.00021	0.0133	0.00002	0.6038	0.006316	0.5788	0.00736	0.00640	0.0001462	0.00618	0.0001238
Paracetamol/MCC 101 L (20%)	0.0090	0.00025	0.0090	0.00031	0.8435	0.0323	0.8417	0.04055	0.00526	0.0001813	0.004955	0.0002648
Paracetamol/MCC 101 L (40%)	0.0107	0.00020	0.0106	0.00022	0.8573	0.01609	0.8569	0.01709	0.00488	0.0001953	0.004752	0.0001761
Mefenamic acid/ MCC 101 L (20%)	0.0130	0.00050	0.0134	0.00050	0.687	0.02717	0.6694	0.02527	0.00466	0.000369	0.004514	0.0003011
MCC 102 G (100%)	0.0160	0.00071	0.0161	0.00094	0.5824	0.07407	0.5832	0.06701	0.01021	0.0009444	0.01007	0.0009158
Mefenamic acid/ MCC 102 G (20%)	0.0103	0.00050	0.0108	0.00005	0.9561	0.04252	0.9305	0.04685	0.00338	0.0003149	0.003211	0.0003774
Mefenamic acid/ MCC 102 G (40%)	0.0071	0.00054	0.0083	0.00042	1.221	0.05801	1.126	0.04216	0.00236	0.0003452	0.002278	0.0003239
Paracetamol/ MCC 102 G (30%)	0.0156	0.00016	0.0154	0.00030	0.7544	0.01147	0.7752	0.01631	0.00974	0.0004921	0.009589	0.0004011
Emcompress (100%)	0.0017	0.00006	0.0016	0.00006	0.5658	0.00589	0.5688	0.05731	0.00025	0.0000106	0.000272	0.0000167
Starch 1500 (100%)	0.0038	0.00016	0.0035	0.00017	0.8692	0.01423	0.894	0.01696	0.00107	0.000216	0.000917	0.000208

observation of the first loading plot (see Figure 6) and PLS regression coefficients.

The wave-number range from 10600 cm^{-1} to 11520 cm^{-1} was excluded due to high ordinate offset which ncl could not account for. The best tensile strength model was obtained when the Standard Normal Variate (SNV) pretreatment was applied to correct for the linear baseline shifts and subsequently Savitsky-Golay first derivative to correct for the ordinate offset which enabled the wave numbers from 10600 cm^{-1} to 11520 cm^{-1} to be included in the calibration (see Figure 7). The first loading vector was observed to check the wave number regions, that is, variables that were modeled (see Figure 8).

After the preprocessing of the data, the spectra and the measured relative density and tensile strength reference values were subjected to PLS regression. The overview of the figures of merit of the created calibration models for all the formulations is given in Table 6.

Created calibration models were compared in terms of performance (RMSEP) and it was noticed that all the models for the prediction of relative density and tensile strength of the tablets made by high tableting speed show worse performance (higher RMSEP) comparing

				Leuenberger equation							
Critical				Gamma				S_{tmax}			
tra	SD	pre	SD	tra	SD	pre	SD	tra	SD	pre	SD
0.1406	0.0344	0.1446	0.01911	0.0125674	0.000685747	0.0149438	0.00100839	7.31092	0.26855	6.77104	0.305785
0.3494	0.01054	0.3668	0.01615	**0.0027709**	0.000285917	**0.002664**	0.000224636	**19.3791**	1.46086	**19.9551**	1.33466
0.401	0.00704	0.405	0.02799	**0.0018087**	0.000264631	**0.00172073**	0.000304936	**15.1827**	1.91932	**15.8972**	1.5243
0.2869	0.00961	0.2864	0.02591	0.0033108	0.000440024	0.00457211	0.000718201	12.9792	1.35817	10.0376	1.14665
0.1145	0.02022	0.109	0.017	**0.0055040**	0.000360343	**0.00576584**	0.000360343	**17.0828**	0.842176	**16.438**	0.842176
0.34	0.03353	0.3277	0.03165	0.00556456	0.000627079	0.00523316	0.000537957	5.79902	0.425104	6.03112	0.411804
0.4277	0.01526	0.4254	0.01502	0.00552612	0.000859025	0.00670111	0.00602235	3.10846	0.308401	6.64314	5.29407
0.281	0.01209	0.291	0.01578	0.0036032	0.000371788	0.00415382	0.000354897	8.20486	0.623178	7.6377	0.449094
0.442	0.01531	0.4349	0.01531	0.00331118	0.000440024	0.00260538	0.000440024	7.58712	1.35817	9.18249	1.35817
0.4095	0.009965	0.4178	0.009578	0.00288876	0.00134468	0.00277918	0.000795574	8.84878	3.21327	9.4519	2.10216
0.3667	0.00358	0.358	0.02421	No fitting		No fitting		No fitting		No fitting	
0.4608	0.007228	0.4863	0.01083	No fitting		No fitting		No fitting		No fitting	
0.1992	0.009304	0.2099	0.007997	0.00147601	0.000143389	0.000927921	0.000230489	48.0388	4.26322	74.6734	17.5723
0.2899	0.01385	0.3079	0.02068	**0.00276639**	0.000285917	**0.00279528**	0.000224636	**18.019**	1.46086	**17.8554**	1.33466
0.3739	0.0137	0.3621	0.01176	**0.0006**	0.000276681	**0.00172073**	0.000276681	**36.9461**	2.22764	**15.8972**	2.22764
0.3279	0.02752	0.3384	0.02274	0.00831021	0.00176721	0.0106034	0.00306169	6.33417	0.664641	4.72677	0.694805
0.122	0.04701	0.1267	0.03961	**0.003504232**	0.000719011	**0.00221382**	0.000601465	**20.3556**	3.36363	**30.7218**	7.33262
0.4407	0.03456	0.451	0.03211	0.00608481	0.000899005	0.00596524	0.000877234	4.46376	0.422988	4.54984	0.433131
0.5126	0.03159	0.5185	0.02997	0.00410826	0.000854952	0.00350502	0.00125187	2.40258	1.04732	2.66629	0.754081
0.201	0.02412	0.209	0.01699	0.00422058	0.000376117	0.00217636	0.00058681	8.03293	0.516722	14.1599	3.39755
0.3667	0.003998	0.3588	0.005941	No fitting		No fitting		No fitting		No fitting	
0.4314	0.03572	0.4555	0.03657	No fitting		No fitting		No fitting		o fitting	

to low tableting speed models (Figure 9). It was noticed that later models needed fewer latent variables to obtain the optimal model performance. This fact can be attributed to the poorer compaction reproducibility when the high tableting speed is applied to the powder bed since shorter dwell time gives less chances for particle bonding and the variations in compact density distribution are more pronounced.[41] The numerous powder formulations showed really individual compaction properties in terms of compressibility which enhanced the differences in the models obtained for the low and high tableting speed tablets. The difference in prediction accuracy was observed between the MCC 101L and MCC 102G. The smaller mean particle size of MCC 101L comparing to MCC 102G contributed to the smaller difference between the relative density (RD) and tensile strength (TS) prediction accuracy of the tablets compacted under low and high tableting speed. Small particles have higher specific surface area and higher probability of particle bonding and thus, are less sensitive to dwell time, that is, tableting speed. A difference in predictions for high and low tableting speed was observed for dicalcium phosphate tablets,

which is attributed to the tablet density inhomogenity, that is, picking and cracking.

Comparison of numerical factors values, measured with traditional and predicted approach

Every single tablet of the produced batches was investigated with NIRS. The measured data signal was then applied to the prediction model and the predicted values for relative density and tensile strength were determined and recorded.

In a second step, the diameter, height and hardness of the tablet were measured manually, which allowed us to calculate in the traditional way the relative density and the hardness of the tablets.

The two data sets (traditional method and prediction model) were applied on the Heckel-Plot, the modified Heckel-Plot and the Leuenberger equation. With this fitting step, a calculation of the technical factor values of the three applied equations could be performed.

A reliable evaluation of the designed prediction method for hardness and relative density with following determination of mathematical equation factor values (Heckel-Plot, modified Heckel-Plot and Leuenberger equation) prerequisited a scientific comparison of the final outcome values for the technical factors k, A, C, ρ_c, γ and σ_{tmax}.

Table 7 gives an overview on the technical factor values for all investigated formulations. The outcomes are divided into one column for the traditional approach and one column for the NIR-approach.

A significant finding was the really small difference between the fitted values of the traditional method and the values, determined with the designed predictive method for the factors k of the Heckel-Plot and C of the modified Heckel-Plot.

The range of difference between the outcome values of the two methods was found to be within the standard deviation of both methods.

This outcome similarity between the two methods is illustrated graphically in Figures 10 and 11.

A similar outcome could be found for the factor critical density ρ_c of the modified Heckel-Plot. As shown in Figure 12 the value difference between the ρ_c of the traditional method and the predictive method was also very small and was found to be in the standard deviation range of the data sets.

This outcome underlined the usability of the designed NIR – method for the reliable fitting of the used formulations to the Heckel-Plot and the modified Heckel-Plot. The particle size of the investigated powder did not show to influence the measurement in a negative way.

The comparison outcomes of the factors γ and σ_{tmax} in Figures 13 and 14 show some bigger value differences between the fitting results of the traditional and the predicted approach. Even though, for some formulations the value differences between the methods are very low, other formulations showed an essential difference between the methods.

The reason for this difference can be explained with the three dimensional structure of the Leuenberger plot and also with the strong sensitivity of the fitting process to single data points.

For a further scientific substantiation of the found similarity of the equation factor outcomes between the traditional approach and the designed method with support of NIR, all the factor values were applied to a two-dimensional diagram. The data points were then fitted to the trendline according to Equation 6. An example for this fitting step is shown in Figure 15.

In the following Table 8 the values of λ and ϕ can be seen for all investigated technical factors. A similarity between two data sets can be shown when λ is close to 1, ϕ is close to 0 and especially the r^2 is higher than 0.95.

These conditions are fulfilled for the technical factors of the Heckel and the modified Heckel equation. The different particle size of the several chosen formulations did not show any influence on the reliability of the technical factor analysis with NIR.

The factors γ and σ_{tmax} of the Leuenberger equation showed a significant deviation from the conditions for similarity. Especially the r^2 – values have shown much lower values for these technical factors. This outcome underlines the non-similarity of the factor values for the Leuenberger equation between the traditional method and the approach with NIRS.

Conclusion

For the investigated formulations, the designed NIR method for determining the factors of the Heckel-Plot and the modified Heckel-Plot showed reliable results and outcomes.

Essentially different outcome values were reached with the NIRS method for the factors of the Leuenberger equation (γ, σ_{tmax}).

In this range of tablet numbers, the mathematical fitting to the Leuenberger equation showed a high sensitivity to deviations of the relative density and tensile strength of some single tablets.

This sensitivity could be determined as essential reason of high outcome deviation between the traditional approach and the predicted method. The relatively high standard deviations of the calculated values for γ and σ_{tmax} are an additional hint for this sensitivity.

The choice of the formulations to be investigated in this study was made with the focus set on the different materials showing a widest possible range of particle size and a wide range of compression mechanisms. These factors showed not to influence the data outcomes of the designed method with NIRS.

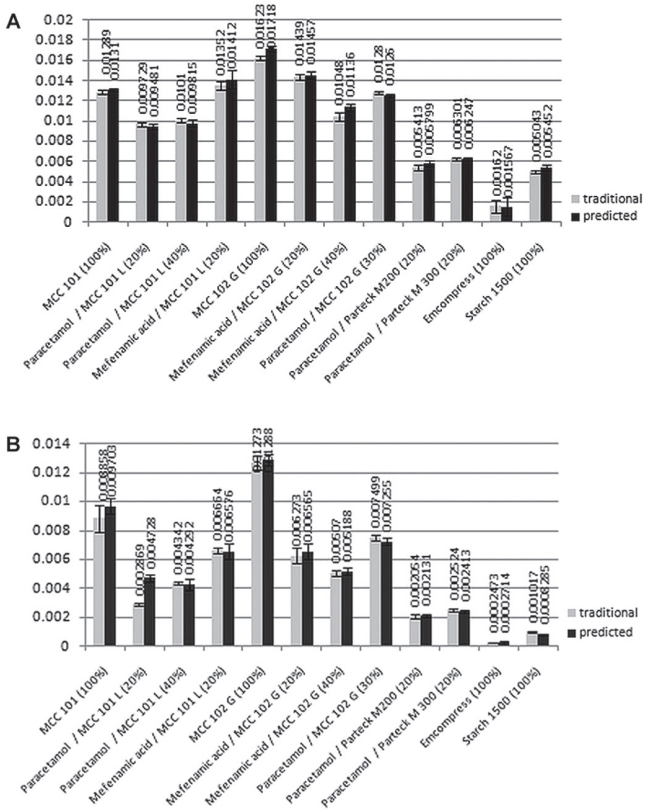

Figure 10. Low speed batches: values k (a) and C (b) of investigated formulations.

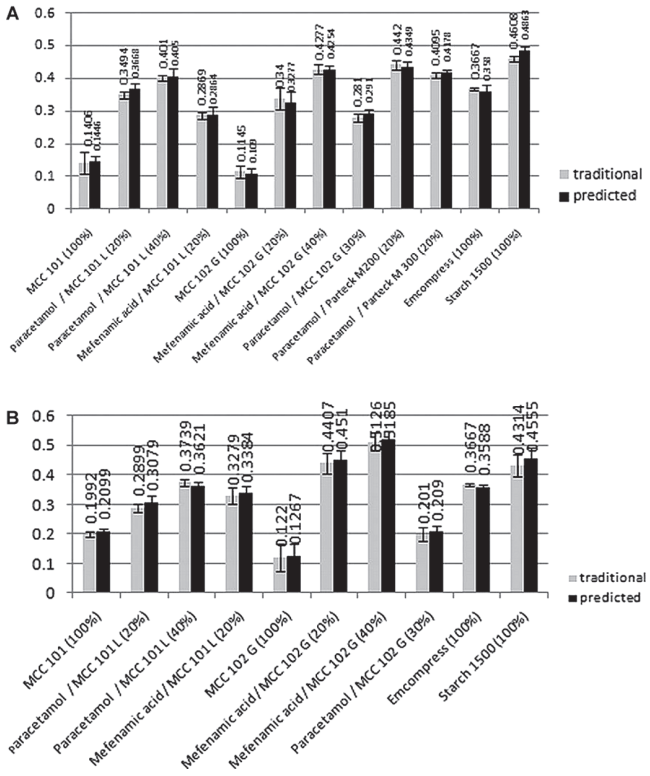

Figure 12. $\rho_{critical}$ data comparison: (a) low speed batches; (b) high speed batches.

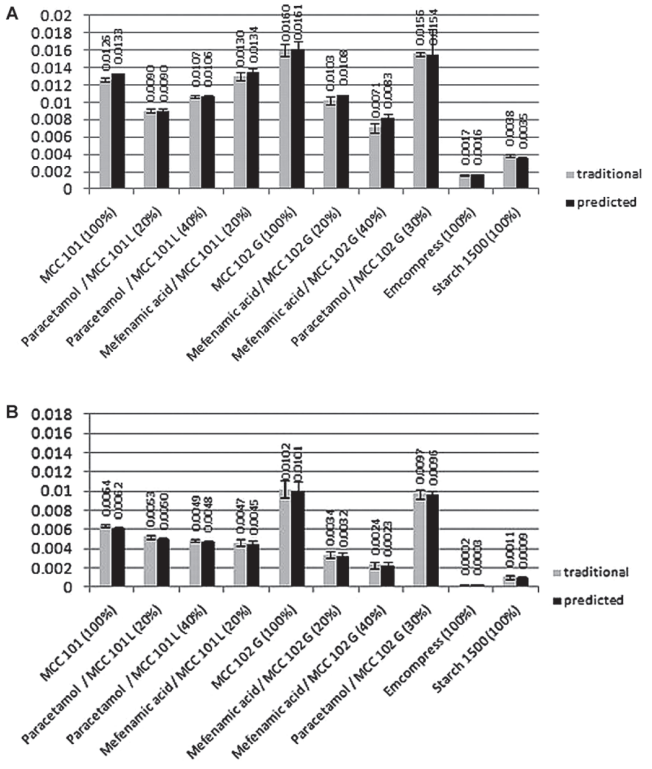

Figure 11. High speed batches: values k (a) and C (b) of investigated formulations.

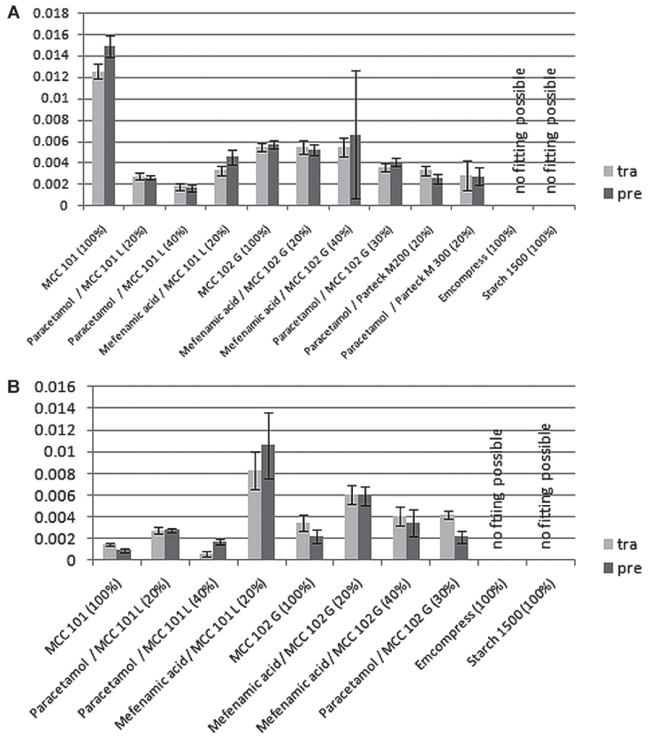

Figure 13. γ data comparison: (a) low speed batches; (b) high speed batches.

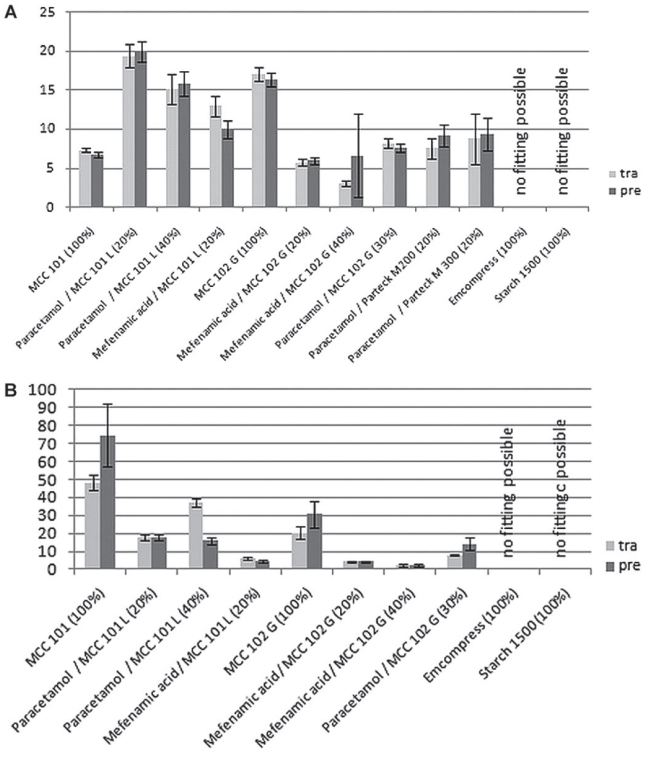

Figure 14. σ_{tmax} data comparison: (a) low speed batches; (b) high speed batches.

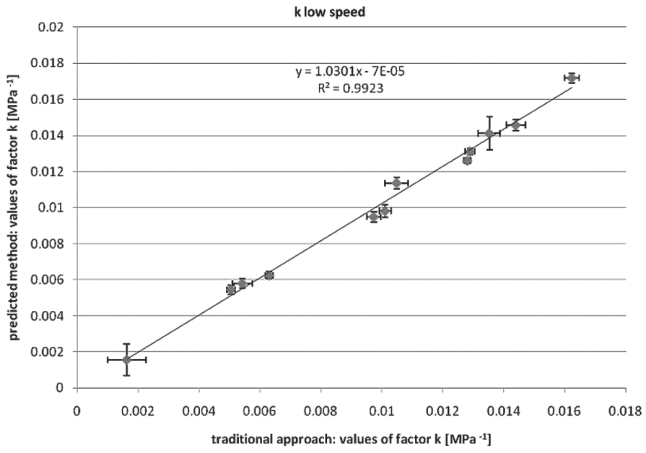

Figure 15. Similarity evaluation of factor k for the investigated formulations. (See colour version of this figure online at www.informahealthcare.com/phd)

The newly designed method is suggested as a promising approach for a non-destructive compressibility measurement of powder formulations. A potential usage of NIRS inline during tablet production could be underlined with this study in a remarkable way.

Declaration of interest

The authors report no conflicts of interest. The authors alone are responsible for the content and writing of the article.

Table 8. Values of λ and ϕ for the technical factors.

	λ	ϕ	r^2
Low speed			
k	1.0301	−0.00007	0.9923
A	0.95	0.0281	0.9757
C	1.0054	0.0002	0.9745
ρ_c	1.0213	−0.044	0.991
γ	1.2244	−0.0006	0.9727
σ_{tmax}	0.8516	1.9632	0.9009
High speed			
K	1.0076	0.0002	0.9908
A	0.8964	0.0707	0.9788
C	0.9892	−0.00009	0.9994
ρ_c	0.9997	0.0074	0.9925
γ	1.1682	−0.0008	0.8328
σ_{tmax}	1.1952	−0.9466	0.7014

References

1. Rasenack N, Müller BW. Crystal habit and tableting behavior. Int J Pharm 2002;244:45–57.
2. Michafry A, Michafry M, Kadiri M, Dodds JA. Predictions of tensile strength of binary tablets using linear and power law mixing rules. Int J Pharm 2007;333:118–126.
3. Celik M, Marshall K. Use of a compaction simulator system in tabletting research, Drug Dev Ind Pharm 1989;15:759–800.
4. Barra J, Falson-Rieg F, Doelker E. Influence of the organization of binary mixes on their compactibility. Pharm Res 1999;16: 1449–1455.
5. Nyström C, Karehill PG. The importance of Intermolecular Bonding Forces and the Concept of Bonding Surface Area. Drugs Pharmaceut Sci 1996;71:17–54.
6. Ragnarsson G. Force-Displacements and Network Measurements. Drugs Pharmaceut Sci 1996;71:77–97.
7. Celik M. Overview of compaction data analysis techniques. Drug Dev Ind Pharm 1992;18:767–810.
8. van Veen B, Van der Voort Maarschalk K, Bolhuis GK, Frijlink HW. Predicting mechanical properties of compacts containing two components. Powder Technol 2004;139:156–164.
9. Holman L, Leuenberger H. The significance of slopes of the semilogarithmic relationship between hardness and solid fraction of porous compacts. Powder Technol 1991;64:233–247.
10. Wu CY, Best SM, Bentham AC, Hancock BC, Bonfield W. A simple predictive model for the tensile strength of binary tablets. Eur J Pharm Sci 2005;25:331–336.
11. Kawakita K, Luedde K. Some considerations on Powder compression Equations. Powder Technol 1970;4:61–68.
12. Denny P. Compaction equations: a comparison of the Heckel and Kawakita equations. Powder Technol 2002;127:162–172.
13. Kuentz M, Leuenberger H. Pressure susceptibility of polymer tablets as a critical property: a modified Heckel equation. J Pharm Sci 1999;88:174–179.
14. Leuenberger H. The compressibility and compactibility of powder systems. Int J Pharm 1982;12:41–55.
15. Cruz J, Blanco M. Content uniformity studies in tablets by NIR-CI. J Pharm Biomed Anal 2011; in press.
16. Dou Y, Sun Y, Ren Y, Ju P, Ren Y. Simultaneous non-destructive determination of two components of combined paracetamol and amantadine hydrochloride in tablets and powder by NIR spectroscopy and artificial neural networks. J Pharm Biomed Anal 2005;37:543–549.
17. Ito M, Suzuki T, Yada S, Nakagami H, Teramoto H, Yonemochi E et al. Development of a method for nondestructive NIR transmittance spectroscopic analysis of acetaminophen and

caffeine anhydrate in intact bilayer tablets. J Pharm Biomed Anal 2010;53:396–402.
18. Blanco M, Eustaquio A, González JM, Serrano D. Identification and quantitation assays for intact tablets of two related pharmaceutical preparations by reflectance near-infrared spectroscopy: validation of the procedure. J Pharm Biomed Anal 2000;22: 139–148.
19. Alvarenga L, Ferreira D, Altekruse D, Menezes JC, Lochmann D. Tablet identification using near-infrared spectroscopy (NIRS) for pharmaceutical quality control. J Pharm Biomed Anal 2008;48: 62–69.
20. Karande AD, Heng PW, Liew CV. In-line quantification of micronized drug and excipients in tablets by near infrared (NIR) spectroscopy: Real time monitoring of tabletting process. Int J Pharm 2010;396:63–74.
21. Blanco M, Peguero A. Influence of physical factors on the accuracy of calibration models for NIR spectroscopy. J Pharm Biomed Anal 2010;52:59–65.
22. Heise HM, Winzen R. Fundamental chemometric methods. In: Siesler HW, Ozaki Y, Kawata SH, Heise M, (eds). *Near-infrared Spectroscopy: Principles, Instruments, Applications*. Germany: Wiley–VCH, 2002: p. 125.
23. Kirsch JD, Drennen JK. Nondestructive tablet hardness testing by near-infrared spectroscopy: a new and robust spectral best-fit algorithm. J Pharm Biomed Anal 1999;19:351–362.
24. Blanco M, Alcalá M. Content uniformity and tablet hardness testing of intact pharmaceutical tablets by near infrared spectroscopy: A contribution to process analytical technologies. Anal Chim Acta, 2006;557:353–359.
25. Blanco M, Cueva-Mestanza R, Peguero A. Controlling individual steps in the production process of paracetamol tablets by use of NIR spectroscopy. J Pharm Biomed Anal 2010;51:797–804.
26. Short SM, Cogdill RP, Wildfong PL, Drennen JK 3rd, Anderson CA. A near-infrared spectroscopic investigation of relative density and crushing strength in four-component compacts. J Pharm Sci 2009;98:1095–1109.
27. Heckel RW. Density-Pressure relationships in powder compaction. Trans Met Soc AIME 1961;221:671–675.
28. Heckel RW. An analysis of powder compaction phenomena. Trans Met Soc AIME 1961;221:1001–1008.
29. Kuentz M, Leuenberger H. A new theoretical approach to tablet strength of a binary mixture consisting of a well and a poorly compactable substance. Eur J Pharm Biopharm 2000;49:151–159.
30. Leuenberger H, Jetzer W. The compactibility of powder systems. A novel approach. Powder Technol 1984;37:209–218.
31. Bastien P, Vinzi VE, Tenenhaus M. PLS generalised linear regression. Comput Stat Data Anal, 2005;48:17–46.
32. Picciochi R, Diogo HP, Minas da Piedade ME. Thermochemistry of paracetamol. J Therm Anal Calorim 2010;100:391–401.
33. Adam A, Schrimpl L, Schmidt PC. Some physicochemical properties of mefenamic acid. Drug Dev Ind Pharm 2000;26:477–487.
34. Kothari SH, Kumar V, Banker GS. Comparative evaluations of powder and mechanical properties of low crystallinity celluloses, microcrystalline celluloses, and powdered celluloses. Int J Pharm 2002;232:69–80.
35. De la Luz Reus Medina M, Kumar V. Comparative evaluation of powder and tableting properties of low and high degree of polymerization cellulose I and cellulose II excipients. Int J Pharm 2007;337:202–209.
36. Abdel-Hamid S, Alshihabi F, Betz G. Investigating the effect of particle size and shape on high speed tableting through radial die-wall pressure monitoring. Int J Pharm 2011;413:29–35.
37. Kimura G, Puchkov M, Betz G, Leuenberger H. Percolation theory and the role of maize starch as a disintegrant for a low water soluble drug. Pharm Dev Technol 2007;12:11–19.
38. Ilkka J, Paronen P. Prediction of the compression behaviour of powder mixtures by the Heckel equation. Int J Pharm 1993;94:181–187.
39. Martens H, Naes T. *Multivariate calibration*. Wiley, 1989: p. 337
40. De Boer A, Bolhuis G, Lerk C. Bonding characteristics by scanning electron microscopy of powders mixed with Magnesium Stearate. Powder technol 1978;20:75–82.
41. Tye CK, Sun CC, Amidon GE. Evaluation of the effects of tableting speed on the relationships between compaction pressure, tablet tensile strength, and tablet solid fraction. J Pharm Sci 2005;94: 465–472.

3. Conclusion

ICH defines robustness of an NIRS analytical method as a measure of its capacity to remain unaffected by small, deliberate changes in method parameters. It provides an indication of the method's reliability during routine usage. Robustness tests examine the effects of operational parameters on the performances of NIRS method. For the determination of robustness of NIRS method for prediction of drug content in tablets, a number of method parameters, such as compression pressure, pre-compression pressure, tableting speed, formulation parameters, environmental temperature, are varied within a realistic range, and the quantitative influence of the variables is determined. Design of Experiments methodology is a systematic tool to study the factor effects with all the interactions and squared effects unlike conventional method which involves the study of one variable at a time.

If the influence of the studied parameter is within a previously specified limit, the parameter is said to be within the method's robustness range. Obtaining conclusions from DoE study helps to assess whether a method needs to be revalidated when one or more process or other parameters are changed, for example, tableting speed or compression pressure. In the ICH Q2B document, it is recommended to consider the evaluation of a method's robustness during the phase of method development, and any factors that are critical for the method, i.e. significantly affect method performance should be documented.

In the process of NIRS method development and its progression from feasibility study to method validation, several groups are usually responsible to run the method and insure its suitability for the early clinical phases to the commercial manufacturing. For that reason the method robustness is particularly important. The NIRS method should provide reliable data, both on a wide range of equipment and in the hands of several operators. It is not uncommon in development and validation of NIRS procedures that the robustness is not sufficient. If robustness is not built into methods in early stages of development, the result will likely be loss of efficiency during routine quality control testing or a lengthy and complicated validation process. The alternative to conventional robustness testing where the tests are performed after the NIRS method has been already developed, innovative approach suggests building in the robustness during the method development. The approach is in line with the Quality by Design initiative which suggests that the quality of the product should be built in by design of the process and not tested into a product.

In this study, tableting process parameters were chosen to be studied in detail. Pre-compression pressure, compression pressure and tableting speed are often varied during the scale-up of tableting process. Robust method needs to insure the long-term stability of the NIRS model predictions and for that reason, it is crucial to define the tableting process factors that significantly influence the NIRS model performance. The list of the factors that potentially influence the performance of the NIRS

methods developed in this work is not exhaustive. The aim of the author was to point out the need for systematic approach to studying these effects with DoE methodology as a suggested tool. The setup of the DoE study, i.e. the selection of factors and responses, is another critical point that needs to be taken into account. The right design of the DoE study enables the saving of time and resources and even more importantly, ensures the relevancy of the conclusions from the study. This is particularly important in case of NIRS method development for the analysis of tablets since the list of potential factors that may influence the method performance is very long.

Systematic and science-based approach in studying critical factors of tableting process affecting NIR spectra and calibration model performance was proposed in this work. DoE study was carefully designed with particular attention to the responses studied. The author suggests the use of Average Euclidean Distance (AED) as a response reflecting the influence of tableting process parameters on NIR spectral features. The effects of the studied factors on the AED are independent of the spectral pretreatments or any other parameter used during the calibration step. The disadvantage of evaluating the factor effects based on AED is the fact that AED does not reflect directly the performances of the developed NIRS model. The second studied response was Root Mean Squared Error of Prediction (RMSEP). RMSEP value reflects the performances of the NIRS method but is dependent on spectral pretreatments and parameters chosen during modeling phase (PCs, wavenumber range). The author suggests the use of both responses during the interpretation of the tableting process factor effects on the NIR spectral information of tablets.

Response Surface Modeling study revealed that compression pressure and tableting speed have shown significant effect on the responses Root Mean Squared Error of Prediction and Average Euclidean Distance in DT measurement mode. DR spectral information of the intact tablets was significantly affected by the compression pressure, pre-compression pressure and tableting speed.

Conclusions of the *Design of Experiments* study were confirmed on five independent test sets of caffeine tablets. Test sets were predicted by the developed global and local calibration models in both studied measurement modes and RMSEP was calculated. The effect of the studied factors on the RMSEP of the five test sets confirmed the conclusions of the DOE study.

Developed global calibration models for tablet caffeine content prediction in diffuse reflectance and transmittance measurement mode were compared in terms of performances and it was found that the DT global model shown better performances exhibiting RMSEP of 1.21 % compared to 1.54 % for the global DR model. Both global calibration models have shown comparable performances to the UV-spectrophotometric reference method which performed with the standard error of 1 %. Global models were suitable for implementation in Content Uniformity Test of the tablets since the total error limit of 5% of nominal drug content was not exceeded.

The conclusions from the performed study certainly need more supporting cases. The sample sets used for the DoE study were based on twenty samples which is considered to be the minimum

statistically relevant number of observations. For higher reliability of the results the larger data set is needed.

The conclusions of the DoE study are formulation dependent. Different deformation behavior of the formulation components would lead to different conclusions. For that reason, the author suggests the study to be replicated with the formulations that would show different deformation behavior.

The list of the process, formulation, environmental and acquisition factors influencing NIR spectral information of tablets is very long. Process factors studied in this work represent some of them. For complete picture of the relevant variables, further studies are necessary.

The D-optimal design was chosen in this work as the optimum for the tailor made and problem specific solutions. It allows great flexibility in the specifications of the problem. The author suggests the study to be replicated with classical designs.

Simultaneous NIRS quantification of two APIs in powders and tablets requires several challenges to be overcome. Overlapping absorption peaks of formulation components result in method specificity problem. Strategy for the design of the sample sets for NIRS method development is of crucial importance. Robustness towards the formulation factors is critical to insure since the problem of co-linearity in case of complex formulations is quite frequent. The experimental setup for the development of NIRS method for quantitation of Hydrochlorothiazide (HTZ) and Metoprolol Tartrate (MTP) in powders and tablets proposed in this work is suggested for the feasibility study stage of the method development. EMA, ICH and PASG guidelines on NIRS method development and validation suggest that feasibility study should be done at the onset of method development. Simulation of industrial scale tablet machines using tablet press replicator - *Presster*® and Balance Reference Method (BRM) as an alternative to HPLC and UV-spectroscopy which are traditionally used as reference methods in NIRS method development, could be a good solution for the feasibility study stage. With a proposed experimental setup, the resource savings are evident bearing in mind that the further stages of NIRS method development would require industrial scale tablet press instead of tablet press replicator and validated official reference method instead of Balance Reference Method in order to be able to validate the procedure with the relevant regulatory authorities.

Metoprolol Tartrate and Hydrochlorothiazide were simultaneously determined in powder and tablet samples using NIR spectroscopy with satisfying accuracy. Balance reference method was shown to be accurate enough, fast and convenient for feasibility studies at the onset of method development. The proposed approach involving compaction simulator for sample set design and manufacture, quick and simple gravimetrical reference method for developing the NIR calibration model, presents a fast and cost-effective alternative that could be applied for the initial stages of NIR method development. The proposed approach could be applied in feasibility study step, optimization of sample presentation and scanning, study of the variables affecting spectral response, evaluation of the quality of the scans, i.e.

repeatability, effect of inhomogeneities. For the further steps in method development an official reference method, validated according to ICH Q2 guidelines should be used.

The developed NIR method for determining the factors of the Heckel-plot and the modified Heckel-plot have shown promising results for the studied powder formulations.

Essentially different outcome values were reached with the Near-Infrared spectroscopy method for the Prediction of the factors of Leuenberger equation (γ, σ_{tmax}) using developed NIR method have shown descrepancies when compared to the traditional approach which could be attributed to the relatively small data set used for modeling and the high influence of the outliers in the data set.

The choice of the studied formulations was made with the focus set on the different materials showing a widest possible range of particle size and a wide range of compression mechanisms. These factors have shown no influence on the NIR predictions of the studied technical factors. The proposed method is suggested as a promising approach for a non-destructive compressibility measurement of powder formulations. However, it should be noted that the study has been performed off-line with a time delay between the production and the actual measurements. The promising results suggest that an on-line and in-line sampling approach should be attempted which would bring higher benefits to process control and optimization.

4. References

1. Saeed M., 2011 “Pharmaceutical Tablets and Near-infrared Spectral Information – Investigation of Sampled Tablet Sections and Press Effect on Predictions”, PhD dissertation, University of Basel, Switzerland.

2. Davies, T. "The history of near infrared spectroscopic analysis: Past, present and future-From sleeping technique to the morning star of spectroscopy." Analusis 26.4 (1998): M17.

3. Maxwell, J. C. The Scientific Papers of James Clerk Maxwell. Vol. 1. Cambridge University Press, 2011.

4. Planck, M. "On the law of distribution of energy in the normal spectrum." Annalen der Physik 4.553 (1901): 1.

5. Pasquini, C. "Near infrared spectroscopy: fundamentals, practical aspects and analytical applications." Journal of the Brazilian Chemical Society 14.2 (2003): 198-219.

6. Wahr, J. A., et al. "Near-infrared spectroscopy: theory and applications." Journal of cardiothoracic and vascular anesthesia 10.3 (1996): 406-418.

7. Ben-Gera, I. T. A. M. A. R., and Norris. H. K. "Direct spectrophotometric determination of fat and moisture in meat products." Journal of Food Science 33.1 (1968): 64-67.

8. Wilson, Edgar Bright. Molecular vibrations: the theory of infrared and Raman vibrational spectra. DoverPublications. com, 1955.

9. Quack, Martin. "Spectra and dynamics of coupled vibrations in polyatomic molecules." Annual Review of Physical Chemistry 41.1 (1990): 839-874.

10. Sokolnikoff, I. S., and Dickerson S. R. Mathematical theory of elasticity. Vol. 83. New York: McGraw-Hill, 1956.

11. Rychlewski, J. "On Hooke's law." Journal of Applied Mathematics and Mechanics 48.3 (1984): 303-314.

12. Workman, J. J. "NIR spectroscopy calibration basics." Practical Spectroscopy Series 13 (1992): 247-247.

13. Cozzolino, D., and I. Murray. "Effect of sample presentation and animal muscle species on the analysis of meat by near infrared reflectance spectroscopy." Journal of Near Infrared Spectroscopy 10.1 (2002): 37-44.

14. Siesler, Heinz W., et al., eds. Near-infrared spectroscopy: principles, instruments, applications. Wiley. com, 2008.

15. Wendlandt, W. W., and Harry G. H. Reflectance spectroscopy. Vol. 110. New York: Interscience, 1966.

16. Fuller, M. P., and Griffiths P. R. "Diffuse reflectance measurements by infrared Fourier transform spectrometry." Analytical Chemistry 50.13 (1978): 1906-1910.

17. Simmons, E. L. "Diffuse reflectance spectroscopy: a comparison of the theories." Applied optics 14.6 (1975): 1380-1386.

18. Steinke, J. M., and Shepherd A. P. "Comparison of Mie theory and the light scattering of red blood cells." Applied Optics 27.19 (1988): 4027-4033.

19. Kubelka, P. "New contributions to the optics of intensely light-scattering materials. Part I." JOSA 38.5 (1948): 448-448.

20. Nobbs, James H. "Kubelka—Munk theory and the prediction of reflectance." Review of Progress in Coloration and Related Topics 15.1 (1985): 66-75.

21. Zaccanti, G., and P. Bruscaglioni. "Deviation from the Lambert-Beer law in the transmittance of a light beam through diffusing media: experimental results." Journal of Modern Optics 35.2 (1988): 229-242.

22. Langhals, H., G. Abbt-Braun, and F. H. Frimmel. "Association of Humic Substances: Verification of Lambert-Beer Law." Acta hydrochimica et hydrobiologica 28.6 (2000): 329-332.

23. Workman, J. J., and Donald A. Burns. "Commercial NIR instrumentation." PRACTICAL SPECTROSCOPY SERIES 27 (2001): 53-70.

24. Osborne, B. G. et al. Practical NIR spectroscopy with applications in food and beverage analysis. Longman scientific and technical, 1993.

25. Shenk, J. S., and Westerhaus M. O. "Accuracy of NIRS instruments to analyze forage and grain." Crop science 25.6 (1985): 1120-1122.

26. Malinen, J. et al. "LED-based NIR spectrometer module for hand-held and process analyser applications." Sensors and Actuators B: Chemical 51.1 (1998): 220-226.

27. Pasquini, C. "Near infrared spectroscopy: fundamentals, practical aspects and analytical applications." Journal of the Brazilian Chemical Society 14.2 (2003): 198-219.

28. Armstrong, P. R., et al. "Comparison of dispersive and Fourier-transform NIR instruments for measuring grain and flour attributes." Applied engineering in agriculture 22.3 (2006): 453.

29. Cozzolino, D., et al. "Prediction of colour and pH in grapes using a diode array spectrophotometer (400-1100 nm)." Journal of near infrared spectroscopy 12.2 (2004): 105-111.

30. Vandeginste, B. G. M., et al. "Chemometrics: a textbook." (1988): 20-21.

31. Aiken, L. S. et al. "Multiple linear regression." Handbook of psychology (2003).

32. Jolliffe, I. Principal component analysis. John Wiley & Sons, Ltd, 2005

33. Kohavi, R. "A study of cross-validation and bootstrap for accuracy estimation and model selection." IJCAI. Vol. 14. No. 2. 1995.

34. Geladi, Paul, and Bruce R. Kowalski. "Partial least-squares regression: a tutorial." Analytica chimica acta 185 (1986): 1-17.

35. Seasholtz, Mary Beth, and Bruce R. Kowalski. "The effect of mean centering on prediction in multivariate calibration." Journal of chemometrics 6.2 (1992): 103-111.

36. Savitzky, A., and Golay J. E. M. "Smoothing and differentiation of data by simplified least squares procedures." Analytical chemistry 36.8 (1964): 1627-1639.

37. Faber, N. M. "Multivariate sensitivity for the interpretation of the effect of spectral pretreatment methods on near-infrared calibration model predictions." Analytical chemistry 71.3 (1999): 557-565.

38. Isaksson, T., and Naes T. "The effect of multiplicative scatter correction (MSC) and linearity improvement in NIR spectroscopy." Applied Spectroscopy 42.7 (1988): 1273-1284.

39. Barnes, R. J. et al. "Standard normal variate transformation and de-trending of near-infrared diffuse reflectance spectra." Applied spectroscopy 43.5 (1989): 772-777.

40. Shenk, J. S., and M. O. Westerhaus. "Population definition, sample selection, and calibration procedures for near infrared reflectance spectroscopy." Crop science 31.2 (1991): 469-474.

41. FDA 2005: "ICH Harmonized Tripartide guideline, Q2 (R1), Validation of Analytical Procedures: Text and Methodology".

42. European Medicines Agency "Guideline on the use of Near Infrared Spectroscopy (NIRS) by the pharmaceutical industry and the data requirements for new submissions and variations." (2012): 1-28.

43. PASG NIR subgroup "PASG guidelines for the development and validation of near-infrared (NIR) spectroscopy methods" (2001): 1-41.

44. Shenk, J. S. et al. "Application of NIR spectroscopy to agricultural products." PRACTICAL SPECTROSCOPY SERIES 27 (2001): 419-474.

45. Eriksson, L. "Design of experiments: principles and applications". MKS Umetrics AB, 2008.

46. Levin, M., ed. Pharmaceutical process scale-up. CRC Press, 2001.

47. Sinka, I. C., et al. "The effect of processing parameters on pharmaceutical tablet properties." Powder Technology 189.2 (2009): 276-284.

48. Marshall, K. "A new technique for investigating the process of tablet compression: A preliminary report." Journal of Pharmacy and Pharmacology 15.1 (1963): 413-421.

49. Sheikh-Salem, M., and J. T. Fell. "Compaction characteristics of mixtures of materials with dissimilar compaction mechanisms." Int. J. Pharm. Tech. Prod. Mfr 2.1 (1981): 19-22.

50. Kesavan, Jothi G., and Garnet E. Peck. "Pharmaceutical granulation and tablet formulation using neural networks." Pharmaceutical development and technology 1.4 (1996): 391-404.

51. Sun, C. and Grant D. J. W. "Influence of crystal structure on the tableting properties of sulfamerazine polymorphs." Pharmaceutical research 18.3 (2001): 274-280.

52. Sun, C. and Grant D. J. W. "Effects of initial particle size on the tableting properties of L-lysine monohydrochloride dihydrate powder." International Journal of pharmaceutics 215.1 (2001): 221-228.

53. Berggren, J. and Alderborn G. "Effect of drying rate on porosity and tabletting behaviour of cellulose pellets." International Journal of Pharmaceutics 227.1 (2001): 81-96.

54. Stiel, D. M. "Method invoking tabletting compression force control for optimizing tabletted formulation parameters." U.S. Patent No. 4,121,289. 17 Oct. 1978.

55. Vezin, W. R. et al. "Adjustment of precompression force to reduce mixing-time dependence of tablet tensile strength." Journal of pharmacy and pharmacology 35.9 (1983): 555-558.

56. Tye, C. K. et al. "Evaluation of the effects of tableting speed on the relationships between compaction pressure, tablet tensile strength, and tablet solid fraction." Journal of pharmaceutical sciences 94.3 (2005): 465-472.

57. Lin, S. Y. "Effect of excipients on tablet properties and dissolution behavior of theophylline-tableted microcapsules under different compression forces." Journal of pharmaceutical sciences 77.3 (1988): 229-232.

58. Sebhatu, T. et al. "Effect of moisture sorption on tabletting characteristics of spray dried (15% amorphous) lactose." Pharmaceutical research 11.9 (1994): 1233-1238.

59. Kanig, J. L. "DIRECT COMPRESSION TABLETTING." U.S. Patent No. 3,873,694. 1975.

60. Çelik, M. and Marshall K. "Use of a compaction simulator system in tabletting research." Drug Development and Industrial Pharmacy 15.5 (1989): 759-800.

61. Neuhaus, T. "Investigation and optimisation of the presster: a linear compaction simulator for rotary tablet presses" Verlag Dr. Hut, 2007.

62. M. Saeed, L. Probst, G. Betz. Assessment of diffuse transmission mode in near-infrared quantification – part II: comparison of information depth with diffuse reflection. Journal of Pharmaceutical Sciences. Volume 100, Issue 3, pages 1130–1141, March 2011.

63. Ben-Gera, I., and K. H. Norris. "Determination of moisture content in soybeans by direct spectrophotometry." Isr. J. Agric. Res 18.3 (1968): 125-132.

64. Ben-Gera, I. T. A. M. A. R., and KARL H. NORRIS. "Direct spectrophotometric determination of fat and moisture in meat products." Journal of Food Science 33.1 (1968): 64-67.

65. Saeed et al. Assessment of diffuse transmission mode in near-infrared quantification - part I: The press effect on low-dose pharmaceutical tablets. Journal of Pharmaceutical Sciences. 2009, 98 (12), 4877-4886.

66. Cruz J, Blanco M. Content uniformity studies in tablets by NIR-CI, J Pharm Biomed Anal 2011;in press

67. Dou Y, Sun Y, Ren Y, Ju P, Ren Y. Simultaneous non-destructive determination of two components of combined paracetamol and amantadine hydrochloride in tablets and powder by NIR spectroscopy and artificial neural networks, J Pharm Biomed Anal 2005;37: 543-549

68. Ito M, Suzuki T, Yada S, Nakagami H, Teramoto H, Yonemuchi E, Terada K. Development of a method for nondestructive NIR transmittance spectroscopic analysis of acetaminophen and caffeine anhydrate in intact bilayer tablets, J Pharm Biomed Anal 2010; 53: 396-402

69. Blanco M, Eustaquio J, Gonzalez, Serrano D. Identification and quantitation assays for intact tablets of two related pharmaceutical preparations by reflectance near-infrared spectroscopy: validation of the procedure, J Pharm Biomed Anal, 2000;22: 139-148

70. Alvarenga L, Ferreira D, Altekruse D, Menezes JC, Lochmann D. Tablet identification using near-infrared spectroscopy (NIRS) for pharmaceutical quality control, J Pharm Biomed Anal, 2008;48: 62-69

71. Karande A, Heng P, Liew C. In-line quantification of micronized drug and excipients in tablets by near infrared (NIR) spectroscopy: Real time monitoring of tabletting process, Int J Pharm,2010;396: 63-74

72. Sekulic, S. Sonja, et al. "On-line monitoring of powder blend homogeneity by near-infrared spectroscopy." Analytical Chemistry 68.3 (1996): 509-513.

73. Hailey, P. A., et al. "Automated system for the on-line monitoring of powder blending processes using near-infrared spectroscopy part I. System development and control." Journal of pharmaceutical and biomedical analysis 14.5 (1996): 551-559.

74. Rosa, Sílvia S., et al. "Development and validation of a method for active drug identification and content determination of ranitidine in pharmaceutical products using near-infrared reflectance spectroscopy: A parametric release approach." Talanta 75.3 (2008): 725-733.

75. Luypaert, J., D. L. Massart, and Y. Vander Heyden. "Near-infrared spectroscopy applications in pharmaceutical analysis." Talanta 72.3 (2007): 865-883.

76. Gemperline, Paul J., Laurie D. Webber, and Frank O. Cox. "Raw materials testing using soft independent modeling of class analogy analysis of near-infrared reflectance spectra." Analytical Chemistry 61.2 (1989): 138-144.

77. Candolfi, A., et al. "Identification of pharmaceutical excipients using NIR spectroscopy and SIMCA." Journal of pharmaceutical and biomedical analysis 19.6 (1999): 923-935.

78. Blanco, M., and M. A. Romero. "Near-infrared libraries in the pharmaceutical industry: a solution for identity confirmation." Analyst 126.12 (2001): 2212-2217.

79. Blanco, Marcelo, and Manel Alcalá. "Content uniformity and tablet hardness testing of intact pharmaceutical tablets by near infrared spectroscopy: a contribution to process analytical technologies." Analytica chimica acta 557.1 (2006): 353-359.

80. Blanco, Marcelo, et al. "A process analytical technology approach based on near infrared spectroscopy: tablet hardness, content uniformity, and dissolution test measurements of intact tablets." Journal of pharmaceutical sciences 95.10 (2006): 2137-2144.

81. Blanco, M., et al. "Quantitation of the active compound and major excipients in a pharmaceutical formulation by near infrared diffuse reflectance spectroscopy with fibre optical probe." Analytica chimica acta 333.1 (1996): 147-156.

82. Chalus, Pascal, Serge Walter, and Michel Ulmschneider. "Combined wavelet transform–artificial neural network use in tablet active content determination by near-infrared spectroscopy." Analytica chimica acta 591.2 (2007): 219-224.

83. Mantanus, Jérôme, et al. "Active content determination of non-coated pharmaceutical pellets by near infrared spectroscopy: Method development, validation and reliability evaluation." Talanta 80.5 (2010): 1750-1757.

84. Moes, Johannes J., et al. "Application of process analytical technology in tablet process development using NIR spectroscopy: Blend uniformity, content uniformity and coating thickness measurements." International journal of pharmaceutics 357.1 (2008): 108-118.

85. Sulub, Yusuf, et al. "Real-time on-line blend uniformity monitoring using near-infrared reflectance spectrometry: A noninvasive off-line calibration approach." Journal of pharmaceutical and biomedical analysis 49.1 (2009): 48-54.

86. Lyon, Robbe C., et al. "Near-infrared spectral imaging for quality assurance of pharmaceutical products: analysis of tablets to assess powder blend homogeneity." AAPS PharmSciTech 3.3 (2002): 1-15.

87. Ely, David, Sai Chamarthy, and M. Teresa Carvajal. "An investigation into low dose blend uniformity and segregation determination using NIR spectroscopy." Colloids and Surfaces A: Physicochemical and Engineering Aspects 288.1 (2006): 71-76.

88. Morisseau, Karen M., and Christopher T. Rhodes. "Near-infrared spectroscopy as a nondestructive alternative to conventional tablet hardness testing." Pharmaceutical research 14.1 (1997): 108-111

89. Donoso, M., D. O. Kildsig, and Evone S. Ghaly. "Prediction of tablet hardness and porosity using near-infrared diffuse reflectance spectroscopy as a nondestructive method." Pharmaceutical development and technology 8.4 (2003): 357-366.

90. Santos, A. F., E. L. Lima, and J. C. Pinto. "In-line evaluation of average particle size in styrene suspension polymerizations using near-infrared spectroscopy." Journal of Applied Polymer Science 70.9 (1998): 1737-1745.

91. Rantanen, Jukka, et al. "On-line monitoring of moisture content in an instrumented fluidized bed granulator with a multi-channel NIR moisture sensor." Powder Technology 99.2 (1998): 163-170.

92. Zheng, Yiwu, et al. "Determination of moisture content of lyophilized allergen vaccines by NIR spectroscopy." Journal of pharmaceutical and biomedical analysis 46.3 (2008): 592-596.

93. Andersson, Martin, et al. "Quantitative analysis of film coating in a fluidized bed process by in-line NIR spectrometry and multivariate batch calibration." Analytical chemistry 72.9 (2000): 2099-2108.

94. Pérez-Ramos, José D., et al. "Quantitative analysis of film coating in a pan coater based on in-line sensor measurements." Aaps Pharmscitech 6.1 (2005): E127-E136.

95. Römer, Meike, et al. "Prediction of tablet film-coating thickness using a rotating plate coating system and NIR spectroscopy." Aaps Pharmscitech 9.4 (2008): 1047-1053.

96. Lee, Min-Jeong, et al. "In line NIR quantification of film thickness on pharmaceutical pellets during a fluid bed coating process." International journal of pharmaceutics 403.1 (2011): 66-72.

97. Aldridge, Paulá K, and S. á Sonja Sekulic. "Determination of end-points for polymorph conversions of crystalline organic compounds using on-line near-infrared spectroscopy." Analyst 122.6 (1997): 549-552.

98. Blanco, Marcelo, et al. "Application of NIR spectroscopy in polymorphic analysis: Study of pseudo-polymorphs stability." Journal of pharmaceutical sciences 94.6 (2005): 1336-1342.

99. Otsuka, Makoto, Fumie Kato, and Yoshihisa Matsuda. "Determination of indomethacin polymorphic contents by chemometric near-infrared spectroscopy and conventional powder X-ray diffractometry." Analyst 126.9 (2001): 1578-1582.

100. Schneider, Ralph Carsten, and Karl-Artur Kovar. "Analysis of ecstasy tablets: comparison of reflectance and transmittance near infrared spectroscopy." Forensic science international 134.2 (2003): 187-195.

101. Trafford, AndrewáD, RogeráD Jee, and AnthonyáC Moffat. "A rapid quantitative assay of intact paracetamol tablets by reflectance near-infrared spectroscopy." Analyst 124.2 (1999): 163-167.

102. Chalus, Pascal, et al. "Near-infrared determination of active substance content in intact low-dosage tablets." Talanta 66.5 (2005): 1294-1302.

103. Feng, Yan-Chun, and Chang-Qin Hu. "Construction of universal quantitative models for determination of roxithromycin and erythromycin ethylsuccinate in tablets from different manufacturers using near infrared reflectance spectroscopy." Journal of pharmaceutical and biomedical analysis 41.2 (2006): 373-384.

104. Laasonen, Magali, et al. "Development and validation of a near-infrared method for the quantitation of caffeine in intact single tablets." Analytical chemistry 75.4 (2003): 754-760.

105. Dyrby, M., et al. "Chemometric quantitation of the active substance (containing C≡ N) in a pharmaceutical tablet using near-infrared (NIR) transmittance and NIR FT-Raman spectra." Applied spectroscopy 56.5 (2002): 579-585.

106. Gottfries, J., et al. "Vibrational spectrometry for the assessment of active substance in metoprolol tablets: a comparison between transmission and diffuse reflectance near-infrared spectrometry." Journal of pharmaceutical and biomedical analysis 14.11 (1996): 1495-1503.

107. Abrahamsson, Christoffer, et al. "Time-resolved NIR spectroscopy for quantitative analysis of intact pharmaceutical tablets." Analytical chemistry 77.4 (2005): 1055-1059.

108. Saeed, M., et al. "Assessment of diffuse transmission mode in near-infrared quantification—part I: The press effect on low-dose pharmaceutical tablets." Journal of pharmaceutical sciences 98.12 (2009): 4877-4886.

109. Ito, Masatomo, et al. "Development of a method for nondestructive NIR transmittance spectroscopic analysis of acetaminophen and caffeine anhydrate in intact bilayer tablets." Journal of pharmaceutical and biomedical analysis 53.3 (2010): 396-402.

110. Meza, Carlos Peroza, María A. Santos, and Rodolfo J. Romañach. "Quantitation of drug content in a low dosage formulation by transmission near infrared spectroscopy." Aaps Pharmscitech 7.1 (2006): E206-E214.

111. Xiang, Dong, et al. "Development of robust quantitative methods by near-infrared spectroscopy for rapid pharmaceutical determination of content uniformity in complex tablet matrix." Analyst 134.7 (2009): 1405-1415.

112. Ito, Masatomo, et al. "Development of a method for the determination of caffeine anhydrate in various designed intact tables by near-infrared spectroscopy: A comparison between reflectance and transmittance technique." Journal of pharmaceutical and biomedical analysis 47.4 (2008): 819-827.

113. Xiang, Dong, et al. "Evaluation of transmission and reflection modalities for measuring content uniformity of pharmaceutical tablets with near-infrared spectroscopy." Applied spectroscopy 63.1 (2009): 33-47.

114. Mark, Howard, et al. "Validation of a near-infrared transmission spectroscopic procedure, part A: validation protocols." Journal of pharmaceutical and biomedical analysis 28.2 (2002): 251-260.

115. Wu, W., et al. "Artificial neural networks in classification of NIR spectral data: design of the training set." Chemometrics and intelligent laboratory systems 33.1 (1996): 35-46.

116. Borer, Matthew W., et al. "Evaluation of key sources of variability in the measurement of pharmaceutical drug products by near infrared reflectance spectroscopy." Journal of pharmaceutical and biomedical analysis 17.4 (1998): 641-650.

117. Rutan, Sarah C., Onno E. de Noord, and Ronald R. Andréa. "Characterization of the sources of variation affecting near-infrared spectroscopy using chemometric methods." Analytical chemistry 70.15 (1998): 3198-3201.

118. Blanco, Marcelo, and Anna Peguero. "Influence of physical factors on the accuracy of calibration models for NIR spectroscopy." Journal of pharmaceutical and biomedical analysis 52.1 (2010): 59-65.

119. Data Reduction and Error Analysis for the Physical Sciences, Second Edition, by Philip R. Bevington and D.Keith Robinson, McGraw-Hill Inc., 1992.

120. European Medicines Agency "Guideline on the use of Near Infrared Spectroscopy (NIRS) by the pharmaceutical industry and the data requirements for new submissions and variations." (2012): 1-28.

121. PASG NIR subgroup "PASG guidelines for the development and validation of near-infrared (NIR) spectroscopy methods" (2001): 1-41.

122. Hailey, P. A., et al. "Automated system for the on-line monitoring of powder blending processes using near-infrared spectroscopy part I. System development and control." Journal of pharmaceutical and biomedical analysis 14.5 (1996): 551-559.

123. Momose, Wataru, et al. "Process analytical technology applied for end-point detection of pharmaceutical blending by combining two calibration-free methods: Simultaneously monitoring specific near-infrared peak intensity and moving block standard deviation." Powder Technology 210.2 (2011): 122-131.

124. ISO 12099:2010 – Animal feeding stuffs, cereals and milled cereal products Guidelines for the application of near infrared spectrometry, http://www.iso.org ; 2010.

125. Williams, P. C. 2001. Implementation of near-infrared technology. Pages 145–169 in Near-Infrared Technology in the Agriculture and Food Sciences. 2nd ed. P. Williams and K. Norris, ed. Am. Assoc. Cereal Chem., St. Paul, MN.

126. Carol J. Bruegge ; Arthur W. Springsteen ; Albert E. Stiegman and Richard A. Rainen "Use of Spectralon as a diffuse reflectance standard for in-flight calibration of earth-orbiting sensors", Opt. Eng. 32(4), 805-814 (Apr 01, 1993). ; http://dx.doi.org/10.1117/12.132373

127. Garg, Gopal, Shailendra Saraf, and Swarnlata Saraf. "Spectrophotometric and column high-performance liquid chromatographic methods for simultaneous estimation of metoprolol tartrate and hydrochlorothiazide in tablets." Journal of AOAC International 91.5 (2008): 1045-1550.

128. Rawool, N. D., and A. Venkatchalam. "Analytical Method for the Simultaneous Estimation of Hydrochlorothiazide and Metoprolol Tartrate using RP HPLC." Indian journal of pharmaceutical sciences 73.2 (2011): 219-223.

129. Gupta, K. R., M. R. Tajne, and S. G. Wadodkar. "New spectrophotometric method for simultaneous determination of metoprolol tartarate and hydrochlorthiazide in tablets." Indian journal of pharmaceutical sciences 70.4 (2008): 511.

130. Gao, Feng, et al. "Simultaneous quantitation of hydrochlorothiazide and metoprolol in human plasma by liquid chromatography–tandem mass spectrometry." Journal of pharmaceutical and biomedical analysis 52.1 (2010): 149-154.

131. Stolarczyk, M. A. R. I. U. S. Z., et al. "Determination of metoprolol and hydrochlorothiazide by derivative spectrophotometric method in pharmaceutical preparations." Acta Poloniae Pharmaceutica 63 (2006): 169-173.

132. Ramadan, Nesrin K., Heba M. Mohamed, and Azza A. Mostafa. "Miniaturized membrane sensors for potentiometric determination of metoprolol tartrate and hydrochlorothiazide." Acta chimica Slovenica 59.2 (2012): 344-352.

133. Alnajjar, Ahmed O., et al. "Capillary Electrophoresis Assay Method for Metoprolol and Hydrochlorothiazide in their Combined Dosage Form with Multivariate Optimization." Journal of chromatographic science 51.1 (2013): 92-97.

134. Dou, Ying, et al. "Artificial neural network for simultaneous determination of two components of compound paracetamol and diphenhydramine hydrochloride powder on NIR spectroscopy." Analytica chimica acta 528.1 (2005): 55-61.

135. Dou, Ying, et al. "Determination of compound aminopyrine phenacetin tablets by using artificial neural networks combined with principal components analysis." Analytical biochemistry 351.2 (2006): 174-180.

136. Blanco, M., and M. Alcala. "Simultaneous quantitation of five active principles in a pharmaceutical preparation: Development and validation of a near infrared spectroscopic method." European journal of pharmaceutical sciences 27.2 (2006): 280-286.

Branko Z. Vranic

Address: Schaffhauserstrasse 5, 8006 Zürich, Switzerland
Phone: + 41 76 273 97 27
E-mail: vranic.b@buchi.com
Age: 31

Summary: PhD candidate in pharmaceutical technology with 5+ years of experience in research and development

Professional Experience

05.2014 – present

BUCHI Labortechnik AG, Meierseggstrasse 40, CH-9230 Flawil
Global Application Specialist NIR-Online / Product Specialist NIR-Online Switzerland & Austria

- Global NIR-Online application support for customers, distributor partners and affiliates
- Consulting and implementation plans
- Feasibility studies
- Sales support for Switzerland and Austria

09.2011 – 05.2014

BUCHI Labortechnik AG, Meierseggstrasse 40, CH-9230 Flawil
Global Application and Training Specialist NIR

- Development of near-infrared spectroscopic applications for the clients in pharmaceutical industry
- Consulting and implementation plans
- Installations (IQ, OQ, PQ)
- Method validation
- Feasibility studies
- Collaborative development projects with Academia
- Global application and software support
- Trainings and seminars
- Development of innovative training methodologies
- QA - development of instrument testing procedures and SOPs
- Software and hardware development and testing
- Technology scouting; strategic projects; sales project management
- Interaction with pharmaceutical regulatory bodies (EMA)

09.2008 – 09.2011

University of Basel, Industrial Pharmacy Research Group Klingelbergstrasse 50, CH-4056 Basel
Researcher and Teaching Assistant

- Research in the field of NIR implementation in pharmaceutical production process monitoring and QC of solid dosage forms
- Organization, preparation and execution of practical exercises in pharmaceutical technology, industrial pharmacy and physical chemistry
- Supervision of student research projects in pharmaceutical technology and near-infrared spectroscopy

Education

09.2008 – present

PhD Student - Pharmaceutical Technology, University of Basel, Switzerland

Title of the thesis: ` Design of Experiments Methodology in Studying Near-Infrared Spectral Information of Model Intact Tablets - Simultaneous Determination of Metoprolol Tartrate and Hydrochlorothiazide in Solid Dosage Forms and Powder Compressibility Assessment Using Near-Infrared Spectroscopy`, Department of Pharmaceutical Sciences, University of Basel.

10.2002 – 06.2008 **MSc in Pharmaceutical Sciences**, University of Belgrade, Serbia

Title of the thesis: `*Formulation, Preparation and Evaluation of Modified - Release Verapamil Hydrochloride Matrix Tablets*`, Department of Pharmaceutical Technology, Pharmaceutical Faculty, University of Belgrade.

Skills

Pharmaceutical process technologies:

Fluid bed granulation, drying and coating; drum coating; high-share mixer granulation; roller-compaction; rotary and eccentric tablet presses (Korsch); compaction-simulator (Presster®).

Characterization (QC) methods:

Near-infrared spectroscopy (mixing end-point determination, content determination of API(s) and excipients, CUT, tablet hardness and relative density, LOD, prediction of disintegration time and dissolution profiles, prediction of compression and compaction properties of powders and granules, prediction of particle size); dissolution and disintegration tests; tablet hardness and friability testing; flowability of powders and granules; particle size determination methods (sieve analysis and laser diffraction); specific surface area determination; true, bulk and tapped density determination; powder compressibility and compactibility assessment; SEM; differential scanning calorimetry.

Analytical methods:

NIR, UV, Chromatography.

Process Analytical Technologies:

NIR (at-line, on-line, in-line – fiber optic probes and non-contact NIR), Focused Beam Reflectance Measurement (FBRM), Power Consumption (high-share mixer).

Software skills:

Chemometric software packages: NIRCal, OPUS, XLSTAT, Matlab (basic), Unscrambler
Artificial Neuronal Networks: Synapse
Design of Experiments: Stavex, MODDE, Minitab
Various: CRM (Customer Relationship Management), ERP (Enterprise Resource Planning)

Regulations and Standards:

cGMP; ICH Q2, Q8, Q9 and Q10; USP; EP; ISO 9001:2008; EMA guidelines

Other skills:

Chemometrics, Design of Experiments, Multivariate Data Analysis Methods, QbD, PAT, modified drug-release technologies, compression and compaction physics, descriptive statistics and hypothesis testing, Kaizen, Miller-Heiman strategic selling, Lean Manufacturing.

Languages

English – Full Professional Proficiency
German – Moderate
Russian – Basic

References

Prof. Dr. Thierry F. Vandamme, Pharmaceutical Faculty, University of Strasbourg; E-mail: vandamme@unistra.fr

Christian Lehmann, Product Group Manager NIR, BÜCHI Labortechnik AG; E-mail: lehmann.c@buchi.com

Dr. Volker Frost, Chief Profit Center Spectroscopy, Metrohm AG; E-mail: info@metrohm.com

PD Dr. Gabriele Betz, Department of Pharmaceutical Sciences, University of Basel; E-mail: gabriele.betz@unibas.ch

Prof. Dr. Georg Gescheidt, Graz University of Technology; E-mail: g.gescheidt-demner@tugraz.at

Prof. Dr. Svetlana Ibric; Pharmaceutical Faculty, University of Belgrade; E-mail: svetlana.ibric@pharmacy.bg.ac.rs

LIST OF PUBLICATIONS

1. Alfuzosin milk protein nanoparticles: NIR spectral characterization and floating tablets preparation

   Journal of Pharmaceutical Development and Technology – Under Review

   Elgindy N. [a], **Vranic B.** [b] and Elzoghby A.[a]

   [a] Dept. of Industrial Pharmacy, Faculty of Pharmacy, Alexandria University, Egypt

   [b] BÜCHI Labortechnik AG, Switzerland

2. Assessing compressibility and compactibility of powder formulations with Near-Infrared Spectroscopy

   Journal of Pharmaceutical Development and Technology; Febuary 2013, Vol. 18, No. 1, Pages 156-171 (doi:10.3109/10837450.2012.663388)

   Nicolaos D. Gentis, **Branko Z. Vranic**, Gabriele Betz
   Department of Pharmaceutical Sciences, Industrial Pharmacy Research Group, University of Basel, Basel, Switzerland

3. Effect of simulated precompression, compression pressure and tableting speed on an offline diffuse transmittance and reflectance near-infrared spectral information of model intact caffeine tablets

   Journal of Pharmaceutical Development and Technology; Early Online: 1–9; 2014 Informa Healthcare USA, Inc. DOI: 10.3109/10837450.2014.949267

   Branko Z. Vranic [1, 2], Thierry F. Vandamme [3]

   [1] Department of Pharmaceutical Sciences, University of Basel, Klingelbergstrasse 50, CH-4056 Basel, Switzerland.

   [2] Büchi Labortechnik AG, Meierseggstrasse 40, Postfach CH-9230 Flawil 1, Switzerland.

[3] Université de Strasbourg, Faculté de Pharmacie, CNRS 7199 Laboratoire de Conception et Application de Molécules Bioactives, équipe de Pharmacie Biogalénique, 74 route du Rhin BP 60024 F-67401 Illkirch Cedex, France.

4. Preliminary study of an offline simultaneous determination of metoprolol tartrate and hydrochlorothiazide in powders and tablets by reflectance near-infrared spectroscopy

   Journal of Pharmaceutical Development and Technology; Early Online: 1–6; 2014 Informa Healthcare USA, Inc. DOI: 10.3109/10837450.2014.949268

   Branko Z. Vranic [1, 2], Thierry F. Vandamme [3]

   [1] University of Basel, Department of Pharmaceutical Sciences, Klingelbergstrasse 50, CH-4056 Basel, Switzerland.

   [2] Büchi Labortechnik AG, Meierseggstrasse 40, Postfach CH-9230 Flawil 1, Switzerland.

   [3] Université de Strasbourg, Faculté de Pharmacie, CNRS 7199 Laboratoire de Conception et Application de Molécules Bioactives, équipe de Pharmacie Biogalénique, 74 route du Rhin BP 60024 F-67401 Illkirch Cedex, France.

5. Preliminary assessment of vegetable oil adulteration of pistachio paste by near infrared spectroscopy

   NIR News; Vol. 25 No. 4 June/July 2014; DOI: 10.1255/nirn.1447

   N. Bernardi,[a] G. Benetti,[a] G. Campolongo,[b] G. Ferrari,[b] R. Palermo[b] and **B. Vranic[b]**

   [a]Real Aromi Spa, Italy

   [b]Büchi Labortechnik AG, Switzerland

6. At-Line Determination of Different Quality Parameters of Fresh Meat Using NIR Spectroscopy

   16th International Conference on Near Infrared Spectroscopy – Proceedings (Peer Reviewed) – Published ; P-1342

Charles D. Dago[1], **B. Vranic [2]**, G. Campolongo[2], G. Ferrari[2]

[1] 16 Associazione Italiana Allevatori (A.I.A. - Italian Breeders Association), Rome, 00161, Italy

[2] 27 BUCHI Labortechnik AG – NIR Division, Flawil, 9230, Switzerland

7. Design of Experiments Methodology in Studying Critical Factors Influencing Near-Infrared Diffuse Transmission Spectra of Tablets

   16th International Conference on Near Infrared Spectroscopy – Proceedings (Peer Reviewed) – Published; P-1410

   Branko Vranic[1]

   [1] BUCHI Labortechnik AG – NIR Division, Flawil, 9230, Switzerland

8. Feasibility of FT-NIR Spectroscopy as a Useful Tool for Rapid Process Control 1 in Palm Oil Mill

   16th International Conference on Near Infrared Spectroscopy – Proceedings (Peer Reviewed) – Published; P-1413

   Xue Ni, Ng[1], Siat Pei, Chin[1], Tee Ching Yee[1], Yee Chee Hong[2], Apichai Kittipanprayoon[3], **B. Vranic[4]**

   [1] 14 Chemopharm Sdn Bhd, 20, Jalan SS2/66, 47300 Petaling Jaya. Selangor. Malaysia.
   [2] 25 Milivest Sdn Bhd, Block A, Lot 4, Ground Floor, Taman Grandview, PPM 111 6 Elopura, 90000 Sandakan, Sabah.
   [3] 37 Buchi (Thailand) Ltd., ASEAN Competence Center, 77/121 Sin Sathorn Tower, Krungtonburi Rd.
   8 Klongtonsai, Klongsan, Bangkok 10600, Thailand.
   [4] BUCHI Labortechnik AG – NIR Division, Flawil, 9230, Switzerland

9. Evaluation of the Performance of NIRMaster™ Near-Infrared Spectrometer on Cheese Samples

   16th International Conference on Near Infrared Spectroscopy – Proceedings (Peer Reviewed) – Published; P-1415

G. Campolongo, **B. Vranic**, V. Iplikci

BUCHI Labortechnik AG – NIR Division, Flawil, 9230, Switzerland

10. Critical Factors Influencing NIR Diffuse Transmission Spectra of Intact Tablets

Russian Journal "Drug Development and Registration", ISSN: 2305-2066. (Peer Review) – Under Review

Branko Vranic[1]

[1] BUCHI Labortechnik AG – NIR Division, Flawil, 9230, Switzerland

11. Optimization of Drug Release from Compressed Multiparticulate Units Using Generalized Regression Neural Network

7th Central European Symposium on Pharmaceutical Technology and Biotechnology - Proceedings (Peer Reviewed) – Published; OP021

Ivić B.[1], Ibrić S.[2], Betz G.[3], **Vranic B.**[2], Đuric Z.[2]

[1] R&D Institute, Galenika a.d., Belgrade, Serbia
[2] Institute for Pharmaceutical Technology, Faculty of Pharmacy, University of Belgrade, Belgrade, Serbia
[3] Industrial Pharmacy Research Group, Department of Pharmaceutical Sciences, University of Basel, Switzerland

LIST OF PRESENTATIONS

1. *Evaluation of the Performance of NIRMaster™ Near-Infrared Spectrometer on Cheese Samples:* G. Campolongo, **B. Vranic**, V. Iplikci, 16th International Conference on NIR Spectroscopy, 2. – 7/06/2013, La Grande-Motte, France – poster presentation.

2. *Feasibility of FT-NIR Spectroscopy as a Useful Tool for Rapid Process Control in Palm Oil Mill:* Xue Ni, Ng, Siat Pei, Chin, Tee Ching Yee, Yee Chee Hong, Apichai Kittipanprayoon, **Vranic B.**, 16th International Conference on NIR Spectroscopy, 2. – 7/06/2013, La Grande-Motte, France – poster presentation.

3. *Design of Experiments Methodology in Studying Critical Factors Influencing Near - Infrared Diffuse Transmission Spectra of Tablets:* **Vranic B.**, 16th International Conference on NIR Spectroscopy, 2. – 7/06/2013, La Grande-Motte, France – poster presentation.

4. *At-Line Determination of Different Quality Parameters of Fresh Meat Using NIR Spectroscopy:* Charles D. Dago, **B. Vranic**, G. Campolongo, G. Ferrari, 16th International Conference on NIR Spectroscopy, 2. – 7/06/2013, La Grande-Motte, France – poster presentation.

5. *Examples of Rapid NIR Implementation Solutions in the Food Industry:* **Vranic B.**, Seminar "Automation in Food Industry", Campden BRI, 19/06/2013, Gloucestershire, UK – oral presentation.

6. *Improving Near-Infrared Calibration Model Robustness Against Parameters of Tableting Process:* **Vranic B.**, QbD / PAT Conference 2011, 5. – 7/10/2011, Heidelberg, Germany – oral presentation.

7. *Simultaneous Quantification of Metoprolol – Tartrate and Hydrochlorthiazide in Powders and Tablets Using NIR Spectroscopy*: **Vranic B.**, Frost V., Betz G., 15th International Conference on NIR Spectroscopy, 13. – 20/05/2011, Cape Town, South Africa. – poster presentation.

8. *Compressibility and Compactibility of Powder Formulations - Investigation from a Physico - Mathematical Perspective with Introduction of Near-Infrared Spectroscopy*: Gentis N., **Vranic B.**, Betz G., FIP Pharmaceutical Sciences World Congress, New Orleans, Louisiana, USA, 14. – 18/11/2010. – poster presentation.

9. *Prediction of Active Pharmaceutical Ingredient in Intact Tablets Using NIR Spectroscopy and Multivariate Data Analysis Methods*: **Vranic B.**, Frost V., Betz G., 5th Congress of Pharmacists of Serbia, Belgrade, Serbia, 13. – 17/10/2010. – oral presentation.

10. *Prediction of Drug Content in Intact Tablets Using Near - Infrared Spectroscopy and Artificial Neural Networks*: **Vranic B.**, Frost V., Betz G., Joint Meeting of Universities of Geneve, Zurich and Basel, 18/06/2010. – oral presentation.

11. *At-line Monitoring of Drug Content in Intact Tablets Using NIR Spectroscopy: PAT Initiative*: **Vranic B.**, Frost V., Betz G., University of Belgrade, Serbia, 20/04/2010 – Invited lecture.

12. *Compaction Behavior of Powder Mixtures with the Focus on Variation of Tablet Relative Density*: Gentis N., **Vranic B.**, Betz G., 7th World Meeting on Pharmaceutics, Biopharmaceutics and Pharmaceutical Technology, Valletta, Malta, 8. – 11/03/2010. – poster presentation.

13. *Simultaneous Quantification of Two Actives in Powders and Tablets Using NIR Spectroscopy*: **Vranic B.**, Frost V., Betz G., Annual Research Meeting, University of Basel, Switzerland, 02/2010. – poster presentation.

14. *Near-Infrared Spectroscopy as a Novel Tool for Studying Compressibility and Compactibility of Pharmaceutical Powders*: Gentis N., **Vranic B.**, Betz G., Annual Research Meeting, University of Basel, Switzerland, 02/2010. – poster presentation.

15. *Case Study: Robust Method for the Quantification of Active Pharmaceutical Ingredient in Intact Tablets Using NIR Spectroscopy*: **Vranic B.**, Frost V., Betz G., 7th PAT and Quality by Design Conference, London, UK, 19/01/2010. – oral presentation.

16. *Application of Near - Infrared Spectroscopy in the Prediction of Drug Content in Intact Tablets*: **Vranic B.**, Frost V., Betz G., Symposium BIOFARM 2009, Belgrade, Serbia, 22/10/2009. - poster presentation.

17. *Robust Method for Determination of Caffeine in Intact Tablets by NIR Spectroscopy – Comparison Between Reflection and Transmission mode*: **Vranic B.**, Frost V., Betz G., IPL Symposium, Industrial Pharmacy Lab, University of Basel, Switzerland, 21/08/2009. – oral presentation.

18. *Prediction of Drug Content in Intact Tablets by Near-Infrared Spectroscopy*: **Vranic B.**, Frost V., Betz G., Annual Research Meeting, University of Basel, Switzerland, 02/2009. – poster presentation.

19. *Optimization of Drug Release from Compressed Multiparticulate Units Using Generalized Regression Neural Network*: Ivić B., Ibrić S., Betz G., **Vranic B.**, Đuric Z., 7th Central European Symposium on Pharmaceutical Technology and Biotechnology, Ljubljana, Slovenia,18.–20/09/2008. – oral presentation.

20. *Preparation and Evaluation of pH – Independent Sustained – Release Matrix Tablets of Verapamil Hydrochloride Using Kollidon® SR*: Ibrić S., **Vranic B.**, Parojčić J., Đurić Z. The 1st Conference on Innovation in Drug Delivery, Naples, Italy, 30/09/2007 – 03/10/2007. – poster presentation.